

Discovering the cover. Molecular imaging of *Populus trichocarpa* leaf surface by FT-IR spectroscopy and mass spectrometry techniques

Dissertation

zur Erlangung des akademischen Grades

„ doctor rerum naturalium“ (Dr. rer. nat.)

vorgelegt dem Rat der Biologisch-Pharmazeutischen Fakultät

der Friedrich-Schiller-Universität Jena

von M.Sc. Mina Dost

geboren am 15 Juni 1979 in Kabul

Gutachter:

Prof. Dr. Wilhelm Boland, Max Planck Institut für Chemische Ökologie, Jena

Prof. Dr. Markus Riederer, Julius-von-Sachs-Institut für Biowissenschaften, Biozentrum
Universität Würzburg

Prof. Dr. Lukas Schreiber, Institut für Zelluläre und Molekulare Botanik (IZMB), Universität
Bonn

Verteidigungsdatum:

23 April 2015

List of content

1. Chapter I. Introduction	1
1.1 The plant cuticle – a chemically and structurally complex ‘limiting skin’.....	1
1.2 Major functions of plant cuticle.....	1
1.3 The epicuticular waxes.....	2
1.4 Biosynthesis of plant waxes.....	5
1.5 Relevance of sampling methods in the leaf surface studies.....	6
1.6 Implemented techniques for molecular imaging studies.....	8
1.6.1 Vibrational spectroscopy imaging techniques.....	9
1.6.2 Mass spectrometry imaging techniques.....	10
1.7 Biological system.....	11
1.8 The main objectives of the study.....	12
2. Chapter II. Epicuticular waxes of <i>Populus trichocarpa</i> : their chemistry and role in host recognition process of the leaf beetle, <i>Chrysomela populi</i>	13
2.1 Introduction.....	13
2.2 Results and discussion.....	13
2.2.1 Chemical characterization of the <i>Populus trichocarpa</i> leaf surface.....	13
2.2.2 Method development for <i>in vivo</i> EW isolation.....	21
2.2.3 The role of <i>Populus trichocarpa</i> epicuticular wax layer in the host plant recognition.....	26
2.2.4 Localization of salicin.....	30
2.3 Conclusions.....	33
3. Chapter III Molecular imaging of <i>Populus trichocarpa</i> leaf surface.....	34
3.1 Introduction.....	34

3.2	Results and discussion.....	36
3.2.1	Wound-induced epicuticular wax deposition on the leaf surface of <i>Populus trichocarpa</i> studied by FT-IR spectroscopy imaging.....	36
3.2.2	High resolution TOF-SIMS imaging reveals co-aggregation of <i>Populus trichocarpa</i> leaf surface compounds.....	57
3.3	Conclusions.....	75
4.	Chapter IV Overall conclusions.....	77
5.	Materials and methods.....	81
6.	Supplementary materials.....	91
7.	References.....	98
8.	Summary.....	109
9.	Zusammenfassung.....	112
10.	Acknowledgments.....	115
11.	Curriculum vitae.....	116
12.	Independency statement / Selbständigkeitserklärung.....	119

1. Chapter I Introduction

1.1 The plant cuticle – a chemically and structurally complex ‘limiting skin’

One of the main adaptations of terrestrial plants to their environment is the formation of a cuticle, a lipophilic structure on the outer surface of epidermal cells. Due to its specific physicochemical properties, the cuticle provides plant's integrity and survival. A mechanical barrier is delivered by cutin, a polyester-type biopolymer, which forms the main structural skeleton. Control of non-stomatal water loss as well as flow and exchange of mainly lipophilic molecules, including various secondary metabolites between the environment and the plant is significantly improved by the presence of highly non-polar compounds, the cuticular waxes. Chemical composition, structure, and thickness of cuticular wax layer depends on diverse factors such as plant species, plant organ and its ontogenetic stage. It may also vary with the changes of environmental conditions such as humidity, light intensity, and temperature (Hauke and Schreiber, 1998; Kunst and Samuels, 2003; Schreiber, 2001). It is widely accepted that plant waxes represent a heterogeneous mixture of very long-chain aliphatic compounds, including alkanes, alkylesters, fatty acids, alcohols, aldehydes, and ketones with carbon chain lengths ranging from C₂₀ to C₆₀ (Kolattukudy, 1996; Post-Beittenmiller, 1996).

1.2 Major functions of plant cuticle

The plant cuticle is a multifunctional interface between the plants and their environment. As a consequence of its structural arrangement and chemical composition, the cuticle plays a primary role as a diffusion barrier on the different levels. Next to the stomata, the cuticle allows to control water transpiration, which determines survival of all terrestrial plants. It also impedes the transport of polar and lipophilic organic substances from the apoplastic solution to the environment as well as their uptake from the outside (Schreiber, 2005; 2006) Furthermore, this structure limits the loss and uptake of gasses and vapors, for instance carbon dioxide, oxygen, but also organic volatile compounds like terpenes (Kerstiens, 1996). When the cuticle remains impermeable to a variety of volatiles, the plant is capable to regulate diffusion of those compounds through opening or closing the stomata. This in turn plays a crucial role in chemical communication with the environment that is largely dependent on the release and perception of chemical information through specific blends of volatile cues (Mithöfer and Boland, 2012).

The leaf surface is also involved in one of the most critical processes for maintaining life on Earth, namely photosynthesis. As a main mechanical barrier, it protects plants from excessive light in the visible (VIS) as well as in the ultraviolet (UV) range, which would exert a destructive impact on the complex photosynthetic system of pigments and proteins as well as on other cell constituents (Koch et al., 2010; Krauss et al., 1997; Müller and Riederer, 2005; Warren et al., 2003)

Finally, the cuticle along with other mechanical barriers such as hardened covers, thorns and trichomes (Simmons and Gurr, 2005), is a main site of aboveground biotic interactions, that comprise microorganisms (bacteria, yeast, fungi) as well as herbivorous insects (Kerstiens, 1996; Gatehouse, 2002). For those organisms, crossing the cuticle is a prerequisite for their invasion. Interestingly, cuticle components themselves may serve as signaling molecules for the induction of fungal cutinase gene expression and initiation of plant defense processes (Kolattukudy, 1995). The cascade of plant defensive processes that are activated in response to an injury aims to alarm previously unaffected leaves or neighbouring plants about the threatening danger (Farmer, 2001), attract herbivore specific predators that prevent further plant damage (Kappers et al., 2005; Kessler and Baldwin, 2001), as well as induce healing process on the damaged tissue (Felton and Tumlinson, 2008). Although the latter process was widely explored from the different perspectives (León et al., 2001; Wu, 1973), due to limitations originating either from the employed analytical techniques or sample preparation procedures, the involvement of the epicuticular waxes in the wound – healing process remains largely unknown.

1.3 The epicuticular waxes

It is known, that within cuticular waxes a spatial differentiation exists (Haas and Rentschler, 1984). An inner layer embedding cutin represents the intracuticular waxes that are composed only of traces of aliphatic compounds and are enriched with pentacyclic triterpenoids, ursolic and oleanolic acids (Jetter et al., 2000). An outer layer having direct contact with the environment and thus creating the actual plant surface is formed by the epicuticular waxes (EWs) (**Fig. 1**). They consist of mainly long chain aliphatic compounds. This spacial and chemical differentiation has its biological and ecological implications.

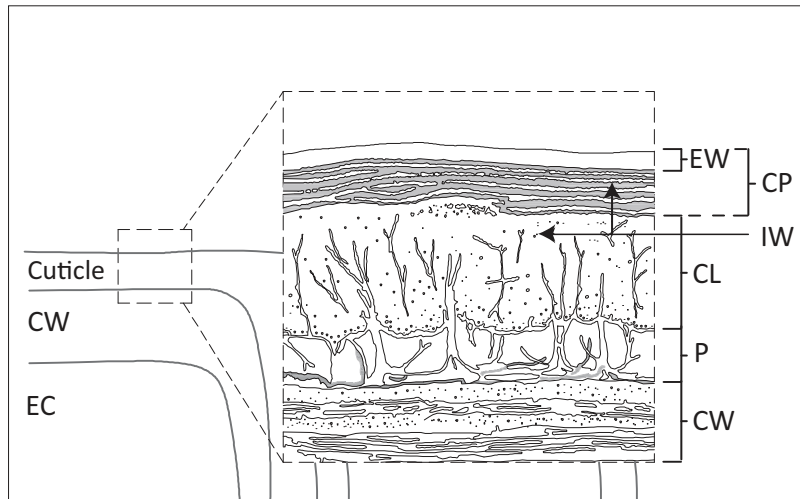


Fig. 1 Cross-section of cuticle layers and upper epidermis (EW – epicuticular waxes, IW- intracuticular waxes, CP – cuticle proper, CL – cuticle layer, P – pectinaceous layer and middle lamella, CW – cell wall, EC – epidermal cell).

EWs exhibit a tremendous morphological diversity ranging from the continuous and smooth layers to the formation of a variety of microstructures. Extend and comprehensive classification of EWs is provided by Barthlott et al. (1998). The most commonly present form of a wax layer is a thin wax film, even of few nm thick (e.g. *Hydrocotyle bonariensis*). Very rarely EWs form crusts: massive wax coverings reaching 10 mm thickness (e.g. *Copernicia cowellii*). Micro and nano structures have different shapes and sizes including granules, rodlets, tubules, platelets and plates. EWs exhibit self-assembly properties, which is prominently visible in the studies on wax recrystallization processes, where isolated waxes form a very similar micromorphology as native crystals observed on the leaf surface (Jetter and Riederer, 1994). This is however not a general rule, since for some plant species recrystallization of EW material on the artificial substrate appeared to be unsuccessful (Barthlott, 1998). It is well known that the morphology of wax microstructures is mainly defined by the chemical composition of EWs. The most abundant wax constituent is usually responsible for the crystal creation. For instance nonacosan-10-ol ($C_{29}H_{60}O$) forms crystals in *Picea pungens* (Jetter Riederer 1994) and in *Wollemia nobilis* (Dragota and Riederer, 2007) whereas the main constituents of EW crystals from the *Nepenthes* species are triacontanal ($C_{30}H_{60}O$) and dotriacontanal ($C_{32}H_{64}O$) (Riedel et al., 2007).

As a consequence of their localization at the interface with the environment, numerous functions are attributed to EWs such as: (1) influence on insect attachment and locomotion

(Eigenbrode and Espelie, 1995; Stoner, 1990); (2) affecting germination and virulence of many phytopathogenic fungi, for instance *Colletotrichum gloeosporioides* or *Metarhizium anisopliae* (Inyang et al., 1999; Kolattukudy et al., 1995; Podila et al., 1993); (3) providing signals for oviposition (Cervantes et al., 2002; Hopkins et al., 1997; Renwick et al., 1992; Spencer, 1996), as well as for host recognition for herbivores (de Boer and Hanson, 1988; Maloney et al., 1988) (**Fig.2**).

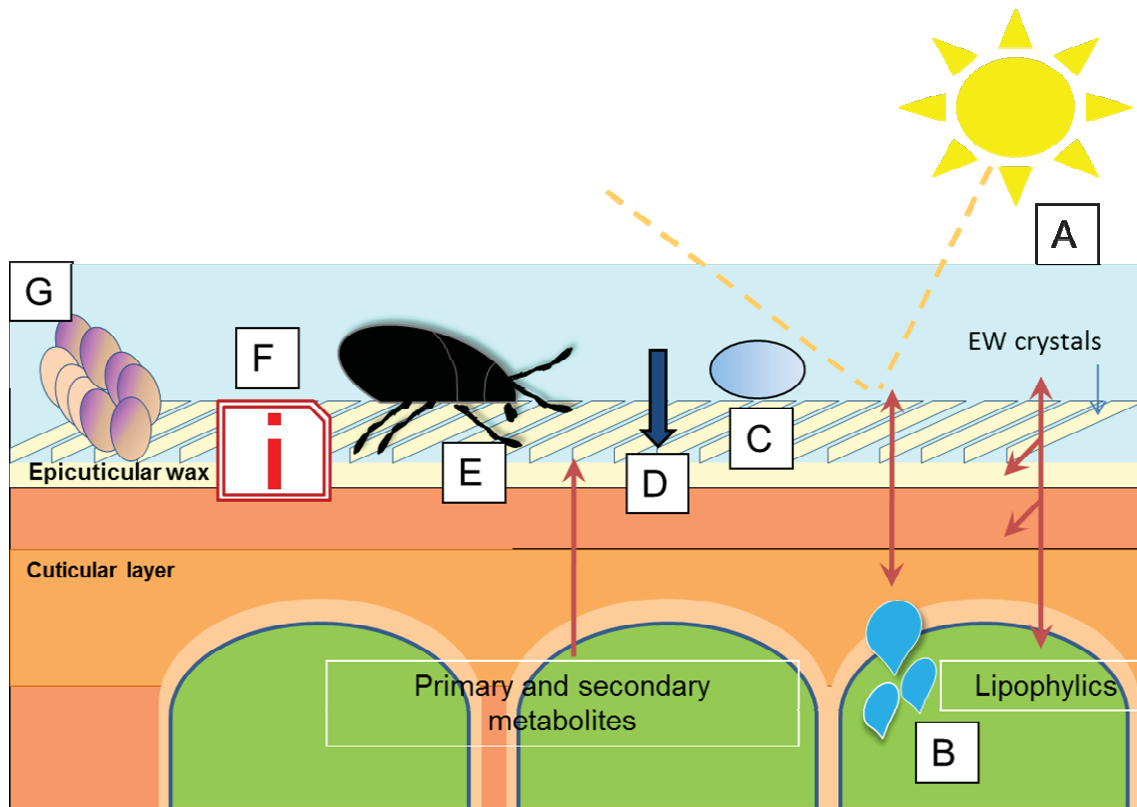


Fig. 2 Functions of leaf surface (A) Reflectance, transmittance, and absorbance of solar radiation; (B) Diffusion of water and other metabolites; (C) Surface wettability, self-cleaning properties; (D) Mechanical resistance against mechanical stress and maintenance of physiological integrity; (E) Adhesion of insect legs and influences of surface characteristics on locomotion; (F) Physical and chemical cues used for host recognition by microorganisms and insects; (G) Attachment of insect eggs (or spores of microorganisms) - usually on the lower leaf surface (Müller and Riederer, 2005; Schreiber, 2005)

Many of the EW functions are the result of unique surface attributes, mainly the interplay between the surface hydrophobicity (i.e. specific chemistry) and its roughness (provided wax sculptures). Due to those joined properties, some plant species demonstrate self-cleaning mechanism (called Lotus-Effect), which allows the removal of microscopic particles, dust, spores and microbes from the leaf surface together with the water droplet (Barthlott and

Neinhuis, 1997). It is one of the phenomenon of nature that has been widely explored in order to develop biomimetic self-cleaning surfaces (Bhushan et al., 2009). In addition, development of microbes like phytopathogenic bacteria or parasitic fungi as well as insects' eggs deposited on the plant surface, is limited by the repellent properties of the leaf surface towards water and aqueous solutions. Furthermore, it was shown that decreased amounts of EW crystals observed in the *M. truncatula* mutant corresponds to a decrease in wax primary alcohol groups. This further leads to reduced spore differentiation of rust fungal pathogens (Uppalapati et al., 2012). Interestingly, not only epicuticular wax crystal abundance but also their arrangement plays a role: enhanced resistance to water loss or light absorption and reflection is attributed to the organization of wax crystals (Koch et al., 2010). It is therefore postulated, that those factors are actively regulated in response to environmental variations. Moreover, despite the micrometer dimensions of EW crystals, they effectively disturb insect's locomotion across the plant surface, which was demonstrated for an example in carnivorous plants, *Nepenthes* spp. The interior surface of pitchers is covered by the wax crystals and their defined structure (next to wax viscosity) hinders insects locomotion by preventing trapped insects from escaping (Gaume et al., 2002; Gorb et al., 2005).

1.4 Biosynthesis of plant waxes

The biosynthetic pathways that lead to the synthesis of wax constituents are largely known from the studies on a model plant, *Arabidopsis thaliana*. It is well known, that epicuticular waxes are synthesized in the epidermal cells and the biosynthesis of wax compounds starts from *de novo* production of long chain fatty acids (C_{16} and C_{18}) in plastids (Kunst and Samuels, 2009; Yeats and Rose, 2013). Those precursors are exported to the endoplasmic reticulum (ER), where they are extended to the VLCFAs (C_{20} – C_{34}). The biosynthesis of wax components includes two main pathways, one leads to the production of primary alcohols that also serve as precursors for wax esters, the second gives rise to alkanes, aldehydes, secondary alcohols and ketones.

Transport of cuticular precursors from the epidermal cells to the leaf surface is a process that requires involvement of at least three different mechanisms. The first is an intracellular transport from the ER to the plasma membrane, the second involves continuation of this process and export of EW components across the cell wall, and finally transport to the leaf surface.

Studies over past years largely contributed to understanding of some of those processes. There is convincing evidence supporting the involvement of an ATP-binding cassette (ABC) in the trafficking of wax compounds across the plasma membrane (Buda et al., 2013; Panikashvili and Aharoni, 2008). It was also demonstrated that all ABC transporters belong to the ABCG subfamily (McFarlane et al., 2010). Although strong genetic evidence supports those findings, confirmation of such substrate specificity by *in vitro* experiments is still missing. Nevertheless, those studies largely contribute to our understanding of the first stage of wax transport. There are also studies enriching our knowledge about the next stage. When highly hydrophobic wax molecules cross the plasma membrane, they need to be transported through a hydrophilic environment of the polysaccharide cell wall. It has long been proposed that lipid transport proteins (LPTs) are engaged in this process (DeBono et al., 2009). Specific properties of those proteins, like their small size, solubility and capability to bind various lipids *in vitro* make them promising candidates. Furthermore, it was shown that their expression is increased during the cuticle development, and *Arabidopsis* mutants that were disrupted in one of those proteins (glycosylphosphatidylinositol - anchored LTP - GLTP) exhibited a reduced amount of alkanes on the plant surface (Lee and Suh, 2012). The final stage, the transport of lipophilic wax constituents through the cell wall to the leaf surface is very poorly understood and is still matter of debates (Kunst and Samuels, 2009; Yeats and Rose, 2013). Thus, despite efforts of many decades, many enigmatic questions about the biosynthesis and transport of cuticular wax compounds remain to be resolved.

1.5 Relevance of sampling methods in the leaf surface studies

The plant surface in many reports was studied without the required selectivity of sampling protocols. EWs have been extensively studied mainly by extraction procedures based on organic solvents (Bianchi et al., 1989; Inyang et al., 1999; Lin et al., 1998; Shepherd et al., 1995; Tsumuki et al., 1989; Tulloch, 1973), where leaves were dipped in organic solvents for different time periods. This procedure however, regardless of immersion duration, yields also intracuticular waxes, which are embedded within a cutin layer. Organic solvents simultaneously penetrate all layers of the cuticle and dissolve not only intracuticular waxes. When stomata are open diverse metabolites from the inner leaf tissue are washed to the surface as well (Reifenrath et al., 2005; Riederer and Schneider, 1989). The required selectivity for the surface studies was first accomplished through application of mechanical isolation protocols. A collodion silver – nitrocellulose polymer, served as an adhesive to

peel-off the wax film (Haas and Rentschler, 1984). However, since the presence of organic solvent was still required (for polymer dissolution), the method was further developed by Jeffree (1996), who used frozen glycerol to transfer surface waxes onto an artificial target. Further modification came from the microscopic studies of epicuticular crystals (Ensikat et al., 2000) and chemical analysis of epicuticular waxes, which employed frozen water as a transfer medium (Jetter et al., 2000). For mechanical probing of the surface waxes, gum arabic (a mixture of polysaccharides and arabinogalactanproteins) may be implemented as an adhesive as well (Gniwotta et al., 2005b; Guhling et al., 2006). Despite of some limitations, it is so far the only reported method that enables *in vivo* experiments, for instance wax regeneration studies (Jetter and Schäffer, 2001).

It is worth to add, that despite the first reports about the differentiation of cuticular waxes into intracuticular waxes and EWs came from the middle 1980s (Haas and Rentschler, 1984) and appropriate sampling techniques were employed since the middle 1990s (Jeffree, 1996), there are still inconsistencies in many reports. The literature terminology concerning leaf surfaces or EWs may be misleading, since EWs are often described as soluble cuticular lipids (SCL), which does not discriminate cuticular waxes. Similarly, terms such as ‘leaf surface’ or ‘surface lipids’ are implemented in studies where organic solvent extraction is applied. Further risk of contamination with the metabolites from the inner tissue increases, when the leaf tissue is cut into discs and subsequently immersed in organic solvent (for instance in hexane for 50 min) (Steinbauer et al., 2004). Recent studies showed, that the selection of an optimal sampling technique is the most critical step when studying the plant surface chemistry (Reifenrath et al., 2005; Städler and Reifenrath, 2009). Glucosinolates, well known feeding stimulants for specialist herbivores were assigned to leaf surface location. This assumption was made when finding this class of compounds in the extracts after leaf immersion in organic solvents (Griffiths et al., 2001; Hopkins et al., 1997; Loon et al., 1992). However, application of highly selective isolation procedures - mechanical wax removal, showed actually the absence of these compounds on the EW layer (Reifenrath et al., 2005). Mechanical wax removal also proved chemical differentiation between the intra and epicuticular waxes (Jetter et al., 2000).

Thus, in the present study, special emphasis was devoted to the selection of most appropriate sampling techniques, optimal for each objective of the study.

1.6 Implemented techniques for chemical imaging studies

The main innovation of the present study is to combine highly selective sampling methods with a variety of powerful techniques such as GC-MS (gas chromatography – mass spectrometry), SEM (scanning electron microscopy), FT-IR (Fourier transform infrared) and Raman microspectroscopy, MALDI-TOF-MS (matrix assisted laser/desorption ionization time-of-flight mass spectrometry) and TOF-SIMS (time-of-flight secondary ion mass spectrometry). All those tools provided complementary information allowing the investigating the leaf surface in a comprehensive manner.

Mass spectrometry is a powerful and standard analytical technique used in a wide range of research disciplines: chemistry, biology, biochemistry, medicine. This method separates ionized particles (atoms, molecules) in respect to their mass to charge ratio (m/z) and can provide not only qualitative, but also quantitative information (Murayama et al., 2009).

GC-MS is a technique of first choice when analyzing the chemical composition of bulk cuticular waxes or selectively isolated epicuticular waxes (Buschhaus et al., 2007; Markstadter et al., 2000; Riederer and Schneider, 1989). Studies aiming at the characterization of a variety of morphological structures present on the leaf surface employed SEM (Baker and Holloway, 1970; Meusel et al., 1994; Wen et al., 2006). Also AFM (atomic force microscopy), which provides higher spatial resolution than SEM, is used to study subtle processes taking place on the leaf surface, for instance wax regeneration or self-assembly processes (Koch et al., 2009c). Nevertheless, GC-MS obviously lacks spatially resolved information and surface specific information. SEM as well as AFM allow studying topographical microstructures without providing required molecular information.

Since one of the main goals of the study was to analyze local distribution of surface compounds, a wide range of imaging techniques providing chemical selectivity was employed: MALDI-TOF-MS, TOF-SIMS imaging and FT-IR as well as Raman spectroscopy imaging. They require minimal sample preparation, and traditional sample staining with dyes or fluorescent labels is eliminated. They are non-invasive, thus samples are not modified throughout the measurement neither structurally nor chemically (the exception is MALDI-TOF-MS where application of matrix is necessary). Furthermore, a single measurement generates sets of spectra that provides molecular profile and information about the distribution of many compounds/class of compounds simultaneously. It is next significant advantage over traditional imaging techniques like immunohistochemistry, based on staining,

labeling or use of specific antibodies. All those advantages has opened up their application to the biological studies. A broad range of compounds was successfully characterized by those techniques, for instance peptides, proteins, plant metabolites or drugs (Barron et al., 2005; Kaspar et al., 2011; Salzer and Siesler, 2009; Svatoš, 2010). The spatial resolution which could be achieved and the chemical specificity strongly depends on the applied imaging techniques and the type of sample as well as investigated molecules.

1.6.1 Vibrational spectroscopic imaging techniques

FT-IR and Raman spectroscopy belong to the most powerful vibrational spectroscopic techniques. They are based on the detection of vibrational signatures of chemical bonds present in the molecules. Energies equivalent to those vibrations and the corresponding wavelengths of the detected signals are specific to defined chemical groups present in the molecule. However, vibration energies of the other chemical groups may overlap and not all vibrations are detectable in both techniques. Consequently, those techniques do not enable identification of single compounds in complex biological samples without the complementary information for example from the mass spectrometry (MS) or nuclear magnetic resonance spectroscopy (NMR). Nevertheless, they offer invaluable chemical information, for instance detection of structural alterations in the proteins, presence of hydrogen bonding as well as monitoring of changes in the chemical profile of the biological material. Therefore, they became attractive analytical tools also in plant science (McCann et al., 1992; Schulz and Baranska, 2007; Schwanninger, 2007). Imaging variances of those techniques offer all the advantages of molecular imaging tools, nevertheless, they are mainly applied in medicine (Lasch et al., 1998; Nallala et al., 2012; Steiner and Koch, 2009).

Coherent anti-Stokes Raman Scattering (CARS) microscopy is another technique that was implemented in this study. CARS is a four-wave mixing process in which a pump beam and a Stokes beam interact with a sample generating a strong anti-Stokes signal, when the resulting frequency matches the frequency of a Raman active molecular vibration. The CARS signal is enhanced in comparison to a spontaneous Raman scattering signal, since Stokes and anti-Stokes signals are emitted coherently. CARS offers chemical contrast without the staining and is a particularly useful tool in biomedical applications. For instance, in imaging tumors in brain tissue by making use of the differences in the lipid density between tumor tissue and healthy tissue (Evans and Xie, 2008). CARS microscopy has been also successfully used *in vivo* (Nan et al., 2006).

1.6.2 Mass spectrometry imaging techniques

Mass spectrometry imaging delivers specific molecular information by providing m/z values of detected ions. Wide range of molecules from the complex samples can be analyzed in a direct and simultaneous manner in a single run. The resulting MS images represent the spatial intensity distribution of defined m/z values, which correspond to the certain compounds. This technique is not limited to the predefined compounds, since any ion detected in the mass spectrometer can be used for an image generation.

MALDI-MS imaging is at present the most widely employed molecular imaging technique applied in bio-analytical chemistry and biomedicine. The mechanism of ion formation is still not fully understood, but it is well known that a crucial role is played by matrix. Its addition serves several purposes (1) extraction of analytes from the sample surface, (2) co-crystallization with the analyte and (3) absorption of laser energy. Most experiments are performed on the spatial resolution of 50 – 200 μm (Benabdellah et al., 2010). Although some procedures like oversampling or solvent-free sublimation matrix application aim to improve the resolution in MALDI imaging, this technique is still placed behind the TOF-SIMS.

TOF-SIMS offers nanometer scale spectral resolution, it is the only available mass spectrometry imaging technique with the potential to visualize distribution of analytes (particularly multiple lipid species) on a cellular and subcellular level (Fletcher et al., 2007; Passarelli and Winograd, 2011a; Winograd, 2005). Traditionally SIMS was employed mainly in analysis of inorganic materials, especially in inorganic surfaces and material science, for semiconductor materials and polymers. In those studies, monoatomic ions such as Ga^+ , Cs^+ , Au^+ , Ar^+ with the capability of high spatial resolution down to 100 nm were employed. However, low sensitivity and a high degree of molecular fragmentation hindered analyses of organic materials. Advances in instrumentation, particularly the introduction of cluster ion beams and TOF analyzers allowed to overcome those drawbacks and opened this technique for the analysis of complex organic molecules (Griffiths, 2008; Winograd, 2005). Cluster ion sources consist of multiple atoms, for instance Bi_3^+ , Au_3^+ , and also C_{60}^+ and SF_5^+ . They have capabilities to lift intact molecules off the surface without inflicting physical and chemical damage during the bombardment process. Consequently, cluster ions reduce sample perturbation, enhance ion yield, and improve the mass range of detection and sensitivity for heavier analytes. Extension of the detected mass range is a consequence of the higher energy

and ion currents characteristic for larger primary ions. Among the various ejected from the surface particles are secondary ions (atoms, molecular fragments, and clusters) and also neutrals that are not detectable by MS.

Although this fact limits the detection and imaging of low abundant molecules, effective ionization in SIMS is achievable without matrix employment. Matrix dissolved in organic solvents and deposited on the sample surface may lead to analyte diffusion (Amstalden van Hove et al., 2010).

Furthermore, tandem MS allows structure elucidation and is presently available for SIMS as well. Major contributions into this advance come from the Winograd group, who has introduced C₆₀ SIMS hybrid-quadrupole orthogonal-TOF-MS with the tandem-MS capabilities (Carado et al., 2008) and the Vickerman group, who has constructed C₆₀ reflectron-TOF-based instrument with the MS/MS mode (Hill et al., 2011).

1.7 Biological system

The most comprehensive studies on plant leaf surfaces were performed on a garden plant, *Prunus laurocerasus* L., commonly known as cherry laurel (Jetter et al., 2000; Perkins et al., 2005). Black cottonwood, *Populus trichocarpa* (Torr. & Gray) on the other hand, is an economically and ecologically important plant and the first long-lived tree that has been sequenced, becoming nowadays a model plant (Bradshaw et al., 2000; Brunner et al., 2004; Taylor, 2002). Nevertheless, knowledge about the leaf surface represented by EWs of this model species is not available, neither chemical characterization, nor its role in the interaction with herbivorous insects. Research on other *Populus* species is very scant as well, and only studies without spatial discrimination were conducted (Alfaro-Tapia et al., 2007; Cameron et al., 2002; Lin et al., 1998). Other works, for instance on *Populus tremuloides* Michx. were limited to the determination of changes in the EW structure without chemical characterization (Mankovska et al., 2005). Scant knowledge about *Populus trichocarpa* is a consequence of the fact that it is a woody plant, therefore its cultivation is demanding. Furthermore, many available reports about this model species are conducted on the field plants. In the present study, plants were cultivated in the growth chambers in order to provide constant environmental conditions crucial for the leaf surface studies.

For the experiments aiming the investigation of the leaf surface role in plant – insect interaction, specialist herbivores were selected. *Chrysomela populi* L. is the most abundant

leaf beetle belonging to the Chrysomelidae family and is a serious forest pest. These leaf beetles are characterized by the high requirements for food quality and a narrow host range, feeding on species of the Salicaceae family. The average period of their activity is limited to a few months during the year (May – September) (Urban, 2006).

The *Populus trichocarpa* - *Chrysomela populi* model system represents a naturally occurring interaction between the host plant and the specialist herbivore, thus, the role played by the compounds on the leaf surface as well as wound-induced processes are particularly interesting.

Furthermore, in contrast to a model plant species in molecular biology, *Arabidopsis thaliana*, the leaf surface of *Populus trichocarpa* provides relatively thicker and homogenous EW imprint (not disturbed by the long and dense trichomes). Therefore, application of molecular imaging techniques that aim scanning leaf surface area and determining local distribution of epicuticular wax constituents was feasible.

So far no studies that combine selective mechanical sampling methods with preservation of the two-dimensional distribution of compounds and high spatial resolution imaging techniques have been reported for any plant species.

1.8 The main objectives of the study

- (1) Chemical characterization of *Populus trichocarpa* leaf surface represented by epicuticular waxes (EWs) using optimal sampling methods and complementary analytical techniques.
- (2) Analysis of the role of *Populus trichocarpa* leaf surface in the host-recognition process of the specialist herbivore *Chrysomela populi*.
- (3) Optimization of molecular imaging techniques such as FT-IR and Raman microspectroscopy as well as MALDI-TOF-MS and TOF-SIMS for leaf surface studies.
- (4) Analysis of the wound-induced processes on the *Populus trichocarpa* leaf surface after *Chrysomela populi* feeding by FT-IR microspectroscopy.
- (5) Characterization of the local distribution of leaf surface constituents using high resolution TOF-SIMS imaging.

2. Chapter II Epicuticular waxes of *Populus trichocarpa*: their chemistry and role in the host recognition process of the leaf beetle *Chrysomela populi*

2.1 Introduction

Terrestrial plants through the evolution have developed fundamental for their survival structure – a cuticle. It covers all aerial plant organs and provides plant's integrity in the constantly altering environment. The most outer cuticle layer represented by EWs consists of a complex mixture of highly lipophilic compounds, therefore significantly enhances plant's impermeability to water as well as to apoplastic solutes. It is present in all plant species which proves its pivotal function. Although leaf surface of many plant species are extensively studied using variety of methods, to date, there are no reports about the actual leaf surface - isolated selectively epicuticular waxes of *Populus trichocarpa*. It is a model plant species and the first sequenced woody plant (Tuskan et al., 2006), nevertheless its chemistry and role in the host plant recognition have not been studied yet. Present study aims to fill the existing gap.

2.2 Results and discussion

2.2.1 Chemical characterization of the *Populus trichocarpa* leaf surface

In order to characterize the chemical composition of epicuticular waxes (EWs) in a selective way, the cryo-adhesive method was applied (Ensikat et al., 2000). The strength of this method is that frozen water acts as a glue (Jetter et al., 2000) and allows mechanical isolation of EWs (**Fig. 3**). Thus, contamination originating from the inner leaf tissue as well as from any external additives is effectively eliminated. Chemical analysis of EWs were performed by GC-MS, which is the most commonly applied technique in insect or plant cuticular wax analysis. In addition, matrix-assisted laser desorption/ionization (MALDI) time-of-flight (TOF) mass spectrometry was applied. The advantage of this technique is its capability to detect high molecular mass compounds, for example wax esters. Ionization of these wax constituents was achieved through application of a LiDHB matrix, which combines the commonly used 2,5-hydroxybenzoic acid and a cationization reagent (Li^+). LiDHB mediates laser energy absorption and gives high ionization efficiency even for highly nonpolar compounds like hydrocarbons (Cvačka and Svatoš, 2003; Kühn et al., 1996). The drawback

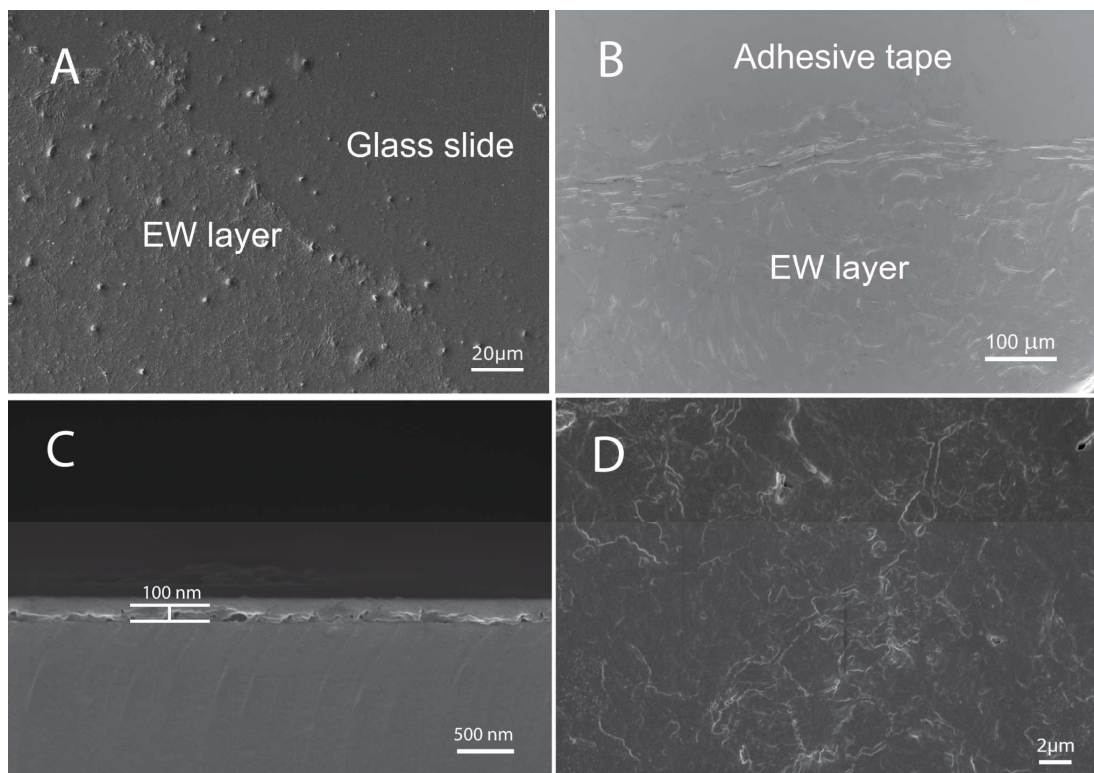


Fig. 3 SEM micrographs of *P. trichocarpa* EWs from the adaxial leaf surface isolated using cryo-adhesive (**A**) and adhesive tape embedding method (**B**). EWs create a thin layer (100 - 300 nm) (**C**) and form continuous amorphous covering without pronounced structures, also wax crystals are absent (**D**), and therefore they may be classified according to Barthlott et al. (1998) as a smooth layer.

of matrix application is the presence of its signals in the spectrum below 250 Da, therefore the detection of low molecular mass compounds by MALDI-TOF-MS is not recommended.

Positive ion MALDI-TOF-MS spectra $[M+Li]^+$ from the adaxial leaf surface of *P. trichocarpa* leaves showed three characteristic homologue series of alkanes, alcohols and esters with the chain length from C_{16} to C_{54} (**Fig. 4**, **Fig. 6A, B**). Their mass analysis compared with the standards, previously published data (Cvačka and Svatoš, 2003; Vrkoslav et al., 2010) as well as GC-MS data reinforced assignments of detected ions. For an example, a signal in the MALDI-TOF-MS profile with m/z value of 429.50 is in accordance with the molecular mass calculated for $C_{30}H_{62}Li$ (429.50) (**Table 1**). This compound was also found in the GC-MS spectra, where comparison of the specific fragmentation pattern and the retention time with the standard allowed its identification. MALDI-TOF-MS appeared to be particularly valuable technique in detecting long chain alcohols and esters with the high molecular masses (up to 795 Da). GC-MS on the other hand, was necessary to detect low

molecular mass homologues as well as unsaturated alkanes and fatty acids (**Fig. 5, Fig. 6C, D**). Further support of compound assignments was provided by the spectroscopic analysis; FT-IR spectrum showed presence of C=O, C-O and O-H vibrations in the frequency ranges corresponding to esters and alcohols (**Fig. 21, Table 4** Chapter III, section 3.2.1). In addition to saturated components, unsaturated wax constituents (C_{25} , C_{27} , and traces of C_{29}) were also detected. Identification of unsaturated alkanes was reinforced by very specific fragmentation pattern under electron impact (EI) conditions (**Fig. 7**). The presence of unsaturated wax esters with the m/z decreased by 2Da comparing with the saturated wax esters was suggested by the signals observed in the MALDI-TOF-MS spectrum (**Fig. S3**). In order to achieve better overall image of surface waxes of *P. trichocarpa*, abaxial (lower) side of leaves was also investigated applying the same, selective isolation method. EW covering the abaxial side of the leaves were significantly poorer in variety of compounds, among more polar compounds only fatty acids C_{16} and C_{18} were present, alcohols were not detected (**Fig. 8**). This stays in opposite to composition of the adaxial side, where significant percentages of wax

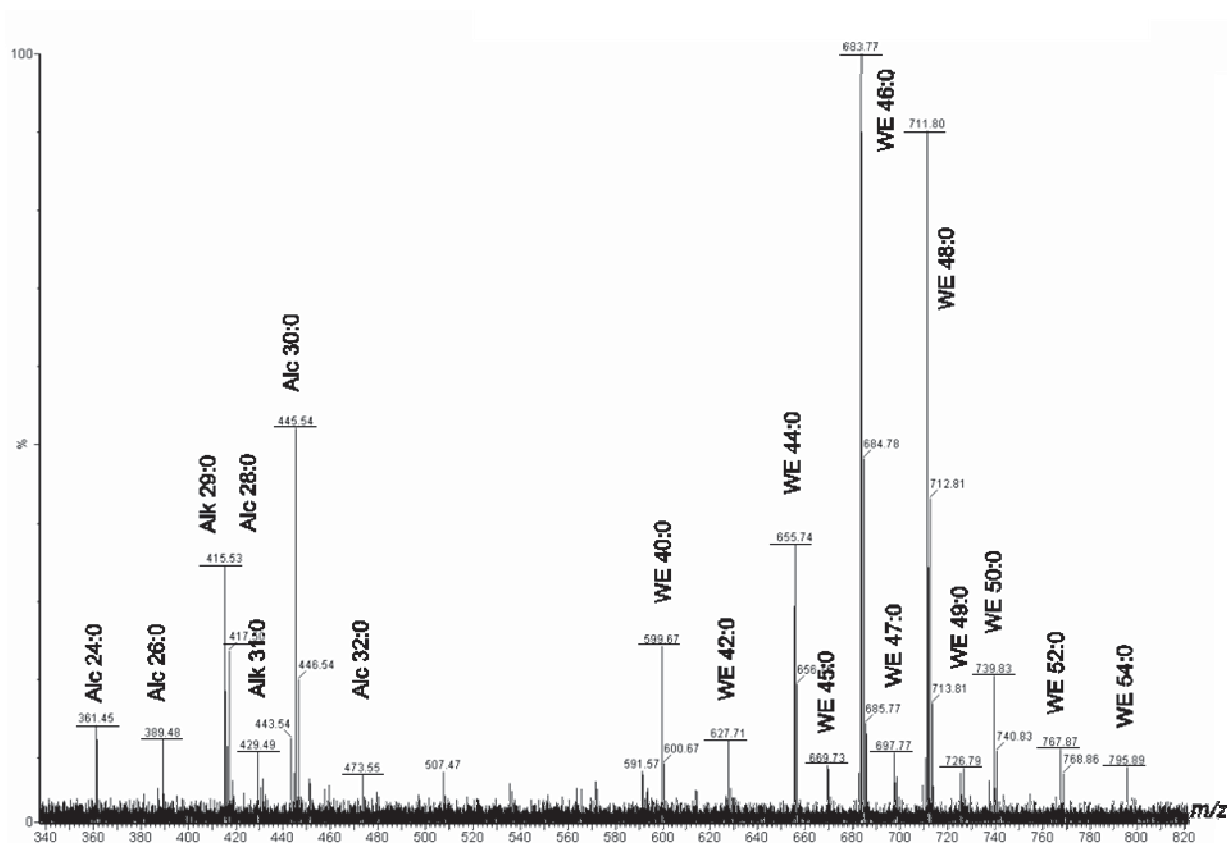


Fig. 4 MALDI-TOF-MS spectrum of EWs isolated from the adaxial side of *P. trichocarpa* leaves using cryo-adhesive isolation method; Alk - alkanes, Alc - alcohols, WE - wax esters.

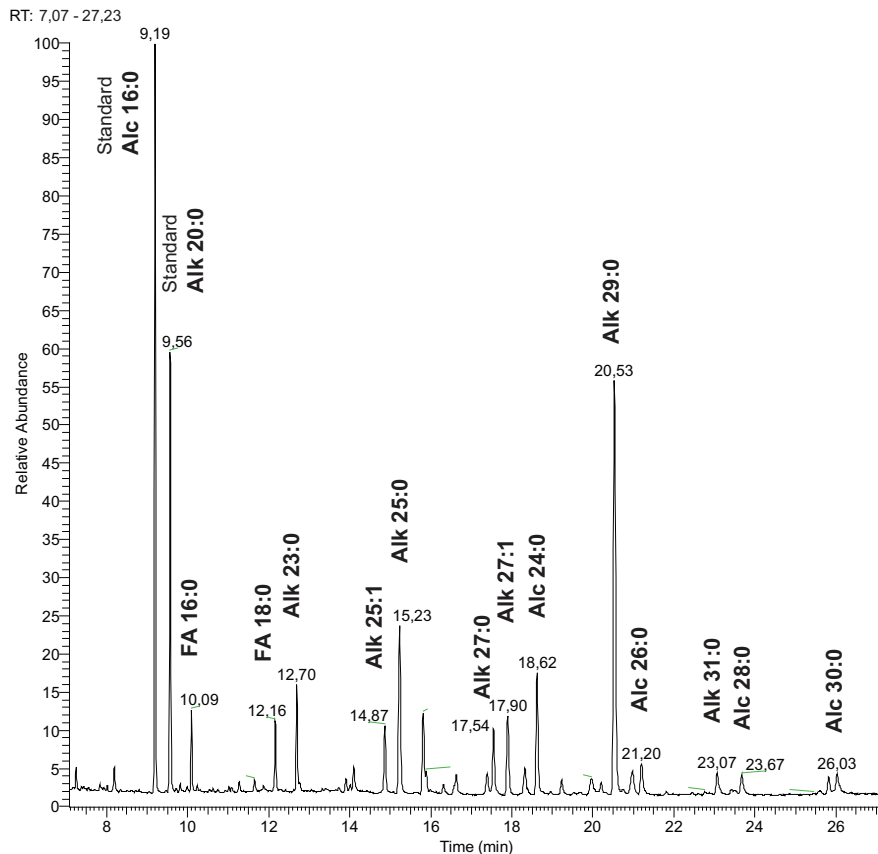


Fig. 5 GC-MS chromatograms (EI) of EWs isolated from adaxial side of *P. trichocarpa* leaves using cryo-adhesive method; DB-5 column. FA – Fatty acids, Alc – Alcohols, Alk – Alkanes.

constituents were long chain alcohols and esters. On the other hand, the level of saturated and unsaturated alkanes was higher comparing to the adaxial side. Abaxial surface of *P. trichocarpa* is thus richer in hydrocarbons, which stays in accordance with the many other plant species reported (Gniwotta et al., 2005a; Jetter et al., 2000; Smith and McClean, 1989).

Although MALDI-TOF-MS and GC-MS provided complementary information with the overlapping regions, direct comparison of quantification results (**Fig. 6, Table S1**) will lead to mismatches due to the varying ionization mechanisms of both techniques. Among all compounds detected by GC-MS in surface waxes of *P. trichocarpa*, the most abundant were saturated alkanes (**Fig. 6 C**), whereas MALDI-TOF-MS with the capability to detect high molecular mass compounds, indicated predominance of wax esters and alcohols (**Fig. 4, Fig. 6 A, B**). Nevertheless, both techniques showed a chain length distribution favoring odd-numbered homologues within alkanes, and even-numbered carbon chain within alcohols (**Fig. 6 A, D**). Additionally, they showed predominance of nonacosane (C₂₉) within alkanes.

Other aliphatic compounds - wax esters detected only by MALDI, also exhibited predominance of even-numbered homologues and C_{46:0} was found to be the most abundant ester (Fig. 6 B, D).

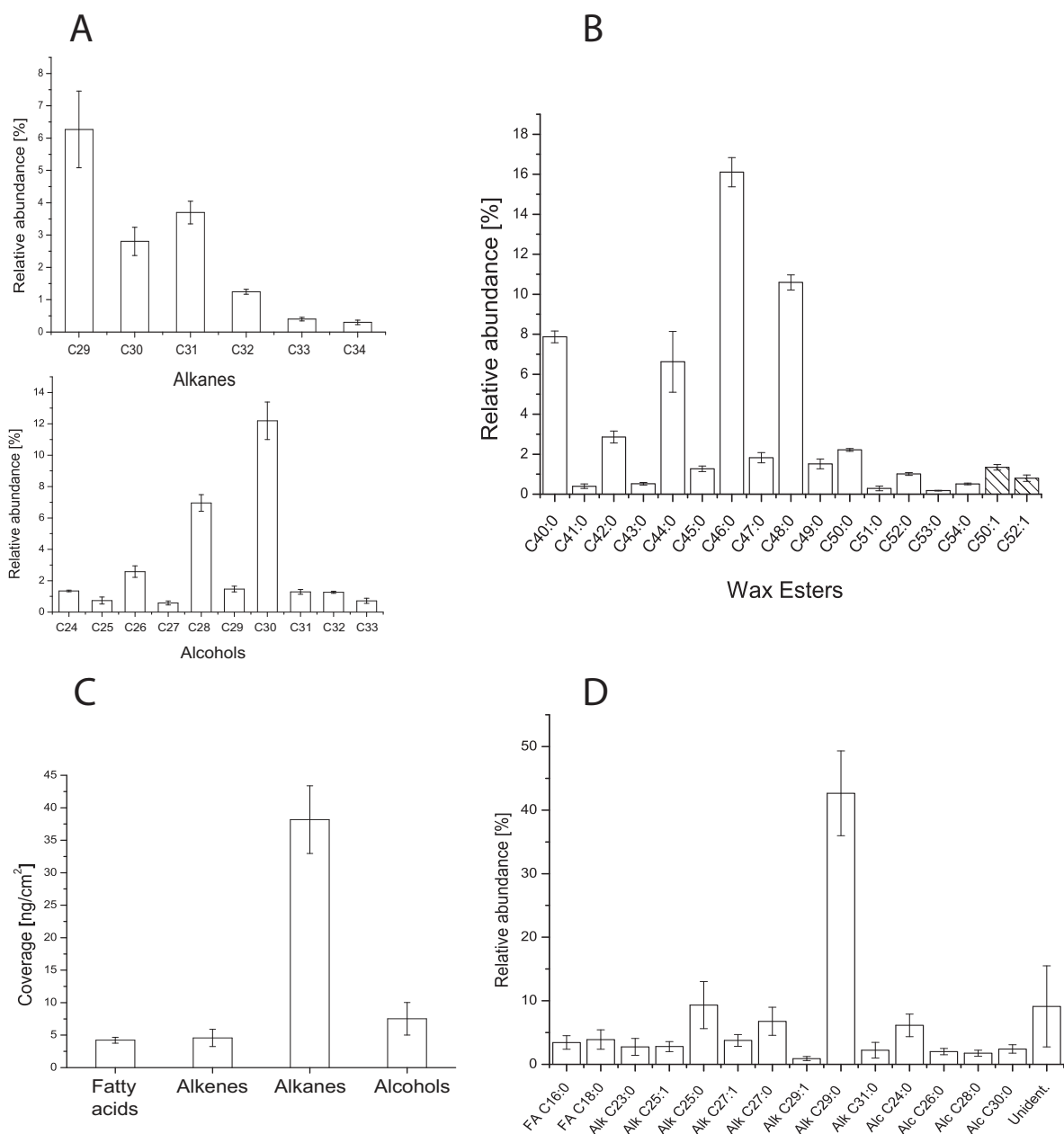


Fig. 6 Composition and chain length distribution of compounds in the EWs isolated from the adaxial side of *P. trichocarpa* leaves using cryo-adhesive method. Relative abundance of individual homologues [%] detected by MALDI-TOF-MS within alkanes and alcohols (A), wax esters (B). Coverage of compound classes [ng cm⁻²] (C) and relative abundance of individual homologues [%] detected by GC-MS (D). FA – Fatty acids, Alc – Alcohols, Alk – Alkanes. The coverage and relative abundance is a mean value ± S.D., n=6.

[M+⁷Li⁺] theor.	[M+⁷Li⁺] detected	Mass difference [mDa]	Assigned sum formula
361.4022	361.4570	54.85	C₂₄H₅₀O
389.4335	389.4753	41.88	C₂₆H₅₄O
415.4855	415.5356	50.17	C₂₉H₆₀
417.4648	417.5088	44.08	C₂₈H₅₈O
429.5012	429,509	7.85	C₃₀H₆₂
443.5168	443.5261	9.37	C₃₁H₆₄
445.4961	445.5371	41.12	C₃₀H₆₂O
459.5117	459.537	25.30	C₃₁H₆₄O
473.5274	473.5636	36.25	C₃₂H₆₆O
599.6318	599.6818	50.03	C₄₀H₈₀O₂
627.6631	627.715	51.90	C₄₂H₈₄O₂
655.6944	655.7461	51.77	C₄₄H₈₈O₂
669.7101	669.7516	41.62	C₄₅H₉₀O₂
683.7257	683.7775	51.80	C₄₆H₉₂O₂
697.7414	697.778	36.65	C₄₇H₉₄O₂
711.757	711.8121	55.17	C₄₈H₉₆O₂
725.7727	725.8095	36.85	C₄₉H₉₈O₂
739.7883	739.8455	57.20	C₅₀H₁₀₀O₂
767.8196	767.8746	55.07	C₅₂H₁₀₄O₂
795.8509	795.9095	58.60	C₅₄H₁₀₈O₂

Table 1 Comparison of detected by MALDI-TOF-MS *m/z* values with the theoretical masses of assigned sum formula.

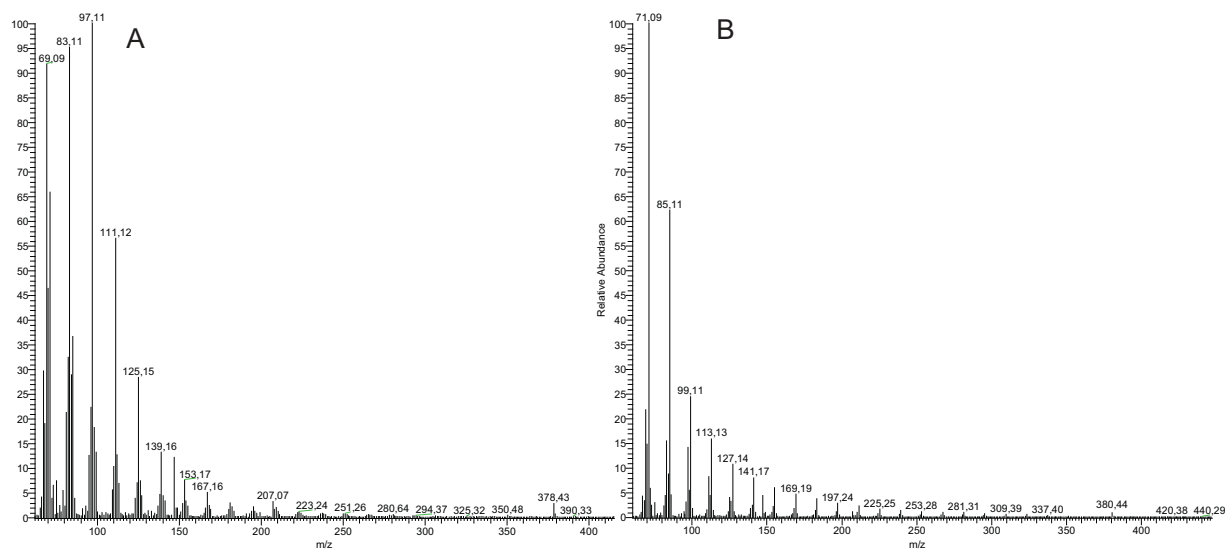


Fig. 7 MS spectra of *P. trichocarpa* EWs (adaxial side). Fragmentation pattern for unsaturated - heptacosene $C_{27:1}$ (A) and saturated alkane - heptacosane $C_{27:0}$ (B). EI quadrupole detector, DB-5ms column.

In the previous studies where EWs were selectively isolated and analyzed by GC-MS, alkanes were also shown to be the most dominant class of compounds in *Brassica oleracea* (Eigenbrode and Jetter, 2002) or *Prunus laurocerasus* (Jetter et al., 2000). However, the dominance of particular groups varies and strongly depends on the investigated plant species as well as its developmental stage and environmental conditions. For example in *Secale cereale* dominating compounds were alcohols (Jetter and Schäffer, 2001; Ji and Jetter, 2008) whereas aldehydes were predominant in the surface waxes of *Nepenthes alata* pitchers (Riedel et al., 2003).

As underlined in the introduction, knowledge about the chemical composition of EWs from other *Populus* species is scant. In the available report on *Populus* species hybrids (*P. deltoids* x *P. nigra* and *P. nigra* x *P. maximowiczii*), bulk samples of cuticular waxes from 3 year old field-grown plants were acquired by solvent extraction without any distinction between the abaxial and adaxial leaf surface (Cameron et al., 2002). Nevertheless, in accordance to results acquired for *P. trichocarpa* in the present study, the most prominent compounds were odd-numbered alkanes and even-numbered alcohols. Dominance of triacontanol (C_{30}) and nonacosane (C_{29}) within those compound classes could be determined. In addition, authors reported also presence of unsaturated alkanes, however in minor amounts and their

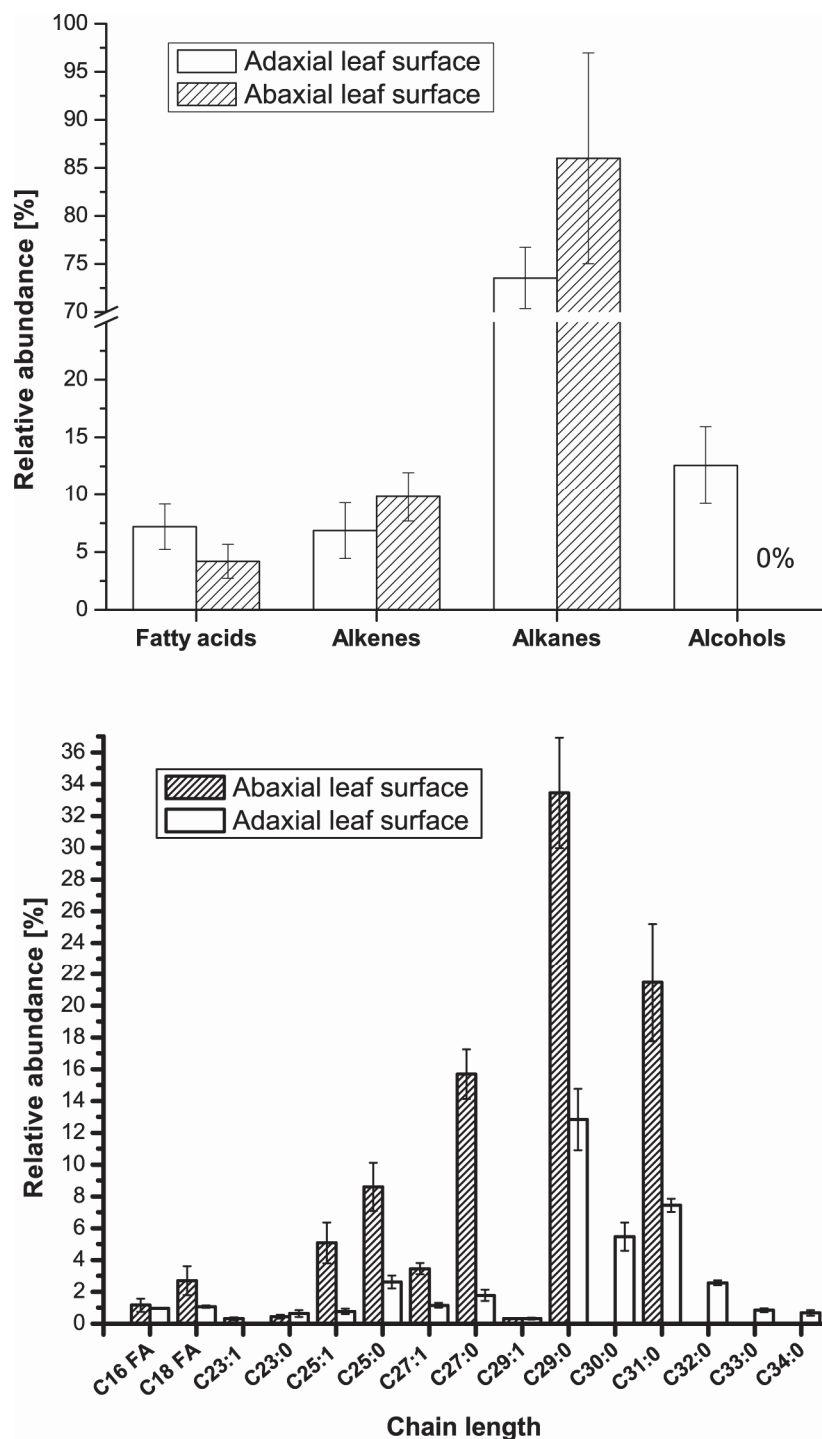


Fig. 8 Composition and chain length distribution of compound classes in the EWs isolated from abaxial and adaxial side of *P. trichocarpa* leaves using cryo-adhesive method and GC-MS. The relative abundance [%] is a mean value \pm S.D., n = 6.

chain length was not determined. In contrast to the present study, wider range of fatty acids (C₂₀ - C₃₀), narrower range of alcohols and alkanes (below C₃₁) was detected. Furthermore,

detection of esters and relative abundance of even-numbered alkanes and odd-numbered alcohols was not investigated.

Through combining the strength of two analytical techniques, MALDI-TOF-MS and GC-MS, more comprehensive and complete knowledge about the chemical compounds present on the leaf surface of *Populus trichocarpa* was acquired. Major chemical classes of aliphatic compounds as well as their chain length is similar to the chemical profiles commonly present in waxes of diverse plant species (Kunst and Samuels, 2003). However, wax esters, which are omitted in many studies on cuticular waxes (Cameron et al., 2002; Jetter et al., 2000; Kosma et al., 2009), were in the present study directly detected by MALDI-TOF-MS. Furthermore, the distinguishable wax components are very long chain unsaturated alkanes, which were detected in minor concentrations, and possibly unsaturated wax esters. All these highly lipophilic constituents determine the primary role of the EW layer, namely its barrier function in the plant-environment interface.

2.2.2 Method development for *in vivo* EW isolation

As a consequence of the most outer location, EW layer forms the first contact zone for any biotic interaction, including herbivores and therefore, they are considered to provide chemical cues in the host recognition process. Previous studies on *Populus* species (*P. deltoids* x *P. nigra*) indicated that the leaf surface chemicals induce feeding in the leaf beetle *Chrysomela scripta* (Lin et al., 1998). However the method for sampling the surface compounds was based on organic solvent extraction. Thus in the present study, selective sampling methods were applied to answer the question if EW layer of *Populus trichocarpa* serves specialist herbivores – *Chrysomela populi* in their process of host plant recognition by employing a selective and optimal sampling method.

For the first time a method for a selective and *in vivo* isolation of EWs was introduced in 2001 by Jetter and Schäffer. It is based on the aqueous suspension of gum arabic (Jetter and Schäffer, 2001) and was employed in behavioral bioassays in previous studies (Blenn et al., 2012). Although it is so far the only available method that fulfils the requirements necessary for *in vivo* leaf surface analysis, it carries several drawbacks. The isolation of EWs with gum arabic is a time consuming procedure and requires coverage of the leaf with a polymer suspension for 1-2 h, depending on the applied thickness and air humidity. Furthermore,

during this time period, the influence of abiotic stress like reduced gas exchange, water transpiration (particularly when both leaf sides are covered by the polymer) or light access, and their influence on plant fitness need to be considered as well. Application of this method for removal of EWs from the abaxial side encounters additional obstacles (due to the liquid state of the polymer) and is practically impossible in case of experiments on the field. Moreover, wax material collected on opaque polymer peels is invisible to the naked eye. The employment of SEM to visualize isolated material may encounter further obstacles if the wax layer is very thin and lack wax crystals, as in the case of *P. trichocarpa* (**Fig. 3**). Inhomogeneous coverage due to leaf surface repellency towards the aqueous polymer suspension, and residues of the polymer remaining on the leaf surface are additional disadvantages of the method. To overcome all these methodological drawbacks, that appeared to be important for the model plant investigated, a new *in vivo* method called adhesive tape embedding was developed. Method evaluation addressed all criteria that need to be fulfilled when studying selectively the role of EWs in the interaction with herbivorous insects in behavioral bioassays.

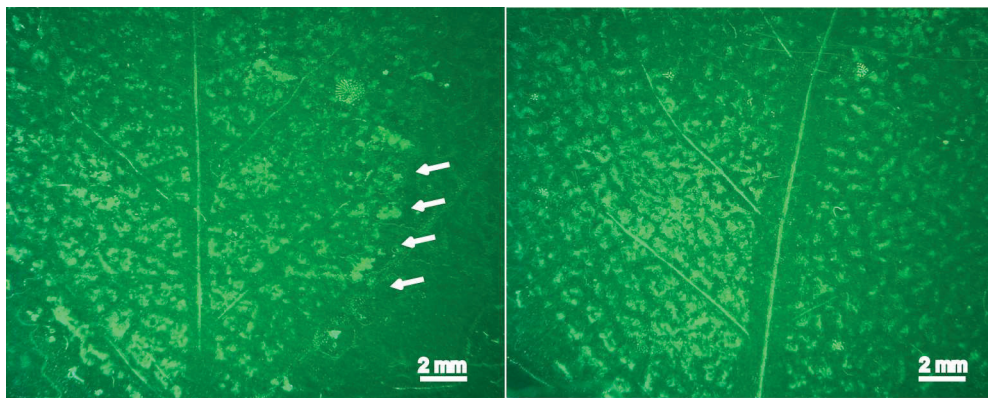


Fig. 9 EWs isolated *in vivo* from the *P. trichocarpa* leaves using adhesive tape embedding are visible by naked eye. Arrows indicate boarder between the clean adhesive tape and the isolated wax layer.

The new method is based on mechanical removal of EWs with the help of commercially available transparent adhesive tape. It fulfills requirements for high selectivity and *in vivo* applicability. Isolated EWs, in opposite to the gum arabic approach, create a visible by naked eye imprint on the adhesive tape surface (**Fig. 9**). Furthermore, the selectivity was microscopically examined in terms of any mechanical damage that could appear on the leaf

tissue after removal of its surface compounds. This aspect was very relevant, since any mechanical removal-based method may cause microscopic mechanical damages of the plant tissue and its repercussions may potentially have an influence on the insect feeding preference. The presence of perturbation of morphological surface structures was already reported for gum arabic method (Buschhaus and Jetter, 2011). Examinations under light microscope showed no disturbances to the epidermal cells. Similarly, no differences were observed considering trichome density in the comparison to the control leaves (**Fig. 10**). In order to achieve even higher resolution and differentiate single trichomes, high resolution SEM analyses were performed. Series of SEM micrographs were generated and leaves after treatments with an adhesive tape, gum arabic and control were compared. The majority of trichomes stayed intact even after six subsequent treatments with a fresh adhesive tape, which was comparable with the single gum arabic treatment (**Fig. 11**). Thus, adhesive tape embedding exhibits better performance considering that aspect. The removal of only single trichomes from the treated leaf area is particularly relevant, since trichomes belong to one of the defense arsenals naturally present on the leaf surface (Philippe and Bohlmann, 2007). Consequently, in course of the leaf surface treatment, they need to be preserved. Further advantages of the adhesive tape embedding method lay in the fact, that the time required for isolation is limited to few minutes. Moreover, the problem of coverage inhomogeneity and the polymer residues that remain on the surface is completely eliminated. The removal of EWs from the adaxial side is equally efficient as for the abaxial side. The method is versatile and can be applied not only to variety of plant organs (fruit, shoots) and variety of plant species (it was successfully tested in *Prunus laurocerasus*, *Armoracia rusticana*, and *Phaseolus lunatus*), but also for non-invasive and selective removal of insects' cuticular waxes. The procedure is particularly promising for field experiments and can be optimized for each application individually.

Additionally, the adhesive tape can also serve as a sample target, since it provides an elastic but flat surface before and after the treatment. After isolation of EWs, the sample can be directly analyzed by SEM or AFM (atomic force microscopy) without further preparation. It opens new applications in studies that focus on EW morphology, for instance wax crystals. It is however not recommended for chemical analysis, since PVC and adhesive material will contaminate the sample, thus, direct quantitative and qualitative chemical data about the selectivity and efficiency of wax removal are not provided.

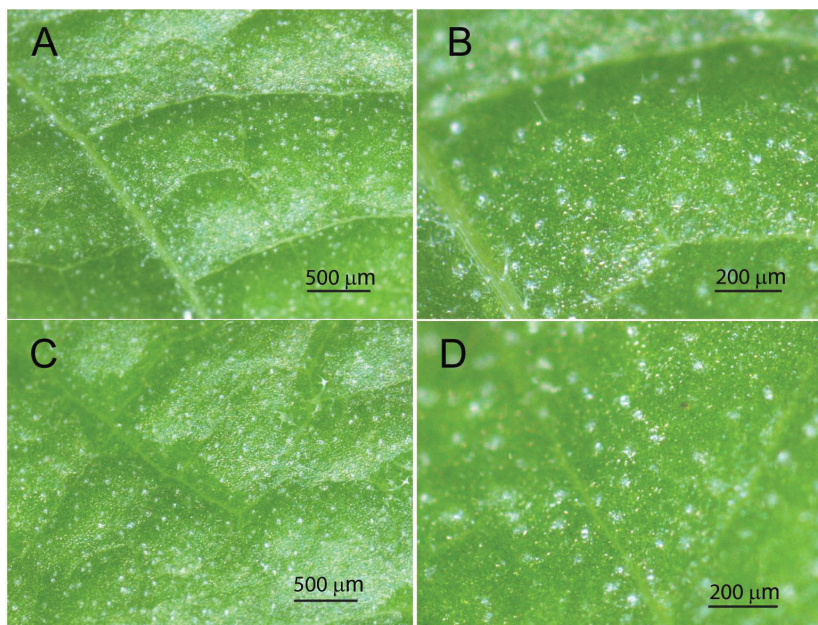


Fig. 10 *P. trichocarpa* leaves (adaxial side) after *in vivo* removal of EW layer using an adhesive tape embedding (6 subsequent treatments) show, that the trichome density of treated leaves (**A, B**) is comparable with the control leaves (**C, D**).

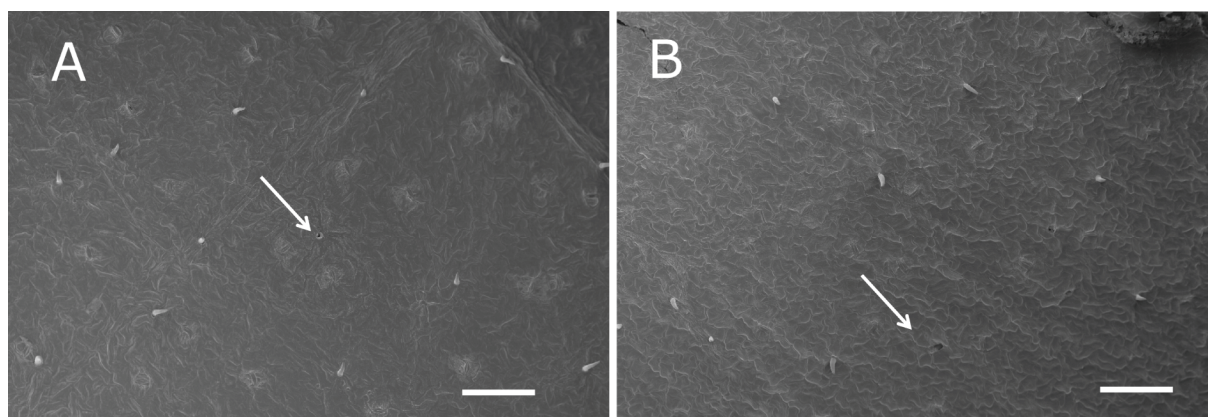


Fig. 11 SEM micrographs of *P. trichocarpa* leaves (adaxial side) after *in vivo* removal of EW layer using an adhesive tape - 6x treatments (**A**) and gum arabic - 1x treatment (**B**). After 6 subsequent treatments with an adhesive tape, only single trichomes were damaged, comparable with single gum arabic treatment. Arrow indicates damaged trichome found on the leaf surface. Scale bar: 100μm.

Nevertheless, EWs were removed by the three available methods: (1) adhesive tape embedding (2) gum arabic treatments and (3) cryo-adhesive. The remained intracuticular waxes (IW) were extracted using organic solvent. Chemical analyses of IW acquired from all methods were compared and results show, that adhesive tape embedding gives satisfactory

performance (**Fig.12**). It is worth to underline, that method based on mechanical removal of EW layer must be at the same time soft enough to leave the surface structures (trichomes) possibly intact. Considering that aspect, the adhesive tape embedding fulfills that crucial requirement.

Overall, the newly developed method allows to preserve the subtle spatial discrimination that exists between different cuticle layers and to remove EWs selectively. It allows *in vivo* application as well as simple handling, provides reproducibility, and lacks many drawbacks known from the previously established methods. Therefore it could be successfully applied in the behavioral experiments.

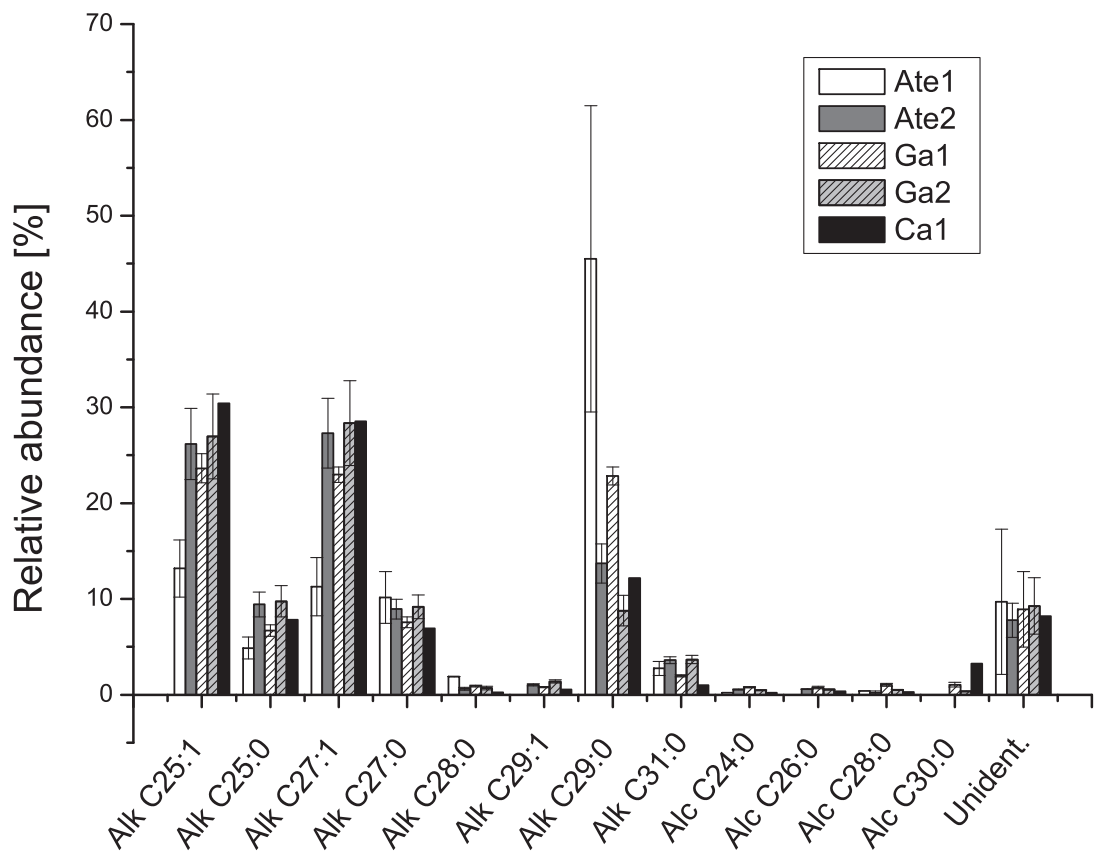


Fig. 12 Chemical composition of cuticular waxes (mainly intracuticular waxes) remained after removal of EWs. Comparison of different sampling methods: adhesive tape embedding (Ate), gum arabic (Ga) and cryo-adhesive (Ca). Alk – alkanes, Alc-alcohols. The number (1) indicates first immersion in organic solvent, the number (2) indicates the second immersion.

2.2.3 The role of *Populus trichocarpa* epicuticular wax layer in the host plant recognition

In order to investigate the role of *Populus trichocarpa* EWs in the plant-insect interaction, particularly in the host plant recognition, behavioral studies with a specialist herbivore, the leaf beetles *Chrysomela populi* were conducted. Due to their adaptation, these insects feed only on a very narrow range of host plants from the Salicaceae (Termonia et al., 2001). Consequently, involvement of the surface compounds in the host recognition process is particularly interesting. EWs were selectively removed *in vivo* using either the method based on adhesive tape embedding or, for comparison, gum arabic treatment. Subsequently, dual choice experiments were performed where the leaf beetles could choose between treated and untreated leaves of *P. trichocarpa*. It is worth to note, that each leaf pair was selected from the same plant from the opposite sides of the stem, thus morphological features as well as developmental stage of both leaves was as similar as possible. Furthermore, beetles were not starved between the experiments and were constantly supplied with *P. trichocarpa* foliage.

Behavioral bioassays based on feeding preference of beetles clearly indicated that insects preferred de-waxed over intact leaves ($P < 0.05$) (**Fig. 13, Fig. 14**). The same preference was observed when EWs were isolated with the adhesive tape embedding ($P < 0.05$) as well as with the gum arabic method ($P < 0.05$). Among 65 independent experiments performed, beetles were selecting de-waxed leaf over control in 49 cases. Preference towards de-waxed leaves was particularly strong when older (7-8 weeks) leaves were chosen as an experimental pair ($P < 0.001$) (**Fig. 13B**). Similar results were obtained in bioassays performed entirely *in vivo*, where leaves after EW isolation were not detached from the plants and were offered to the insects (**Fig. 15**).

Insect's preference was not directed by the absence of trichomes, since only single trichomes were removed in the process of EW isolation, which was carefully investigated during the method development. Although removal of even single trichomes did not contribute to better insects' locomotion, it represents a mechanical damage, which may have further consequences in the plant-insect interaction. Interestingly, many reports have shown that mechanical damage in fact increases the resistance to insect herbivores, which was also shown for the flea beetles, *Phyllotreta cruciferae* (Chrysomelidae family) (Palaniswamy and Lamb, 1993).

Considering all the advantages of the applied method and setup of performed bioassays, it can be concluded that removal of EWs caused significant higher attraction of *C. populi* towards de-waxed leaves.

There are two implications of the acquired results, both correlated with the functions that are assigned to EWs. The observation that leaves of host plant are recognized by specialist leaf beetles despite removal of EWs (from the adaxial and abaxial surface) suggests that those compounds do not play a decisive role in the host recognition process of *C. populi*. Thus, assignment of EW components to serve as chemosensory cues that determine host recognition could not be confirmed in the present study. Secondly, removal of EWs appeared to be in fact a beneficial factor that influenced leaf beetles' behaviour and directed their preference towards de-waxed leaves.

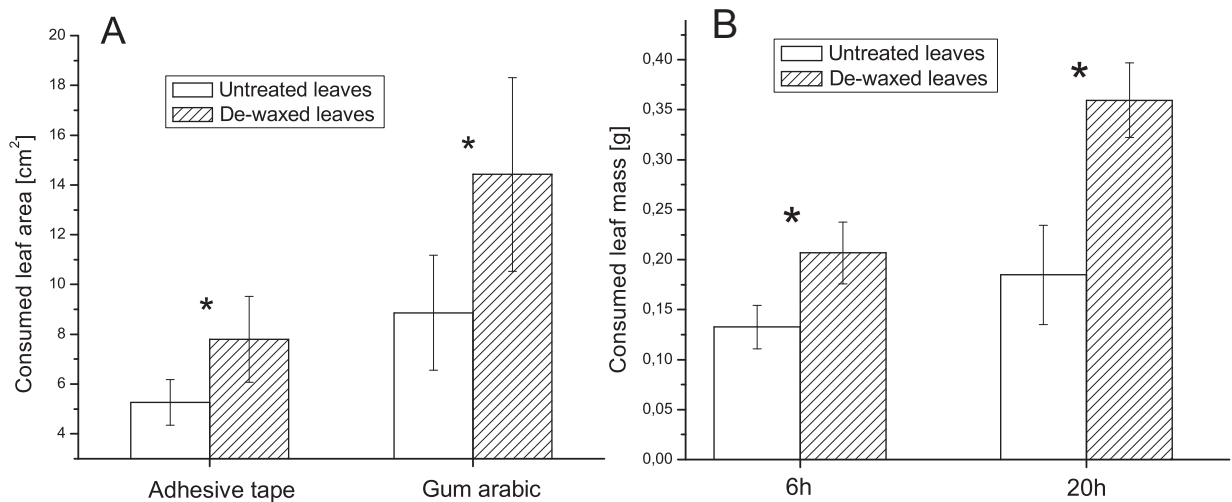


Fig. 13 Feeding preference bioassay: *C. populi* and *P. trichocarpa*. Consumed leaf area after *in vivo* EW removal using adhesive tape embedding (mean ± S.D.; n = 26, $P < 0.05$) and gum arabic method (mean ± S.D.; n = 13, $P < 0.05$) (A). Consumed leaf weight for older leaves (ca. 7-8 weeks old) after given time using adhesive tape embedding (mean ± S.D.; n = 26, $P < 0.001$) (B). Asterisks indicate significant difference determined by paired *t*-test.

As a consequence, other aspects of EW involvement in the plant-insect interaction need to be considered; their plausible role as (1) deterrent compounds, (2) mechanical barrier limiting leakage of actual chemosensory cues (e.g. volatiles from the inner leaf tissue) and/or (3) their role in hindering insects' attachment and locomotion. These aspects were explored in the available literature and will be shortly discussed.

Fig. 14

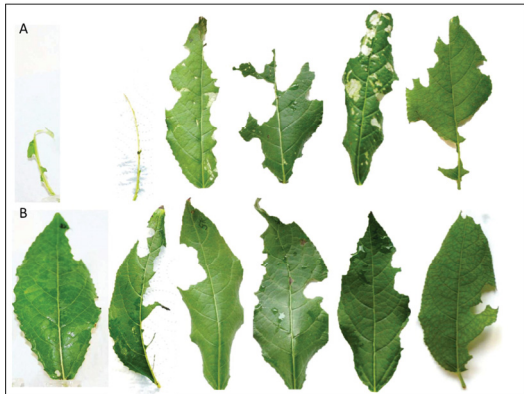


Fig. 15

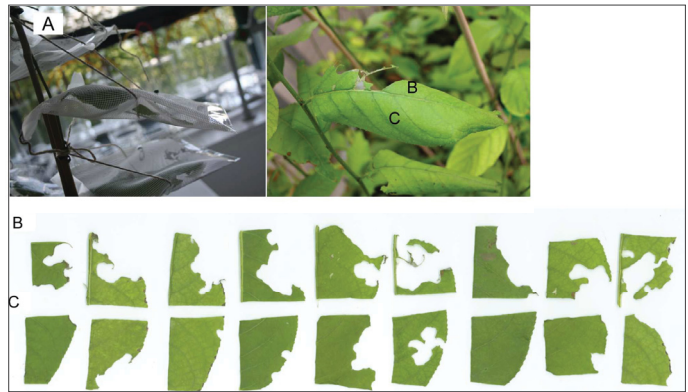


Fig. 14 Feeding preference bioassay, *in vivo* isolation of EWs from the adaxial side of *P. trichocarpa* leaves performed with an adhesive tape embedding. Insects preferred de-waxed leaves (A) over intact leaves (B).

Fig. 15 Feeding preference bioassay performed *in vivo*. EW removal (using adhesive tape embedding) as well as insect feeding was performed on leaves not detached from the plants ($n = 9$). Insects were trapped (A) and had a choice between de-waxed part of the leaf (B) and intact part (C).

The role of leaf surface chemicals in plant – insect interaction was investigated considering their phagostimulatory or deterrent effects on insects (Chapman and Bernays, 1989). The most commonly employed approach in those studies was extraction of surface compounds after leaf immersion in organic solvents. Extracts prepared in that way were subsequently applied onto an artificial surface (paper filter) and used in behavioral experiments; eventually insects' bites were compared with the solvent-treated controls. Phagostimulatory effect of bulk leaf surface extracts was reported for instance in *Poa annua* that induced *Locusta migratoria* feeding (Bernays et al., 1976) or in *Lycopersicon esculentum* that stimulated *Manduca sexta* feeding (de Boer and Hanson, 1988). There were also efforts to discriminate individual compounds or classes of compounds that stimulate feeding. Among compounds indicated to exhibit those properties are long chain alkanes C_{21} - C_{25} and C_{30} - C_{36} from *Artemisia menetriesi*, alkanes C_{28} and C_{29} from *Pyrrhalta humeralis*, and alkanes C_{31} - C_{40} and acids C_{24} - C_{26} from *Galerucella vittaticollis* (Adati and Matsuda, 1993). Primary alcohols also belong to this group, e.g. C_{26} and C_{28} from *M. alba* (Mori, 1982) and C_{22} - C_{30} from *Populus* (*P. deltoids* x *P. nigra*) (Lin et al., 1998).

On the other hand, surface extracts were also shown to induce deterrence in several herbivorous insects investigated on host and non-host plants (Chapman and Bernays, 1989; Yang et al., 1993). *Spodoptera frugiperda* were developing more rapidly when larvae were

fed on corn, *Zea mays* foliage with removed cuticular waxes. In studies on *Sorghum bicolor* and its pest, *Locusta migratoria*, deterrent effects were attributed to p-hydroxybenzaldehyde, n-alkanes (C₁₉, C₂₁ and C₂₃), and ester fractions found in cuticular wax extracts (Woodhead, 1983). Interestingly, alkanes C₁₈ - C₂₈ showed neither deterrent nor phagostimulatory effects.

It is worth to note, that apart from non-selective sampling methods applied in those studies, many compounds postulated to stimulate feeding belong to ubiquitous wax constituents present in many plant species (Kunst and Samuels, 2003). For example, studies on *Populus* and a specialist leaf beetle, *C. scripta*, assigned this role to even-numbered alcohols ranging from C₂₂ to C₃₀ (Lin et al., 1998). Compounds playing a role as chemosensory cues in the process of host recognition are expected to be species-specific, particularly in the case of specialist insects.

Recent studies on Brassicaceae species demonstrated that employing selective isolation methods (based on adhesive properties of gum arabic) is a crucial prerequisite for determining the involvement of leaf surface components in the plant-insect interactions (Reifenrath et al., 2005; Städler and Reifenrath, 2009). These authors proved that the surface wax layer of *Brassica napus* and *Nasturtium officinale* lacks feeding stimulants for the beetle *Phaedon cochleariae*. Moreover, similarly to our study, insects preferred de-waxed over intact leaves. Thus, the postulated function of EW layer is related to its protective role by providing a mechanical barrier limiting leakage of actual information about the host plant. As previously reported, plant volatiles play an essential role in the host recognition process of beetles from the Chrysomelidae family (Fernandez and Hilker, 2007; Kendrick and Raffa, 2006; Kühnle and Müller, 2011). These compounds emitted by the plants provide olfactory cues and attract insects. For instance, the leaf beetle *Agelastica coeruleae* was shown to clearly distinguish between leaf odors from the nine different Betulaceae species (Park et al., 2004). Poplar also produces volatile secondary metabolites (Kendrick and Raffa, 2006; Philippe and Bohlmann, 2007) and as one of few plant species, emits high quantities of isoprene and monoterpenes. Those distinctive volatiles together with the other secondary metabolites may potentially mediate host finding behavior (Schnitzler et al., 2010).

Removal of highly hydrophobic EW layer could have improved insects' access to the characteristic blend of volatile compounds, which consequently could have directed their preference towards de-waxed leaves. Support for this hypothesis can be found in the extensive studies of Schönherr on transport mechanisms through the plant cuticle, where

among all cuticle constituents, cuticular waxes (which include EWs) were proven to be responsible for the barrier properties of cuticles (Schönherr, 1976; Schönherr, 2006).

Further experiments would be required in order to back up this hypothesis, since alternative scenarios in which the enhanced release of volatiles after EW removal overrides the role of EW compounds as chemical cues are also plausible. Those investigations, however, need to address crucial issues like application of the additional EWs onto the intact leaf surface, which is challenging due to (1) the necessity to dissolve EWs in organic solvents, (2) coverage homogeneity, and (3) adequate concentration of EW compounds. Careful consideration of all those aspects is necessary for a factual interpretation of the results. For instance, stimulating effects of the leaf surface extracts have increased with the increasing concentration, however higher concentrations than those naturally occurring, resulted in the opposite feeding response of *M. sexta* larvae (de Boer and Hanson, 1988).

In the present study, the relevant aspect which may also contribute to the insects' behavior is impact of surface waxes on insects' attachment and locomotion. Involvement of EWs in those processes was extensively investigated in various systems (Eigenbrode and Espelie, 1995). Support of presented results – attraction of leaf beetles to the de-waxed leaves could be found in the studies performed on plants characterized by reduced amounts of epicuticular lipids (*Brassica napus*, *Brassica oleracea*, *Pisum sativum*, *Hordeum vulgare*). Those glossy plants were more susceptible to insect attacks (Bodnaryk, 1992; Eigenbrode et al., 2000; Stoner, 1990; Tsumuki et al., 1989). A similar result was obtained for another chrysomelid beetle, *P. cochleariae* (Stork, 1980), which preferred the glossy phenotype of *B. oleracea*. Certainly, it must be mentioned that opposite results such as an increased resistance of glossy phenotypes to insect infestation have been also reported (Eigenbrode and Espelie, 1995; Stoner, 1990). Nevertheless, in some of those studies experiments were conducted in the field and thus influence of predators (and also their improved attachment and thus higher activity) needs to be considered as well.

2.2.4 Localization of salicin

A selective sampling method is crucial not only for analysis of EW chemistry and its involvement in plant-insect interaction. It is also crucial for the determination if some plant secondary metabolites are actually located on the surface. For instance, Reifenrath et al (2005) demonstrated that glucosinolates, well known feeding stimulants for specialist insects feeding on Brassicaceae, are not located on the leaf surface as was suggested previously

(Hopkins et al., 1997), but in the inner leaf tissue. In the literature, salicin is reported as a candidate compound that influences the distribution and food selection of leaf beetles (Rank, 1994; Rowell-Rahier and Pasteels, 1989). This secondary plant metabolite primarily serves the plant for defensive purposes. However Chrysomelina leaf beetles, which includes *C. populi* have adapted this toxic compound for their own protection (Termonia et al., 2001). Salicin along with the other phenolglucosides was detected in *P. trichocarpa* leaf extracts (Palo, 1984; Pearl and Darling, 1971; Warren et al., 2003). However, organic solvent extraction was used in those studies, and hence the question if this polar compound is located on the leaf surface or located only in the inner leaf tissue is still open. In order to answer that question, the surface compounds including the EW layer from the *P. trichocarpa* leaves were isolated using the cryo-adhesive method and analyzed with LC-MS.

Salicin was not detected in the outermost cuticle layer (MDL- method detection limit: 1-10 ng), whereas it was present in the whole leaf extracts (**Fig. 16, 17**). This result suggests that salicin is located preferentially in the inner leaf tissue (below 300 nm). That further supports the results from the behavioral experiments; chemosensory cues are not present among the surface compounds. Removal of the most outer cuticle layer together with all compounds located there does not inhibit recognition of the *P. trichocarpa* by *C. populi*. That process is most probably based on perception of diverse chemicals. In addition, many other factors may influence Chrysomelina host affiliation including biogeographically, genetically, and ecologically driven factors (Fernandez and Hilker, 2007; Termonia et al., 2001).

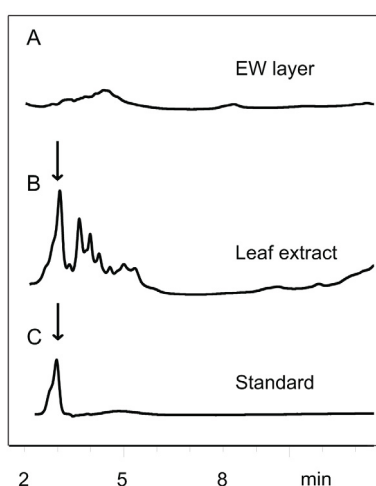


Fig. 16 LC-MS chromatograms of EW layer isolated from *P. trichocarpa* leaves by cryo-adhesive method (A), whole leaf extract (B), and standard – salicin (C). Arrows indicate presence of salicin.

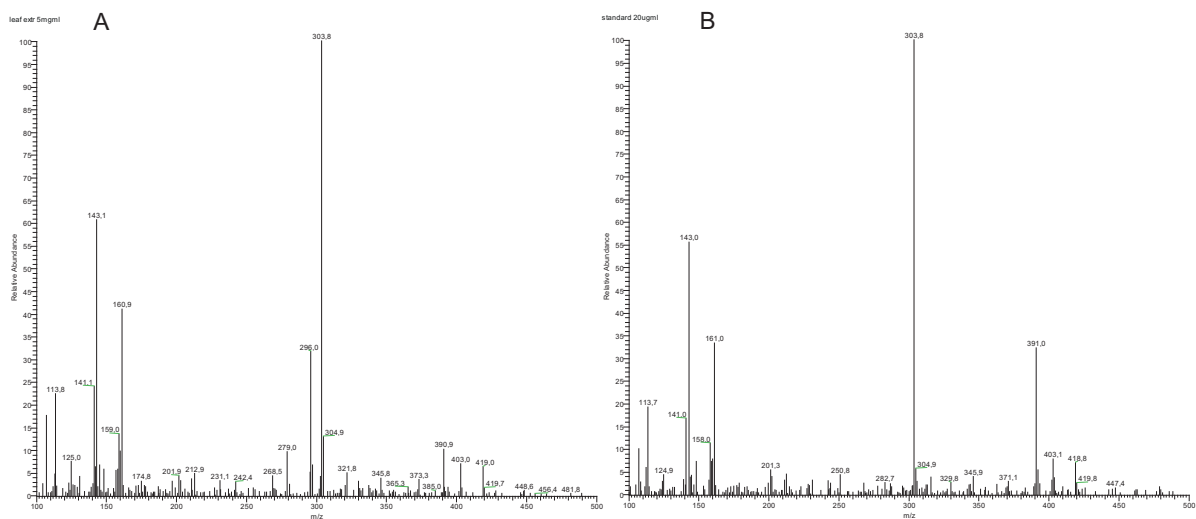


Fig. 17 MS spectra confirming presence of silicin in the whole leaves extracts of *P. trichocarpa* (A), standard (B). Silicin was not found on the leaf surface.

2.3 Conclusions

Employing selective sampling method allowed to characterize the chemical composition of *P. trichocarpa* epicuticular waxes. Besides GC-MS also MALDI-TOF-MS was employed, since this technique allowed direct detection of high molecular mass compounds characteristic for plant waxes. EWs consisted of long chain saturated (C₂₃-C₃₄) and unsaturated alkanes (C₂₅, C₂₇, C₂₉), fatty acids (C₁₆, C₁₈), alcohols (C₂₄-C₃₃) and esters (C₄₀-C₅₄). Apart from the unsaturated constituents, other main classes of aliphatic compounds present in the EWs of *P. trichocarpa* share ubiquitous chemical profile with the other plant species. Recognition of host plant by specialized herbivores is a complex process involving perception of multiple cues including unique plant secondary chemistry. Behavioral experiments with *P. trichocarpa* and its specialist herbivore, *C. populi*, demonstrated that after the removal of EWs in a selective and non-destructive way, leaf beetles were not only able to recognize their host plant but even preferred de-waxed leaves over the control. Thus, the role of EWs as decisive chemosensory cues could not be confirmed in our study. On contrary, acquired results support the hypothesis, that EWs in addition to other components of the cuticle, limit leakage of cues that would serve herbivores to identify the host plant (eg. plant volatiles). Furthermore, salicin reported by previous studies as one of the candidate compounds that may serve as a feeding signal for *C. populi*, was not found among the surface compounds, but was detected in the whole leaf extract.

The novel method – adhesive tape embedding for *in vivo* removal of EWs presented in this study is a promising alternative to reported approaches, particularly for performing behavioral bioassays. It allows removing the EW layer in a selective manner leaving surface structures such as trichomes mainly intact. Its simplicity will allow substituting methods based on organic solvent extraction and help to revise present knowledge on the role of EWs in the processes like host recognition or oviposition for other plant and insect species.

3. Chapter III Molecular imaging of *Populus trichocarpa* leaf surface

3.1 Introduction

There is a knowledge gap about the spatial arrangement of compounds on the leaf surface. Traditionally, plant tissue is investigated by prior extraction of interesting plant structures, for instance cell walls (Chen et al., 1998; Coimbra et al., 1999; Kacuráková et al., 2000; McCann et al., 1997; McCann et al., 1992; Sene et al., 1994; Toole et al., 2004) or cuticle (Villena et al., 2000). This approach involves time consuming procedures and addition of several chemicals. Furthermore, eventual purification steps are necessary, since samples may still be contaminated, for example by cytoplasmic proteins (Chen et al., 1998). As a result, information about the chemical distribution and structure are disrupted or lost.

Other approach is based on the analysis of intact plant tissue for instance with the help of FT-IR spectroscopy (Dubis et al., 1999; Lammers et al., 2009; Yang and Yen, 2002). In those experiments, influence of external chemicals is eliminated and plant can be analyzed *in situ*. However, because particular plant structures are not isolated prior the analysis, authors encounter difficulties to assess exact origin of the acquired signals. Penetration depth of an infrared beam reaches few micrometers (Salzer and Siesler, 2009), which needs to be considered in surfaces research. Plant surface usually represents thin layer; EW layer of *P. trichocarpa* is only few nanometers thick (**Fig. 3**). Thus, signals from the deeper leaf layers, cutin (ω - and mid-chain hydroxy and epoxy C₁₆ and C₁₈ fatty acids) together with intracuticular waxes (triterpenoids) and apoplast (pectins), will be recorded as well. In addition, water must be removed from the plant material, since most techniques require high vacuum (mass spectrometry) or presence of water disturbs data analysis due to its own strong absorbance in the relevant spectrum regions (IR spectroscopy).

Consequently, when investigating plant tissue one needs to make a compromise between the application of invasive procedures with more or less discriminatory potential or examination of an intact tissue. However, in both cases a severe drawback is the presence of spurious or unspecific bands in the spectrum, which originate either from the external chemical additives when applying the first strategy, or from the internal constituents choosing the second. In the

present study, in order to investigate the leaf surface in a comprehensive manner a selective sampling method that overcomes all these drawbacks was employed.

The EW layer is a mixture of compounds that share similar chemical structures. All wax constituents belong to the class of long and very long chain hydrocarbons or its derivatives. The EW layer of *P. trichocarpa* creates a thin film that tightly seals the leaf surface and is characterized by the absence of distinguishable structures (**Fig. 3**). Due to those chemical and morphological properties, a distinction of areas that could be differentiated in images either by morphological features or varying chemical compositions is rather impossible. As a result, image interpretation is a demanding process and requires high resolution techniques. Furthermore, the image interpretation provides additional challenges, since intracellular as well as extracellular transport mechanism of EWs to the leaf surface is still a matter of intense studies and many crucial questions remain open. Thus, it is not known (1) if the same traffic mechanism serves all lipophilic wax constituents, (2) what is the spatial and temporal aspect of their deposition to the leaf surface, (3) whether chemical structure i.e. chain length or chemical class determines the spatial arrangement on the leaf surface, and (4) how environmental factors (abiotic and biotic) influence the local distribution of EW compounds.

Extended and multidisciplinary studies are required to answer all those questions. By employing powerful imaging techniques such as vibrational spectroscopy and high resolution mass spectrometry imaging, the present study provides new insight into some of the processes taking place on the leaf surface and may help to answer some of those questions.

In those techniques, the molecular mass or vibrational energies are used as an endogenous label. In this way interference of potential fluorescent labels or other markers is eliminated, which leaves the investigated biomolecules functionally unmodified. Moreover, many ions or molecular vibrations can be detected in parallel, therefore chemical distribution maps can be generated for exactly the same location and the same physiological state.

The key issues in molecular imaging of biological surfaces such as spatial resolution, molecular selectivity, penetration depth, sensitivity, destructiveness and required sample modifications were taken into consideration in the present study. Simultaneously, employed tools were selected considering their capabilities to answer biologically relevant questions and the practical availability of the instruments for the routine experiments.

3.2 Results and discussion

3.2.1 Wound-induced epicuticular wax deposition on the leaf surface of *Populus trichocarpa* studied by FT-IR spectroscopy imaging

Vibrational spectroscopic imaging for *P. trichocarpa* leaf surface analysis

In order to answer the question what is the local distribution of EW compounds and what changes appear in the response to biotic stress (specialist insects feeding), vibrational spectroscopic imaging techniques were selected. To those tools belong FT-IR and Raman imaging, which have potential to provide information about the local variation of the molecular content in the examined sample. Both techniques were carefully tested considering chemical sensitivity and specificity. Although Raman measurements were performed under different experimental conditions in order to increase the detectability (by employing varying wavelengths of the operating laser), acquired spectra provided only information about the C-H and C-C vibrations, which does not allow to differentiate chemical variation of EW constituents. For an example, Raman spectra acquired with the laser operating at 532 nm, exhibit bands at the wavenumbers 2880 cm^{-1} and 2845 cm^{-1} corresponding to symmetric stretching (ν) of C-H. Deformation vibrations (δ) of CH_3 and CH_2 groups are found in the region 1465 cm^{-1} and 1420 cm^{-1} respectively. Further vibrations of CH_2 group (twisting) appear at 1296 cm^{-1} and 1170 cm^{-1} . Stretching vibrations of C-C are observed at 1135 cm^{-1} , 1060 cm^{-1} and 1032 cm^{-1} (**Fig. 18, Table 2**). The same information were acquired when using a laser excitation wavelength at 633 nm (**Table 2, Table S2**). The samples were prepared in the form of EW imprint on the ZnS sample target using the cryo-adhesive method. That sampling method could not be applied in experiments with the operating laser wavelength at 1064 nm, since higher concentration of analytes was necessary. Measurements were done for bulk samples according to protocol for GC-MS analysis. (**Fig. 18, Table S3**). Nevertheless, that approach has not enriched information available in Raman spectrum.

The second technique that was employed was CARS imaging (Coherent Anti-Stokes Raman). Although CARS was successfully employed and the resonance signals were acquired (**Fig. 19, 20**), this tool have potential to provide images visualizing distribution of only C-H and C-C vibrations.

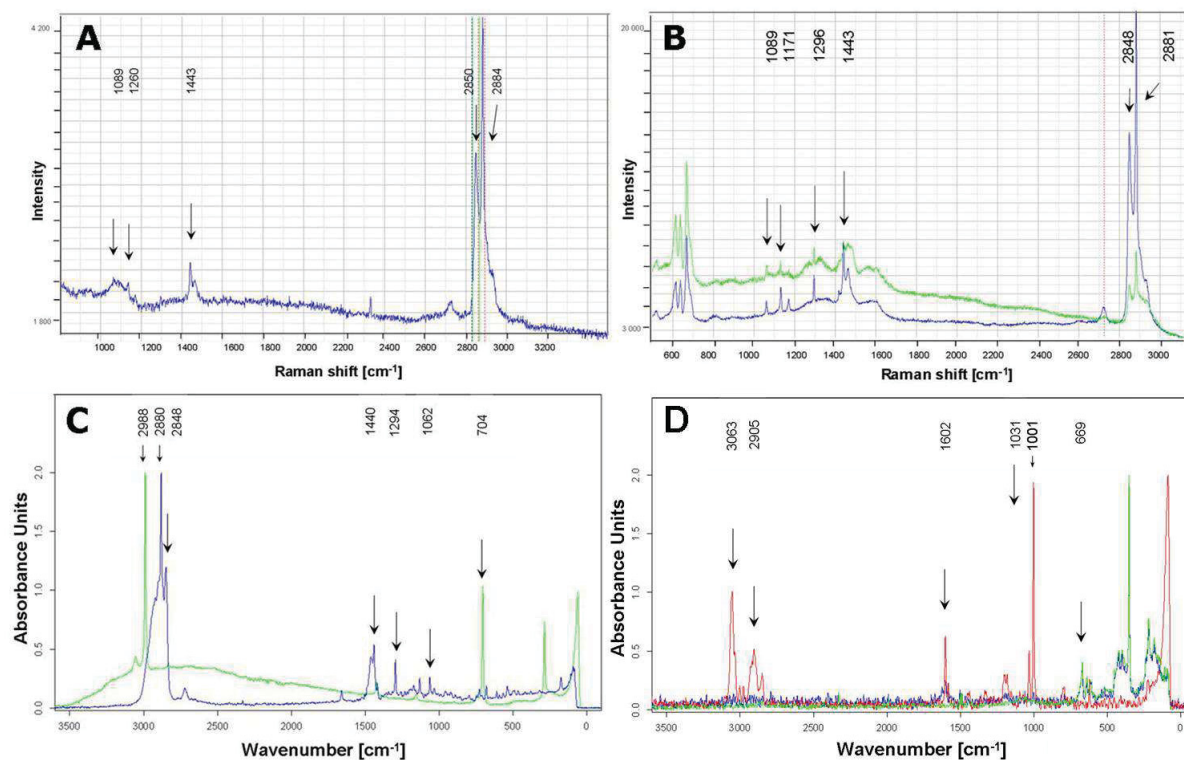


Fig. 18 FT-Raman spectra of *P. trichocarpa* EW imprint (adaxial side) on the ZnS sample target, laser wavelength - 532 nm (A), 633 nm (B, C) (Green line indicates spectrum acquired on the leaf vein, blue line - area without the veins) and 1064 nm (D). Varying colors indicate subsequent measurements.

This is due to the fact, that CARS signals appear exclusively for the vibrations that are Raman active and contribute to the strong bands. As a result, this technique did not contribute to enrichment of biologically relevant information.

Previous reports on employment of CARS in biological studies were mainly based on C-H and C-C vibrations as can be seen in the **Table 3**. Those vibrations are sufficient to differentiate lipids from proteins or to detect lipid droplets in animal tissue, but considering the chemistry of wax samples and the potential to detect more polar groups (C-O, C=O or OH present in long chain fatty acids, alcohols and esters), FT-IR appeared to be a superior technique. Furthermore, the major advantage of the Raman spectroscopy - the possibility to analyze samples containing water, did not play a role due to the sample preparation technique that was applied in the study. Investigations of processes taking place on the leaf surface after herbivore damage were eventually performed using mainly FT-IR mapping coupled with the multivariate statistical and SEM analysis.

Vibration/ Assignment	Raman shift (cm^{-1})	Relative intensity	Laser wavelength			
			1064nm imprint	1064nm imprint extract	633nm imprint	532nm imprint
v sym C-H	2880	Strong	x	√	√	√
lipids (fatty acids)	2845	Strong				
v C-H	2725	Weak	x	√	√	√
v C=O	1710-1750	Weak	x	x	x	x
v C=C	1620-1680	Medium	x	x	x	x
δ (CH_3)	1465	Weak	x	√	√	√
δ (CH_2) deformation	1440	Weak				
	1420	Weak				
t(CH_2) twisting	1296	Weak	x	√	√	√
	1170	Weak				
v C-C	1135	Weak	x	√	√	√
	1060			√	√	x
	1032			√	x	x

Table 2. Comparison of vibrations detected by Raman microspectroscopic analysis of EWs from *P. trichocarpa* imprints or imprint extracts. Symbol x and √ indicate absence and presence of given vibration respectively.

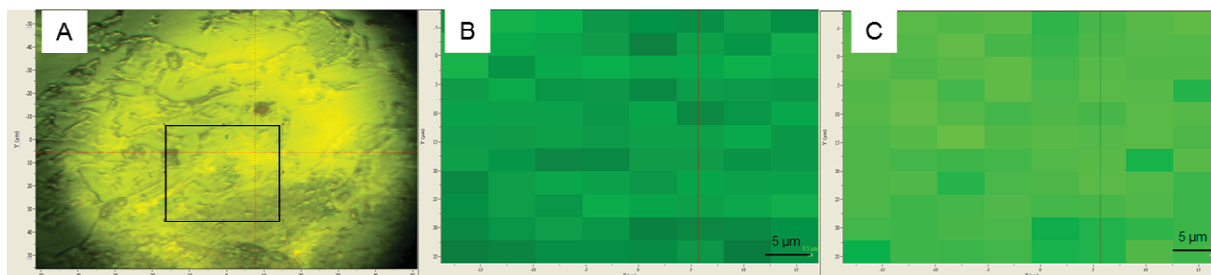


Fig. 19 Bright field image of EW imprint (A) Raman pseudo-color images at 2880 cm^{-1} (B) and at 2845 cm^{-1} (C) showing distribution of compounds containing C-H groups. Lateral resolution - $5 \mu\text{m}$.

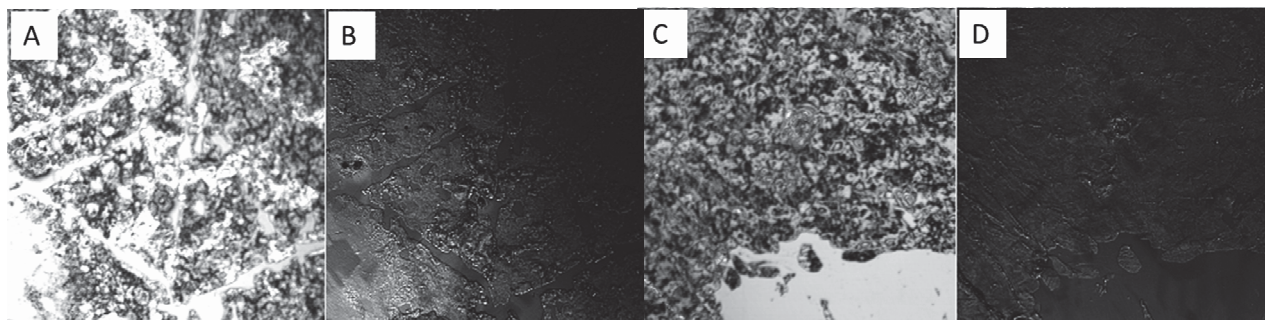


Fig. 20 Bright field images of EW imprint (A, C) and CARS images at 2848 cm^{-1} – resonant signal showing distribution of compounds containing C-H groups (B) and at 2822 cm^{-1} – non resonant signal (D).

References	Technique	Sample investigated	Vibrations detected
(Krafft et al., 2009)	CARS Raman imaging	Colon tissue, $10\ \mu\text{m}$	C–H stretching vibration 2850 cm^{-1} , 1660 cm^{-1} , 1450 cm^{-1} and 1000 cm^{-1}
(Potma and Xie, 2003)	CARS	Erythrocytes - single lipid bilayers, $2\ \mu\text{m}$	C–H stretching vibration
(Strehle et al., 2006)	Raman	Anise seeds	C–H stretching vibration
(Rinia et al., 2007)	CARS	Lipid phase transition	C–H stretching vibration
(Cheng et al., 2002)	F,E,P,C-CARS	Implementation of CARS (four different configurations) in mapping of living cells	F-CARS C–H stretching vibration
(Bergner et al., 2009)	CARS	Quantitative detection of analytes (toluen C_7H_8)	C–H stretching vibration
(Rinia et al., 2008)	CARS	Visualization of the formation and growth of LDs	C–H stretch region C-C stretch region

Table 3. Vibrations detected in various biological materials and in organic compound (toluene) using Raman and CARS microscopy. The list shows that vibrations that serve for Raman and CARS imaging belong mainly to C – H and C – C stretching mode, therefore are optimal for distinction lipids from other biomolecules (e.g. proteins), but deliver poor information considering distinction of different classes of compounds present in EWs (fatty alcohols, fatty acids, esters) with polar functional groups like O-H and C=O or C-O.

FT-IR delivered chemical specificity

The most intense bands present in the FT-IR spectrum of epicuticular waxes (EWs) are at 2917 cm^{-1} and 2849 cm^{-1} and they correspond to asymmetric and symmetric C-H stretching mode of CH_2 (methylene) groups (Dubis et al., 1999) (**Fig. 21**). These vibrations are accompanied by deformation vibration of CH_2 groups, which can be found in the fingerprint region at 1462 cm^{-1} and 729 cm^{-1} . High intensity of these bands is due to the dominance of CH_2 groups in the EW components; hydrocarbons, fatty acids, alcohols and esters with chain lengths ranging from 16-54 carbon atoms, as shown by mass spectrometric analysis (**Fig. 4, 6**). Presence of these bands is therefore very typical for all those long chain aliphatic compounds and can not be used as a diagnostic marker for differentiation of specific groups of compounds.

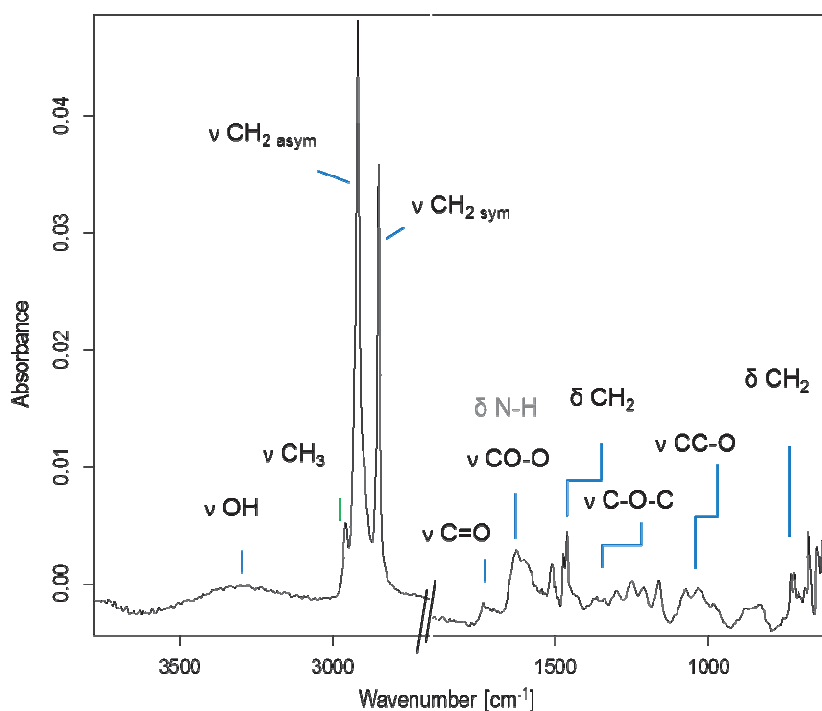


Fig. 21 FT-IR absorption spectrum. Aliphatic EW constituents – alkanes, fatty alcohols, esters exhibit vibration at $2955, 2916, 2848, \sim 1462$ and $\sim 729, 719\text{ cm}^{-1}$ (CH_3 and CH_2), $\sim 3270\text{ cm}^{-1}$ ($\nu\text{ OH}$), 1734 cm^{-1} ($\nu\text{ C=O}$), $\sim 1250 - 1030\text{ cm}^{-1}$ ($\nu\text{ C-O}$).

For this purpose, IR spectroscopy is a superior technique over Raman spectroscopy, since Raman spectra of EWs are dominated by C-H and C-C bond stretching, therefore not very informative. In contrast, functional groups present in alcohols, esters, fatty acids are IR-

active and thus detectable. Esters, one of the main groups of compounds present in EWs of *Populus trichocarpa* and fatty acids can be identified due to carbonyl groups found in the fingerprint region of FT-IR spectrum. Distinguishable bands for C=O groups occur at 1735 cm^{-1} and 1714 cm^{-1} which fits to the typical frequency for esters (1725 - 1750 cm^{-1}) and fatty acids (1700 - 1725 cm^{-1}) (Dubis et al., 1999; van de Voort et al., 2001). Alcohols representing additional prominent constituents of EWs exhibit commonly very broad band at around 3580 - 3200 cm^{-1} due to OH stretching (Socrates, 1994). This band is present in the FTIR spectrum with the absorption maximum at 3364 cm^{-1} . A very informative region located in the low frequencies between 700 - 1500 cm^{-1} provides further confirmation of EW chemical composition. Those series of bands in the fingerprint region have moderate-to-weak intensities, some bands are broad. However, these bands' features are explainable considering the very thin layer of EWs (in the range of hundred nanometers (**Fig. 3**)) and the chemical complexity of the sample.

In all analyzed wax samples (control leaves as well as after insect feeding) bands in the fingerprint region corresponding to the CH_2 vibration belong to the most prominent one and are at the constant frequencies. The scissoring band for CH_2 is present at 1462-63 cm^{-1} and the methylene rocking vibration for CH_2 appeared at 720 cm^{-1} and 729-31 cm^{-1} as doublets. They are indicators of an orthorhombic arrangement of alkyl chains and their shape depends on the phase behavior of cuticular waxes (Merk et al., 1997). Significant are also bands corresponding to C-O stretching vibration, which are present in alcohols, acids and esters. The EWs of *P. trichocarpa* are specially rich in alcohols and esters, therefore we can expect that bands appearing in the range 1000 – 1300 cm^{-1} can be assigned to the C-O stretching mode present in those groups of compounds (Stewart, 1996). In the spectrum are present bands that are characteristic for long chain aliphatic esters; asymmetric stretching vibration C-O can be found near 1161 cm^{-1} and asymmetric stretching vibration C-O near 1075 cm^{-1} . A symmetric deformation band for CH_3 normally found in esters near 1375 cm^{-1} as well as a deformation band for CH_2 from the $-\text{CH}_2-\text{C}(\text{O})-\text{O}-$ group near 1420 cm^{-1} (Socrates, 1994) is also present (at 1374 cm^{-1} and at 1419 cm^{-1} respectively). Bands characteristic for primary alcohols related to C-O stretching are normally found at 1090-1000 cm^{-1} and occur in the overlapping region; nevertheless presence of alcohols is already confirmed by a broad band corresponding to OH stretching at 3364 cm^{-1} (**Table 4**).

Deposition of EWs is detectable on the damage boarder after 6h

In imaging experiments, EWs were isolated from the *P. trichocarpa* leaves after feeding of *C. populi* and samples were scanned over the area where damage was present (e.g. 750/500 μm). Subsequently, FT-IR chemical maps were generated by integration of defined spectral regions corresponding to the characteristic vibrations. Increased absorbance intensities were observed on the damaged areas when compared with the rest of the EW area (**Fig. 22**). Further studies aimed to better understand those processes and determine the temporal dependence of the observed changes.

Bright field images show that the process of EW accumulation takes place on the border line where the leaf tissue was damaged by the insects' feeding (**Fig. 23**). The thickness and the expansion of a supplementary wax coverage depends on the time window available for the

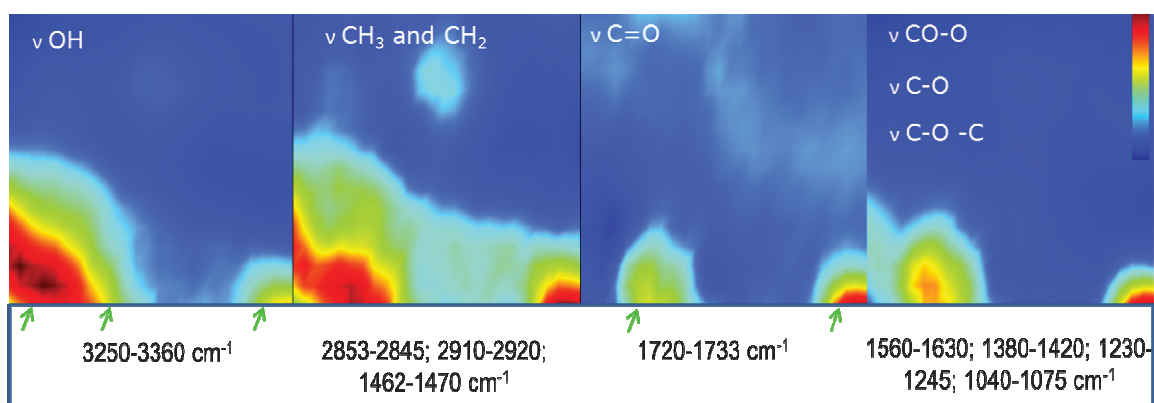


Fig. 22 FT-IR pseudo color images (750/500 μm , Δx , $\Delta y = 80 \mu\text{m}$) of EWs isolated from the *P. trichocarpa* leaves after *C. populi* feeding. In the injury boarder (green arrows) absorption of different chemical groups is significantly higher in comparison to the rest of the sample.

healing process, and is distinctive particularly between 6 h, 24 h and 72 h or 15 days. 1 h after the damage, the deposition is not detectable by the applied techniques. After 6 h the changes on the damage border start to be recognizable under the light microscope and characteristic chemical profile is detectable by FT-IR measurements (**Fig. 24**). Within 24 h these changes become well distinguished and depositions of ca. 50 -200 μm broad wax layers are clearly visible. The morphology of these wax deposits vary, as can be seen in the **Fig. 23** and **Fig. 25**. The thickness measurements could not be performed with high precision, but the estimated thickness reaches ca. 1 μm . The wax deposition visible in the light micrographs

helped to interpret chemical maps generated by IR scanning. It is worth to stress, that the distribution maps are derived from the integrating selective wavenumbers; however, they do not represent a single constituent. It is due to the fact, that chemical

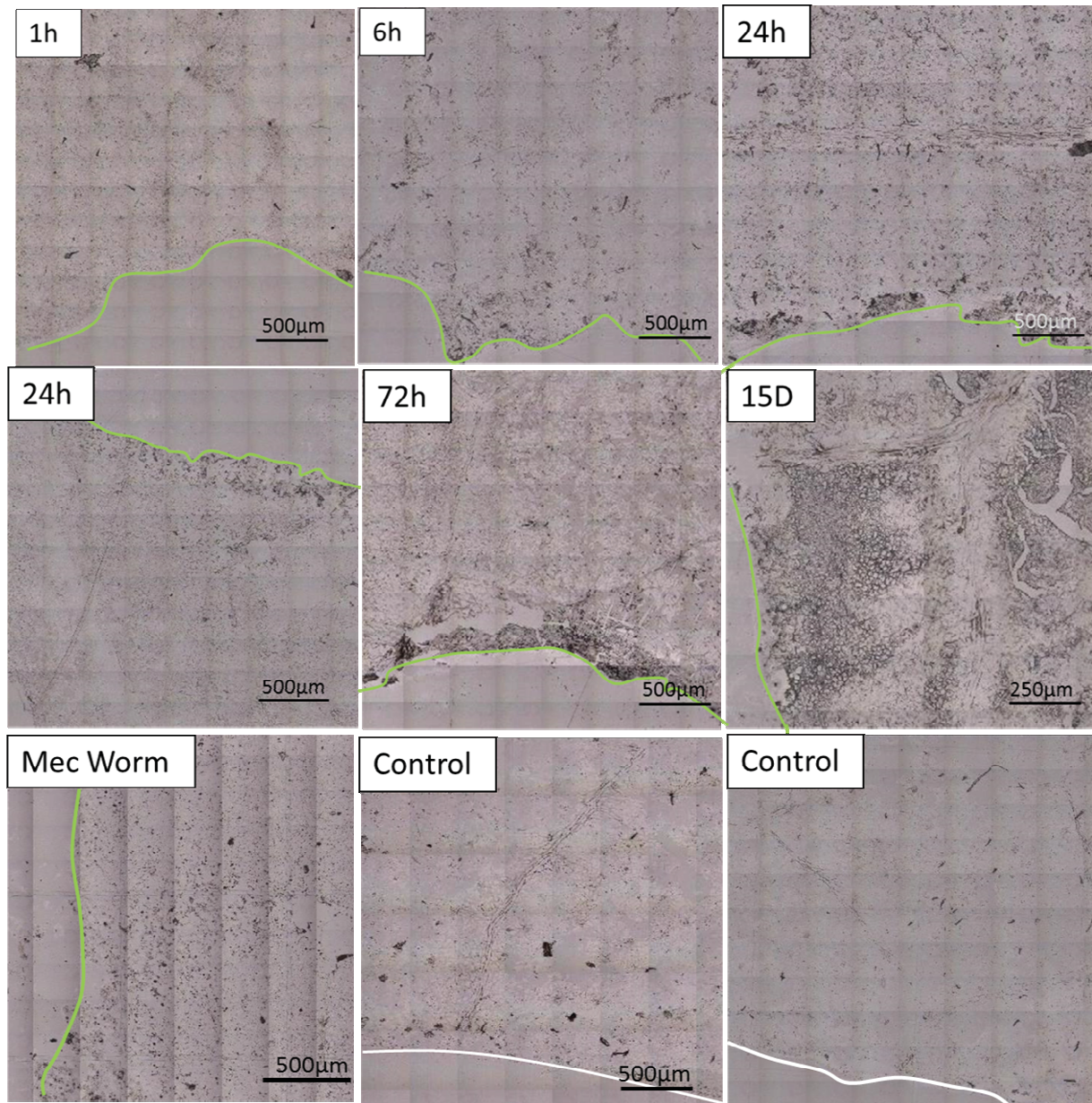
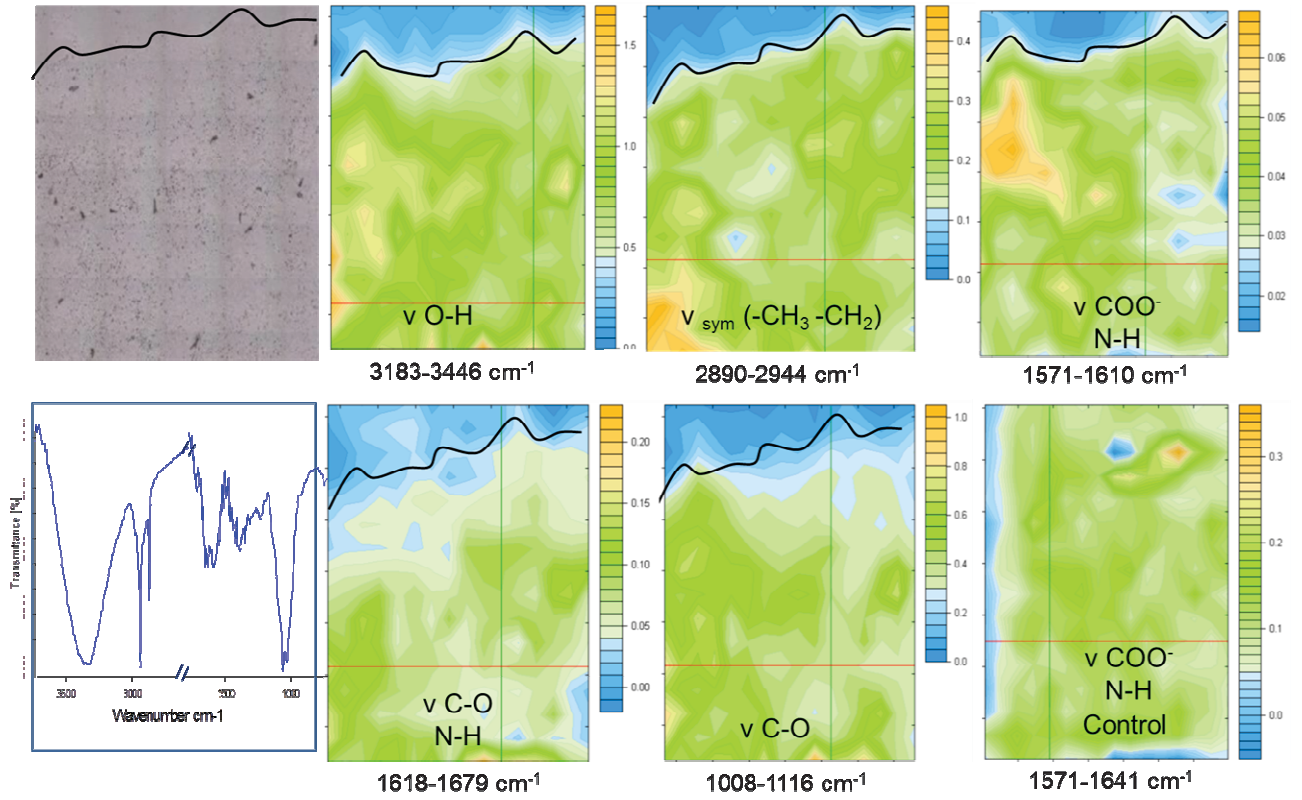
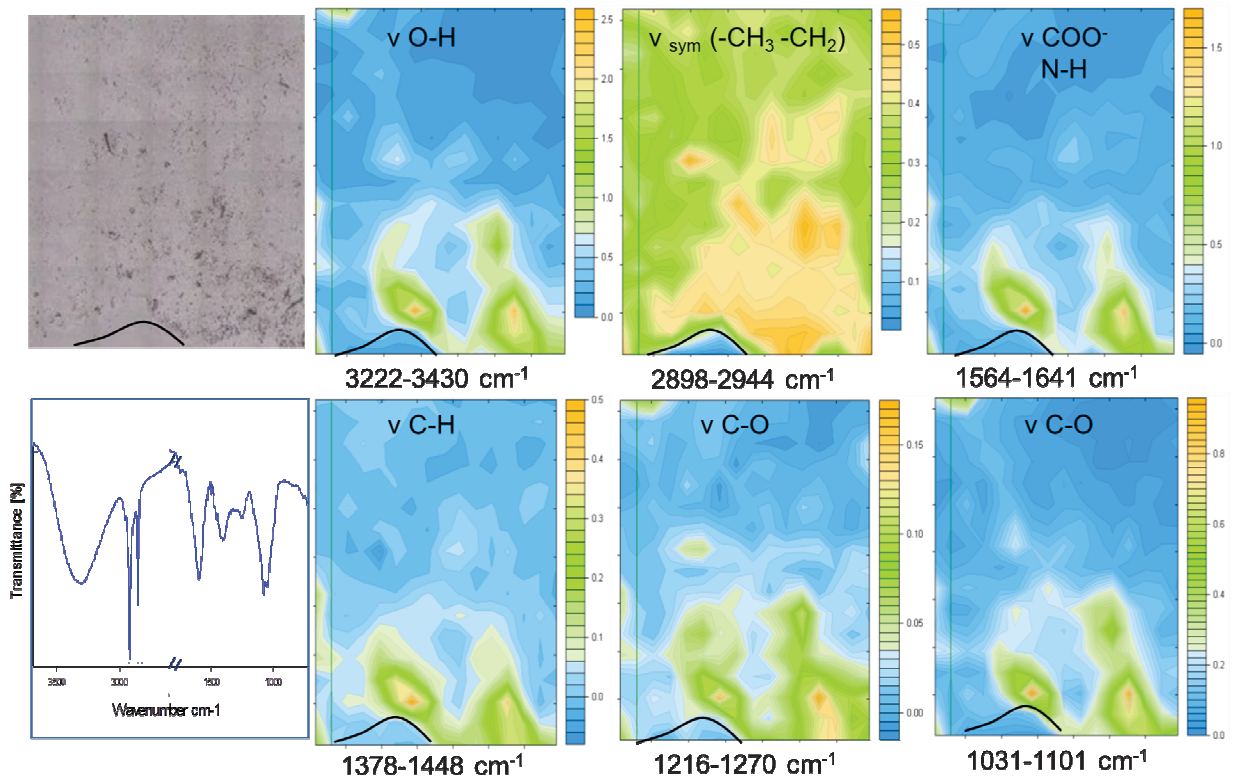
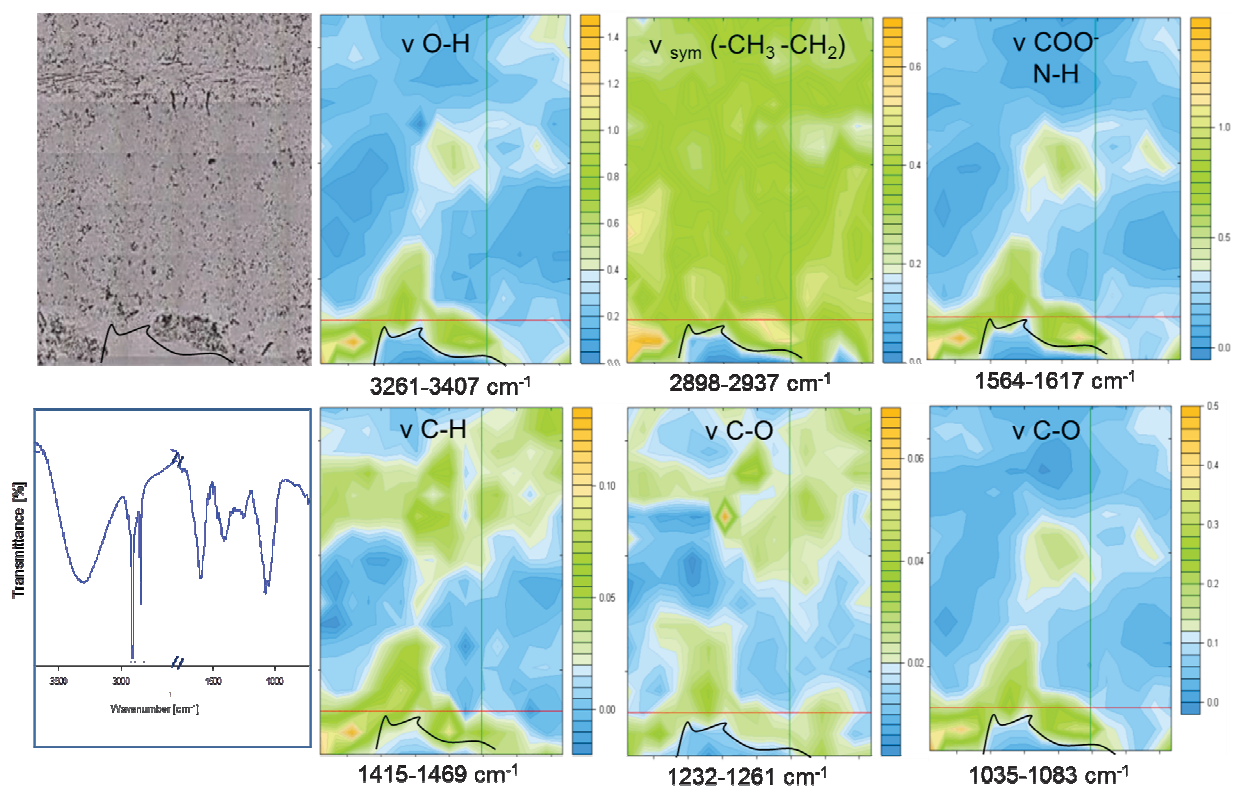


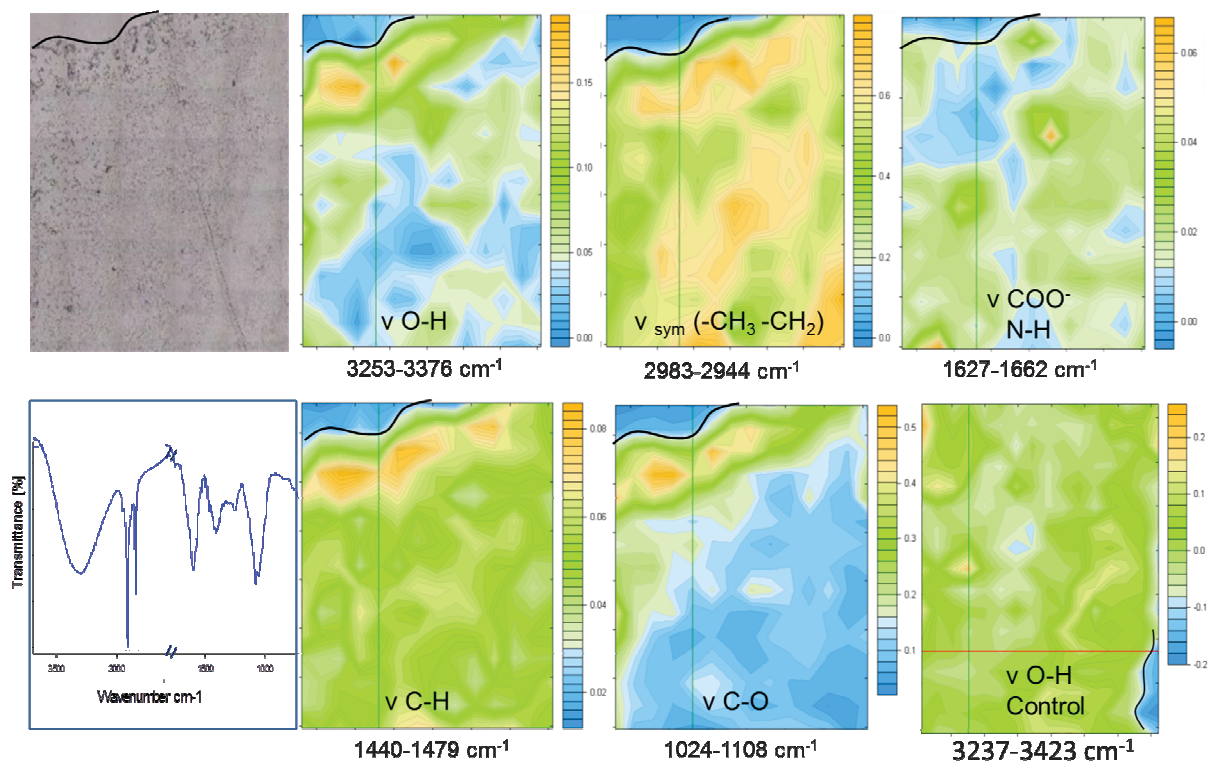
Fig. 23 Bright field images of EWs isolated at the different time windows after *C. populi* feeding. EWs accumulate on the damage boarder (marked by the green line) of the damage caused by insects. For comparison: mechanical damage (Mec Worm) and control samples.

A.**B.**

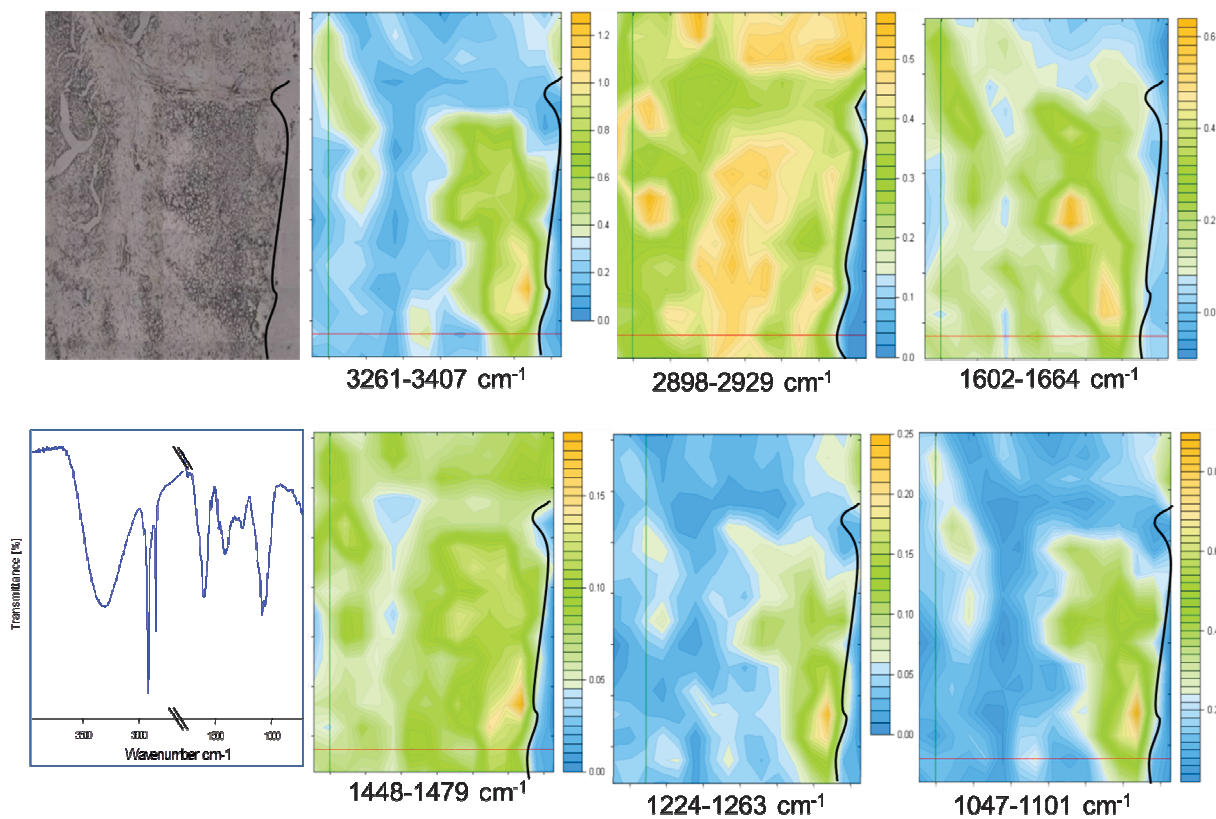
C.



D.



E.



F.

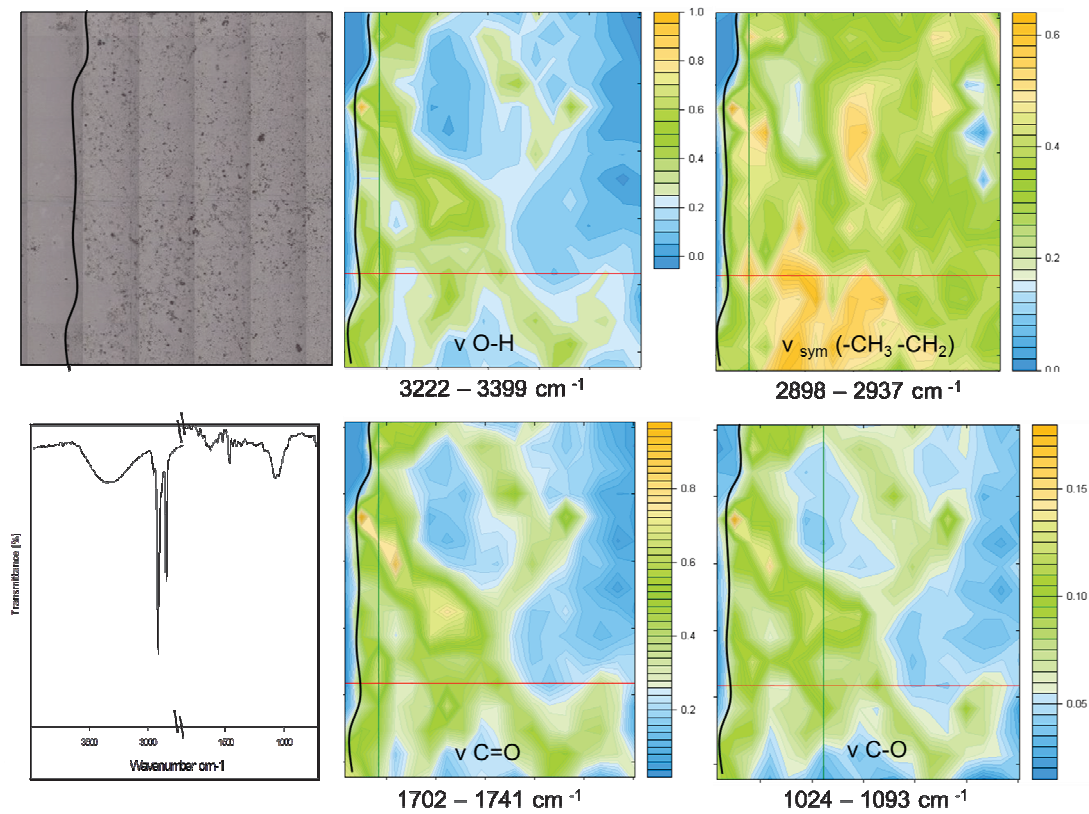


Fig. 24 FT-IR pseudo color images of EW imprint (isolated from *P. trichocarpa* leaves after *C. populi* feeding) at the different time windows after damage; 1h (A), 6h (B), 24 (C,D), 15 days (E). Figure (F) represents EWs after mechanical damage (24h). Distributions of the band intensities in the defined spectral regions exhibit distinctive pattern on the damage boarder (black line).

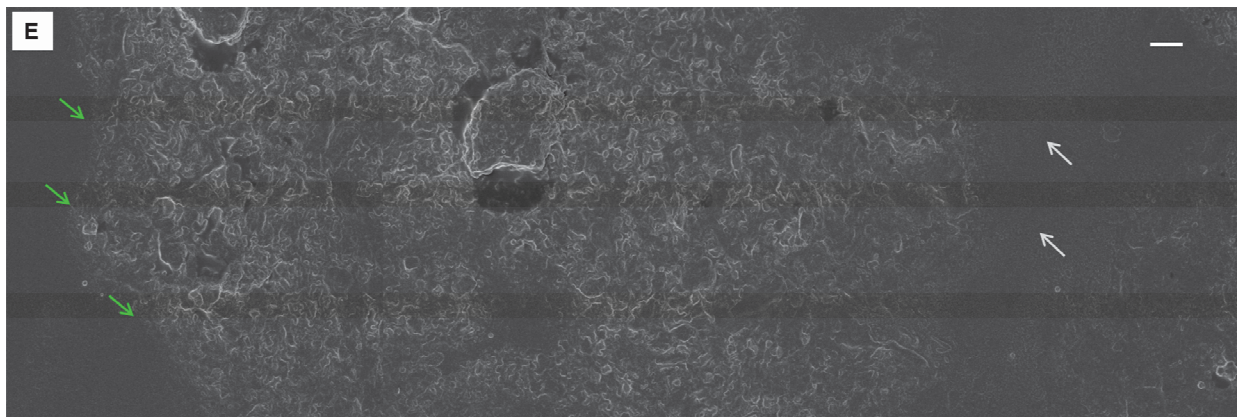
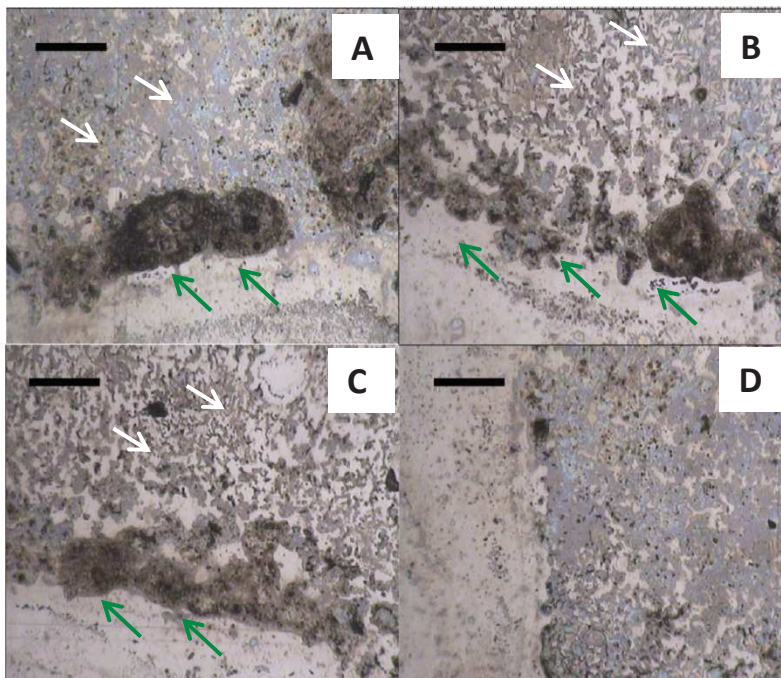


Fig. 25 EWs of *P. trichocarpa* after *C. populi* feeding. EWs accumulate on the boarder (green arrows) of the damage caused by insects. Bright field images (A, B, C - scale bar: 50 μ m) and SEM micrograph (E - scale bar: 2 μ m). For comparison: rest of the sample (white arrows) and D – control sample (without insect damage).

compounds rarely exhibit one diagnostic absorption that is specific for this constituent and not present in any of the other accompanying compounds. This is particularly relevant in biological samples where chemical complexity is a common feature.

Chemical functional group maps acquired over the EW imprint show that the highest absorption (represented by orange colour) of a variety of infrared active chemical groups (such as OH, CH, CO) is detected in the damage line (**Fig. 24**). It is this area, where rigid cell walls are damaged so that the leaf tissue integrity is destroyed; therefore the regeneration processes must be intense. The absorption gradually decreases and is the lowest in the area most distant from the damage site (blue colour). These healing processes occurring on the wounded area involve chemical changes which have not only quantitative nature (represented by higher bands intensity), but also band shifts are observable (**Table 4**). For instance, the maximum absorption of OH in the spectrum acquired on the injury border (that describes the site where leaf tissues was damaged by the insect feeding) is shifted from 3364 cm^{-1} to a lower frequency of 3303 cm^{-1} . Further variances are located in the frequency window between 950 cm^{-1} and 1750 cm^{-1} . The bands assigned to C-O stretching modes at 1170 cm^{-1} is shifted to 1161 cm^{-1} and that at 1538 cm^{-1} is shifted to 1549 cm^{-1} in the wounding border. Additionally, comparing with the control sample two bands at 1234 cm^{-1} and at 991 cm^{-1} , appear in the injury region. On the other hand, in contrast to the control spectrum, the band corresponding to C=O stretching vibration characteristic for carboxylic acids is absent. Band at 1734 cm^{-1} assigned to C=O stretching vibration of esters is still present, as well as two bands due to C-O stretching modes at around 1076 and 1044 cm^{-1} occur in both samples.

The distinction of the spectra acquired on the damage boarder is confirmed by multivariate statistics. For this approach, unsupervised Hierarchical Clustering Analysis (HCA) was employed. HCA is based on finding the smallest 'distances' between the spectra, thus allowing to segment the spectra on the basis of subtle differences in the spectra features like band shape. Five and four clusters from the second-derivative spectra were generated over different spectral windows; $700 - 4000\text{ cm}^{-1}$ and $1750 - 1030\text{ cm}^{-1}$ (**Fig. 26**). The mean cluster spectra, which are encoded in the same colours as the clusters, are presented in the **Fig. 27**. The spectra on the damage area exhibit distinct features in comparison to the spectra acquired from the rest of the sample, therefore HCA segmented these spectra into separate clusters. Notably, there are two clusters in the damage area, which indicates that there are detectable differences in spectral features between the spectra acquired on the damage border

and in the distance of ca. 100-200 μm from this line. This suggests that chemical changes that accompany regeneration processes have complex nature.

Band Position [cm^{-1}]		Assignment	Reference
Control	Damaged		
3364	3303	O –H stretch	(Socrates, 1994)
2917	2917	C –H stretch	(Dubis et al., 1999)
2849	2849	C –H stretch	(Dubis et al., 1999)
1735	1735	C = O stretch	(van de Voort et al., 2001)
1714	-	C = O stretch	(van de Voort et al., 2001)
1656	1656	Amide I; N –H deform.	(Arrondo and Goñi, 1999)
1538	1549	Amide II; N –H deform.	(Arrondo and Goñi, 1999)
1463	1463	C –H deform.	(Merk et al., 1997)
1419	1419	C –H deform. from CH_2	(Socrates, 1994)
1374	1374	C –H deform. from CH_3	(Socrates, 1994)
-	1234	C –O stretch	(Socrates, 1994)
1170	1161	C –O stretch	(Stewart, 1996)
1076	1076	C –O stretch	(Stewart, 1996)
1044	1044	C –O stretch	(Socrates, 1994)
-	991	C –O stretch	(Maréchal and Chanzy, 2000)
731	731	C –H deform.	(Merk et al., 1997)
720	720	C –H deform.	(Merk et al., 1997)

Table 4 Summary of IR bands observed in the EW layer of control and damaged by insect feeding leaves. Band shifts are observed (eg. for ν OH and the δ NH - amide II) as well as appearance of some bands in the damaged leaves (eg. ν CO at 1234 cm^{-1} and 991 cm^{-1}).

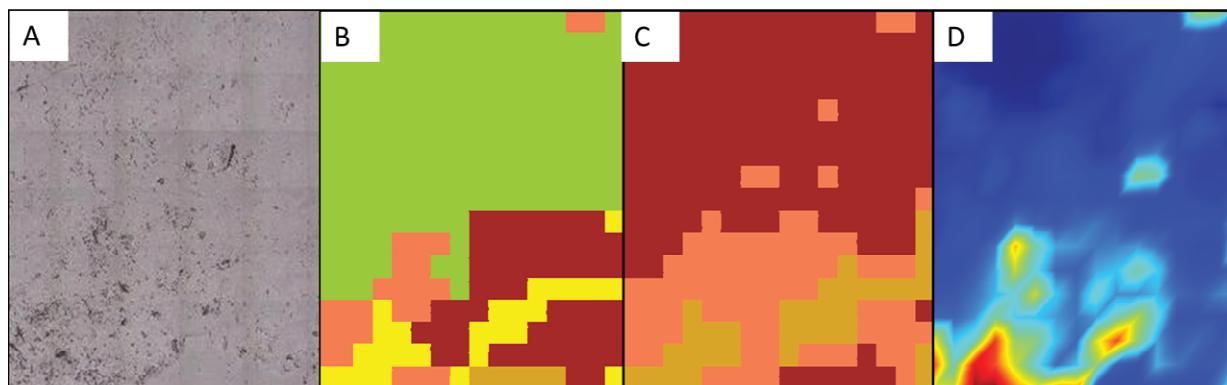


Fig. 26 Bright field image of EW imprint (isolated from leaves damaged by *C. populi*) (A); FT-IR pseudo-color image obtained from hyperspectral data via HCA, 5 clusters 700 – 4000 cm^{-1} (B); 3 clusters 1750 – 1030 cm^{-1} (C); distribution of the absorbance integrated area under the 1080 – 1030 cm^{-1} spectral region (D). Color codes represent the segmentation.

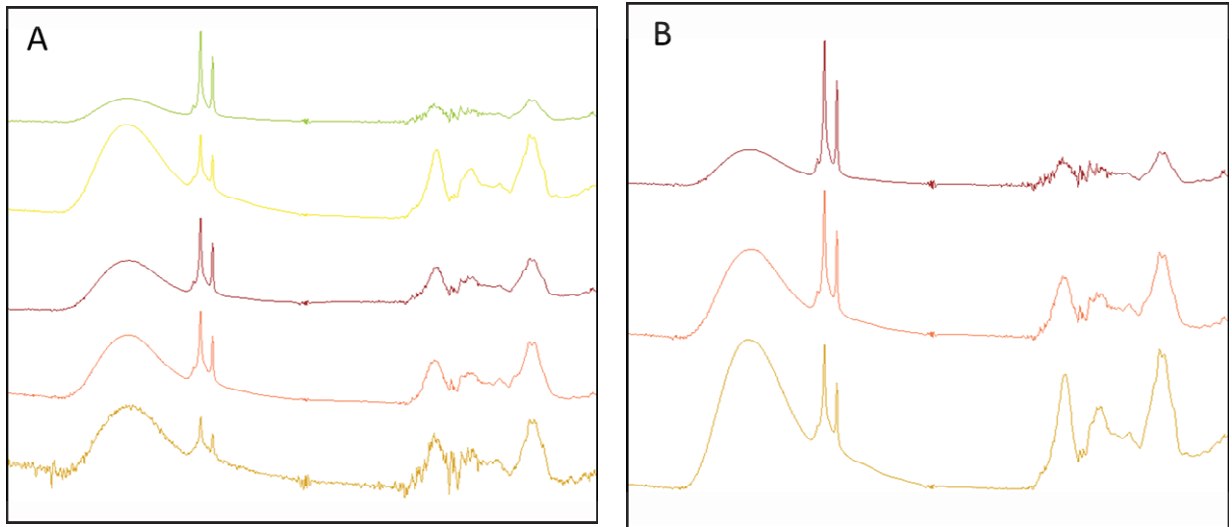


Fig. 27 Average FT-IR mean HCA cluster spectra of the regions shown in the same color for 5 HCA clusters (A) and 3 HCA clusters (B)

FT-IR imaging and selective sampling method allows to investigate the leaf surface comprehensively

Different plant species commonly create a thin layer of EWs and in *P. trichocarpa* this layer is of few hundred nm thick as was shown by SEM (**Fig. 3**). Detection of subtle changes taking place on such a thin layer would encounter difficulties, when the whole leaf is taken for the investigation. Such an approach would also encounter typical obstacles due to interference from the inner leaf tissue or additionally, from fixatives in case of prior tissue fixation (Walsh et al., 2007). Therefore, prior isolation of EWs using an effective and highly selective technique represents the best suitable strategy and allowed the detection of processes occurring on the leaf surface after herbivore damage. Furthermore, the employed sampling procedure allowed to limit problems with the sample thickness variation, which is commonly present when samples are prepared as cross sections (Salzer and Siesler, 2009). Moreover, the exclusive isolation of the EW layer and its thickness of less than a few hundred nanometers (**Fig. 3**) enabled measurements in a transmission mode. Due to these advantages and considering the IR wavelength range used for the measurements, the risks of

non-Beer-Lambert absorption caused by Mie-Type scattering (Mohlenhoff et al., 2005) or the electric field standing wave effect were eliminated (Filik et al., 2012). Both processes may lead to artifacts in the FT-IR spectra of biological samples.

The relevant aspect of the presented results is the fact, that FT-IR chemical maps as well as SEM micrographs represent a direct visualization of processes occurring *in vivo*. The entire feeding experiment was performed *in vivo* while taking special care that the only stress factor applied to the plants was insect feeding. Additional stress factors, which could originate from the bioassays setup, like limitation of the light access, barriers for natural gas exchange (necessary for photosynthesis, respiration and transpiration), or mechanical stress through usage of relatively heavy traps were effectively eliminated (additional details are available in the section ‘Material and methods’).

The chemical composition of *P. trichocarpa* EWs was investigated by means of MALDI-TOF-MS and GC-MS techniques (Chapter II, Section 2.2.1). However, those techniques allowed analyzing only bulk samples without providing information about the spatial distribution of surface compounds. Employing FT-IR microspectroscopy provided possibility to fill this gap and to acquire spatially resolved and chemically specific information without subsequent sample modifications (staining, labelling) as well as in a direct and non-destructive manner.

FT-IR spectra acquired for selectively isolated EWs of *P. trichocarpa* are rich in information; several bands characteristic for particular EW constituents provided confirmation for the presence of characteristic chemical groups. Prior mass spectrometric analysis allowed proposing detailed assignments for most of the bands. The most intense bands were corresponding to CH₂ groups abundant in all wax constituents, whereas bands assigned to OH, C=O and C-O vibrations allowed to confirm the presence of adequate functional groups that occur in the aliphatic primary alcohols, acids and esters (**Fig. 21**).

FT-IR spectroscopy also appeared to be a valuable technique for monitoring leaf surface chemistry after insect infestation. FT-IR spectra of samples originating from the leaves damaged by *C. populi* exhibit notable variances, not only higher absorption but also band shifts are observable. The frequency for OH absorption is shifted from 3364 cm⁻¹ in a native sample to 3303 cm⁻¹ in an injury border. These band shifts suggest structural arrangements within the newly deposited wax compounds. The intermolecular hydrogen bonding belongs to one of the most plausible structure modifications and is best observable by FT-IR

spectroscopy (Kondo and Sawatari, 1996). It is known, that the OH stretching vibration frequency is lowered when hydrogen bonding occurs (Wong et al., 1989). Increase of hydrogen bond strength is displayed by an increase in OH band intensity (Maréchal and Chanzy, 2000). Furthermore it is reported that intermolecular hydrogen bonds are present in plant waxes and that they exert an impact on molecular structure of waxes (Reynhardt, 1997). Intermolecular bonding may appear between esters – alcohols, esters – fatty acids or in fatty acids and alcohol dimers. From MS analysis (**Fig 4, 5**) we know that all those compounds, particularly alcohols and esters are abundantly present in the EW of *P. trichocarpa*. Also presented in this study FT-IR data confirm presence of these aliphatic components. Alcohols belong to long chained and esters to very long chained compounds (number of carbon atoms is in the range of 24 - 32 and 40 – 54 respectively). Hydrogen bonds lead to bridging of adjacent shorter chains (fatty acids, alcohols) by longer ester chains, which prevents phase separation and increases the melting point. This bridging does not occur in the case of paraffinic wax or standard mixtures with the similar chain-length distribution as plant waxes (Reynhardt, 1997).

Further variances are located in the frequency window between 950 cm^{-1} and 1200 cm^{-1} . Bands due to C-O stretching modes at around 1170 , 1076 and 1044 cm^{-1} occur in both samples, whereas a band at 991 cm^{-1} that accompanies those bands only in the damaged leaf surface, may correspond to C-O stretching modes in primary alcohols (Socrates, 1994). Together with a weak band at 1018 cm^{-1} , they suggest several conformations of primary alcohols (Maréchal and Chanzy, 2000), which are revealed in newly deposited waxes. Plausible factors that lead to those variations in spectroscopic features apart from hydrogen bonding and conformational changes could also belong to positional linkage differences (Ribeiro da Luz, 2006).

Water next to the intense OH stretching band near 3288 cm^{-1} exhibits also a HOH bending feature at 1633 cm^{-1} . However, as mentioned before, the samples were vacuum dried in order to limit water interference. Thus, the OH stretching band observed in the spectrum originates from constituents of EW layer (mainly alcohols) which can be confirmed by the presence of C-O vibrations in the fingerprint region (**Table 4**). Bands near 1656 cm^{-1} may be related to amide I due to C=O stretching and contribution from C-N stretching vibration or antisymmetrical stretching of $-\text{COO}^-$ (Villena et al., 2000). However, we find also a band at around 1538 cm^{-1} which may correspond to amide II due to N-H deformation and

contribution from C-N stretching vibration (Arrondo and Goñi, 1999; Sene et al., 1994). Both frequencies also fit into the range characteristic for free amino acids, namely NH_3^+ asymmetric (1656 cm^{-1}) and symmetric (1538 cm^{-1}) deformation vibration (Socrates, 1994). Amide I and amide II bands detected on the leaf surface would suggest the presence of proteins. Interestingly, band shift from 1538 cm^{-1} to 1549 cm^{-1} in the damaged samples may suggest changes in the protein structure (Arrondo and Goñi, 1999; Sene et al., 1994). There are reports in the literature about proteins found on the leaf surface (Pyee et al., 1994). It is also hypothesized that proteins may be involved in the wax transport from the epidermal cells onto the leaf surface. Most plausible candidates named by many authors are lipid transport proteins (LTP) (Kunst and Samuels, 2009; Lee and Suh, 2012; Pyee et al., 1994). On the other hand, presence of free amino acids on the leaf surface can not be excluded as well.

The processes of wax deposition observed in the present study can be compared with the few studies on wax regeneration processes (Koch et al., 2009b; Koch et al., 2004; Neinhuis et al., 2001). Epicuticular waxes in those studies were mechanically removed (usually using glue) and growth of wax layers was investigated using SEM and AFM. Authors observed that during the initial stage of wax formation, the deposited material has a form of patches (also termed ‘terraces’), which are generated on different areas. In the later stages these patches expand. In the present study, it was also observed that new wax layers do not create continuous strips along the damage border, but form irregular aggregates that vary in the thickness and are separated by a thin wax film (**Fig 23, 25**). Alternatively, they create rather continuous layers which are however, significantly thicker in comparison to the rest of the sample. The deposition is limited mainly to the injury border, which is not surprising, since it is an area where the tissue integrity is disrupted and plant investments are largely directed to strengthen these weak points.

In the present study, the deposition of additional EW layers was detectable after 6 hours and the thickness of wax deposits increased further within 24 hours. Wound-related genes are usually induced after few minutes to several hours (León et al., 2001). The healing process on the leaf surface is detectable by applied techniques in 6h after the leaf damage. This suggests, that genes involved in the biosynthesis of complex EW constituents and wax transport to the leaf surface need to be activated in the early stage. As a consequence, wax deposition process can be described as an ‘early process’. Confirmation of that can be found in the wax regeneration studies, where AFM with the potential to acquire higher spatial

resolution micrographs (in comparison with SEM) was employed. Very early steps of wax growth (after 4-13 min from the mechanical wax removal) could be examined and differences of a few nanometres could be detected (Koch et al., 2009a; Koch et al., 2004). These authors observed that waxes start to regenerate immediately after mechanical wax removal and within 6 hours 40% of initial wax amount was regenerated. However, regenerated wax crystals were smaller in size and varying in structure. Regeneration of the complete wax film took place after 10 hours and a multilayer of wax film could be detected after 20 hours. This underlines that protection provided by highly non-polar EW layer is crucial for the leaf survival and the process of EW regeneration as well as its supplementary deposition on the wounding area belong to the important healing processes.

The deposition of EWs on the damaged site can be considered as one stage of the repair processes that is initiated by the plant after insect feeding. A comparable process is observed in the human skin, where formation of clot provides protection of wound tissues by plugging the defective area (Martin, 1997). It is also known, that plant in response to tissue damage induces mechanisms aiming wound closure (Schaller, 2008). Suberin - lipophilic biopolymer and main compound of cork (tissue with multiple layers of dead cells) is actively involved in that process. It seals the cell walls and prevents water loss and infections by bacterial and fungal pathogens (Cottle and Kolattukudy, 1982; Soler et al., 2007). The substances that are observed in the present study to accumulate at the injury site, can not be assigned to suberin. It is due to the fact, that suberin is deposited within the cell wall and not on the most outer cuticle layer (Höfer et al. 2008; Molina et al., 2009; Schaller, 2008). As can be seen in the scheme (**Fig. 1**), any cellular constituents are located below the cuticle. Sampling methods employed in the present study allow to isolate only the most outer cuticle layer - EW layer, without contribution of any compounds from the layers below the cuticle. Further, one of the main constituents of suberin is aromatic polyester (Cottle and Kolattukudy, 1982). Aromatic rings present in phenolic domains would show characteristic absorption in the region 1600-1585 cm^{-1} due to carbon-carbon stretching (Socrates, 1994). That vibration however was not detected in the FT-IR spectra, which excludes presence of aromatic compounds.

Those arguments indicate that observed process is based on deposition of EWs, and not suberin. This further leads to the conclusion, that selective sampling method allowed to detect new wound-healing process. EW deposition at the injury site provides effective diffusion barrier, thus plays similar role as suberinization. Its significance in plant defense is

additionally enhanced, since that process takes place on the plant-environment interface.

Interestingly, processes of EW deposition was not observed after mechanical damage of the leaf (**Fig. 24 F**), suggesting that there is selectivity in activating wax deposition processes. It is known from the literature, that physical damage and the damage caused by herbivore infestation induce different plant responses that vary in their biochemical nature (Maffei et al., 2007). In the latter, perception of elicitors deriving from insects and inducing plant defence responses is involved. During pure physical damage elicitors are obviously not present. This in turn suggests the existence of signalling pathways that link perception of elicitors and activation of wax deposition processes. The question why pure physical damage does not activate similar processes is a subject for further investigations.

For some samples, wax deposition was not observed even after insect damage (data not shown), which suggests that (1) the process did not took place, (2) it occurred but in a minor grade and therefore was not detectable by the applied techniques, (3) the injury border was not transferred to the sample target (ZnS window) during the sample preparation procedure. Considering the fact that the border is in the range of 50-200 μm and the transfer of EW is mechanical, the third option can be a plausible factor. Nevertheless, in the wax regeneration studies, authors also reported that regeneration of wax film investigated on the whole leaf in some cases did not occur (Koch et al., 2009b; Koch et al., 2004; Neinhuis et al., 2001). Similarly, the amount of regenerated wax is also an altering factor, depending on the plant species. Only in one species out of the 24 examined, the waxes were fully restored (Neinhuis et al., 2001). Further, plant developmental stage plays also a role, and in fully developed leaves the regeneration processes may completely not occur.

In the early reports, two hypothesis of wax deposition were presented: the pore hypothesis and the diffusion hypothesis (Anton et al., 1994). The existence of pores in the cuticle was suggested in very early studies (in 1871 by de Bary) and although some later studies aimed to deliver supporting evidence (Miller, 1982), this concept is still a matter of debates. A second group of scientists postulated a mechanism based on diffusion of waxes dissolved in a volatile solvent or water through the cell wall and cuticle (Neinhuis et al., 2001). Interestingly, in the present study as well as in previous ones, the regeneration process did not occur in some cases (within one plant species as well as among different species), which may implicate that passive diffusion is not a conceivable mechanism of EW transport to the cuticle surface. The distinct chemistry of intracuticular waxes located beneath the EW layer

is also an argument that needs to be considered. Furthermore, recent studies identified the first transcription factor regulating wax biosynthesis (MYB96) and authors prompt to discover other key players in controlling the deposition of waxes not only throughout the plant development, but also under diverse biotic and abiotic stresses (Bernard and Joubes, 2013).

3.2.2 High resolution TOF-SIMS imaging reveals co-aggregation of *Populus trichocarpa* leaf surface compounds

Mass spectrometry imaging for *P. trichocarpa* leaf surface analysis

Mass spectrometry imaging became a powerful technique in different disciplines, including medical diagnostics, where it is applied to differentiate diseased from healthy tissues (Schone et al., 2013). MS allows parallel analysis of hundreds of biomolecules, belonging to different molecular classes, thus, providing a specific molecular profile, which serves classification purposes. MS imaging provides much more information than traditional histological approaches and therefore may be applied for detection of early stages of diseases, which is not achievable by standard tools. In the present study, two imaging MS techniques were applied: MALDI-TOF-IMS (matrix-assisted laser desorption/ionization time-of-flight imaging mass spectrometry) and high resolution TOF-SIMS (time-of-flight secondary ion mass spectrometry). In those techniques the sample area is scanned point by point and each pixel of an image represents one spectrum, which contains a number of peaks (depending on sample complexity) at defined mass values and intensities. Although MALDI is a first choice MS imaging technique, progress over last decade enormously extended the capability of SIMS and at present this technique contributes to molecular characterization of complex organic and biological materials (Winograd, 2005).

The challenge of the MS imaging experiments for the leaf surface studies derived from two aspects: (1) long chain compounds consisting mainly of CH₂ groups are not easily ionized; (2) the low thickness of the EW layer of only a few hundred nanometers (standard thickness of tissue sections employed in the MS imaging is 10-20 μm (Goodwin, 2012)) severely limits the available material for ionization. Nevertheless, both MS imaging techniques delivered good quality data (**Fig. 28, 29**). Cumulative spectra exhibited relatively high S/N ratio and many ions were detected, thus localization of many surface compounds could be determined.

For the MALDI-TOF-MS imaging, entire sample was treated by a matrix (light-absorbing organic acid with low molecular weight). Selection of an appropriate matrix is a crucial step, since it drastically affects the ionization efficiency and subsequent detection of analytes. LiDHB was successfully applied in lipidomic research, including plant waxes (Vrkoslav et al., 2010), and was consequently chosen for all MALDI experiments.

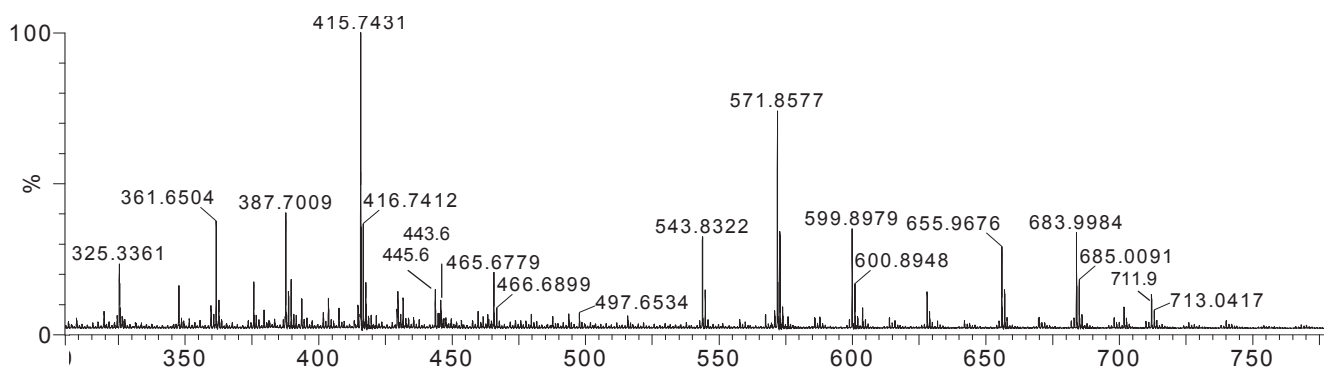
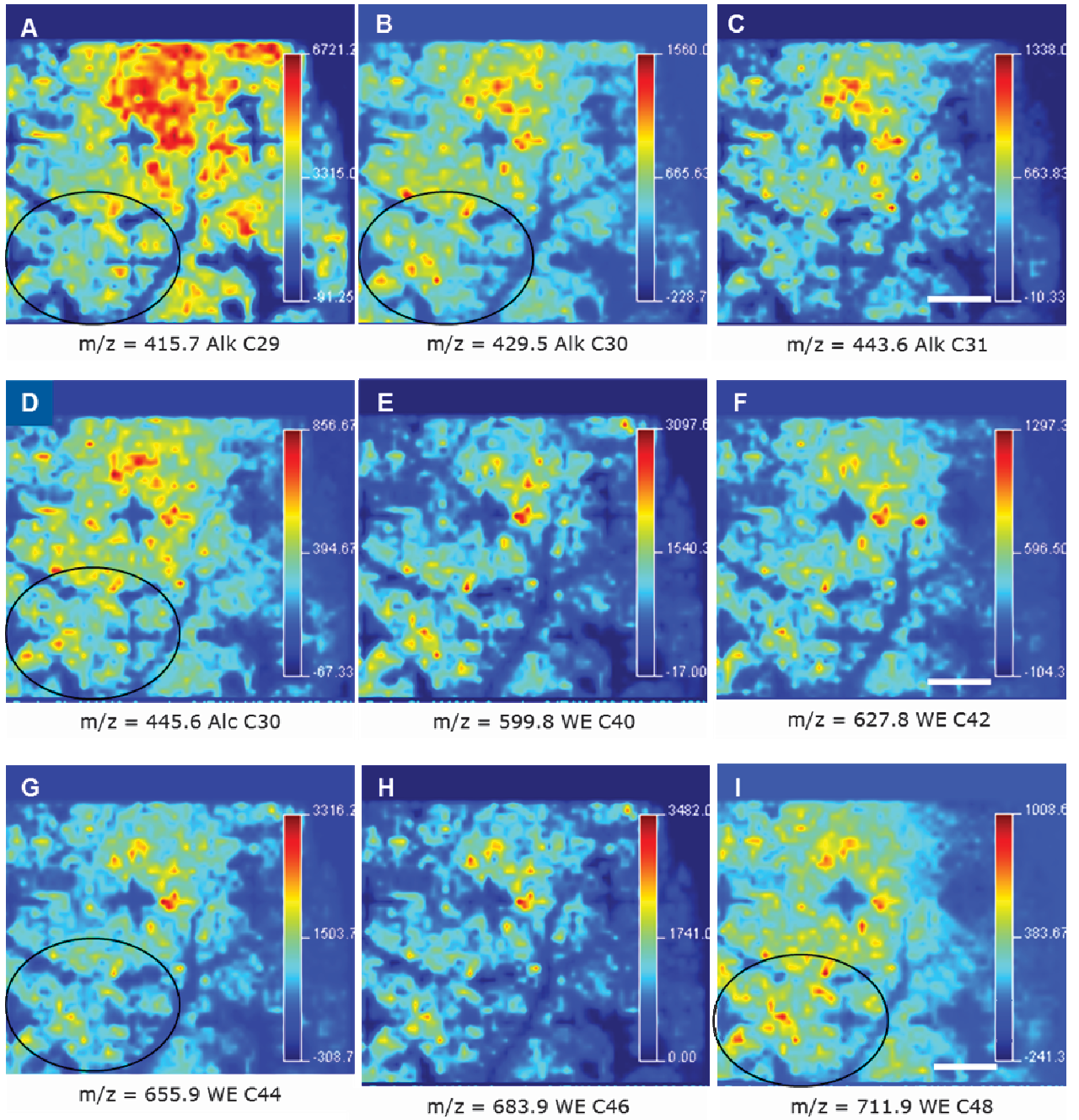


Fig. 28 MALDI-TOF-MS cumulative spectrum and pseudo-color images in the positive ion mode (with LiDHB matrix) of EW imprint (cryo-adhesive method). The color scale indicates signal intensity values for each m/z ; dark blue and red corresponds to the minimum and the maximum signal intensity respectively. Alk - alkanes, Alc - alcohols, WE - wax esters. Pixel size of 200 μm . Scale bar - 5mm

Fig. 28 shows a cumulative spectrum and representative MALDI-TOF-MS images of the scanned leaf surface area which represent plots of an ion intensity at defined m/z values versus their (x,y) position. Because one of the significant advantages of MALDI is ionization of large molecules, it was possible to detect not only ions assigned to alkanes (nonacosane C_{29} , triacontane C_{30} , and hentriacontane C_{31}) and alcohols (triacontanol C_{30}), but also wax esters with m/z above 600 Da. Generated MALDI images for particular m/z values demonstrate the heterogeneous distribution of EW constituents. In the **Fig. 28** those regions are marked by the circles. The color scale corresponds to varying ion intensities, the red color indicates high intensity, and the moderate to low intensity is indicated by the green and blue color respectively. However, this observable heterogeneity might also be a consequence of factors that cannot be excluded in the experiments: (1) possible variations in the thickness of the EW layer, or (2) matrix application – differences in the co-crystallization process and thus ionization efficiency over the sample area. Both those plausible sources of heterogeneity need to be considered when interpreting the data. Due to the relatively low lateral resolution of MALDI IMS (200 μm) and sample treatment, conclusions about the spatial arrangement of wax constituents and their correlation can only be acquired when employing techniques that lack those two drawbacks.

TOF-SIMS is one of the most promising imaging techniques, since in contrast to the widely employed MALDI-IMS, fine structural arrangement of compounds on the sample is not disturbed by matrix application. The common problem with the analyte diffusion during matrix application interrupts the desired information about the local distribution of analytes (Amstalden van Hove et al., 2010). Superiority of this method is also demonstrated by the fact, that SIMS is able to provide nanometer scale spatial resolution, which is not achievable by MALDI –IMS. Furthermore, TOF-SIMS imaging has been successfully employed in examining lipids (Passarelli and Winograd, 2011b) including lipid-related diseases (Tahallah et al., 2008).

TOF-SIMS demonstrated co-aggregation of surface compounds

In the secondary ion mass spectrometry (SIMS), the high energy primary ion beam allows desorption and ionization of analytes from the defined sample area. Secondary ions are released from the surface, directed to the mass spectrometer and a mass spectrum is acquired for each measured position. Similar as in MALDI, generated false color images represent the spatial intensity distribution of defined m/z values, which can correspond to a certain compound. Considering the priority of cluster ion sources over traditional monoatomic sources, SIMS experiments were performed with a bismuth cluster ion source (Bi^+ , Bi_3^+). It provides equivalent emission currents, focus, and lifetime as the Ga ion, and simultaneously lacks main drawbacks of monoatomic ions sources such as extensive molecular fragmentation and surface destruction (Touboul et al., 2005).

For the high resolution SIMS imaging, two approaches were utilized: the first one employed a larger sample area ($700 \times 700 \mu\text{m}$) with a short pulse duration, thus, enabling high mass resolution (**Fig. 31**), while the second aimed to scan only a small sample area ($100 \times 100 \mu\text{m}$) in order to obtain better visualization of compound distribution, however at the expense of the mass resolution (**Fig. 32, 34**). Thus, the first approach was used initially to facilitate the ion peak assignments. In the next step, measurements of smaller sample area allowed precise localization of well-defined ions and confirmed the presence of characteristic features on the sample surface. Moreover, independent and dependent comparisons of the results were performed. Dependent comparisons were employed in case of measures of the same biological sample at different points of time. Independent experiments were used when samples from different leaves were analyzed. Their application aimed to reinforce and confirm the structural arrangement observed in the initial results.

It is worth to underline, that the sampling procedure allowed preserving the structural integrity of the isolated metabolites and their quantitative representations. No treatment was applied on the sample surface. Thus, spatially resolved analysis allowed determining the distribution of detected ions and demonstrating possible correlation between the different wax constituents.

The initial step was to analyze the mean SIMS mass spectrum (**Fig. 29**), which displays the mean intensity of each mass across the entire dataset and served for the generation of all molecular images. SIMS spectra interpretation is more challenging in comparison to

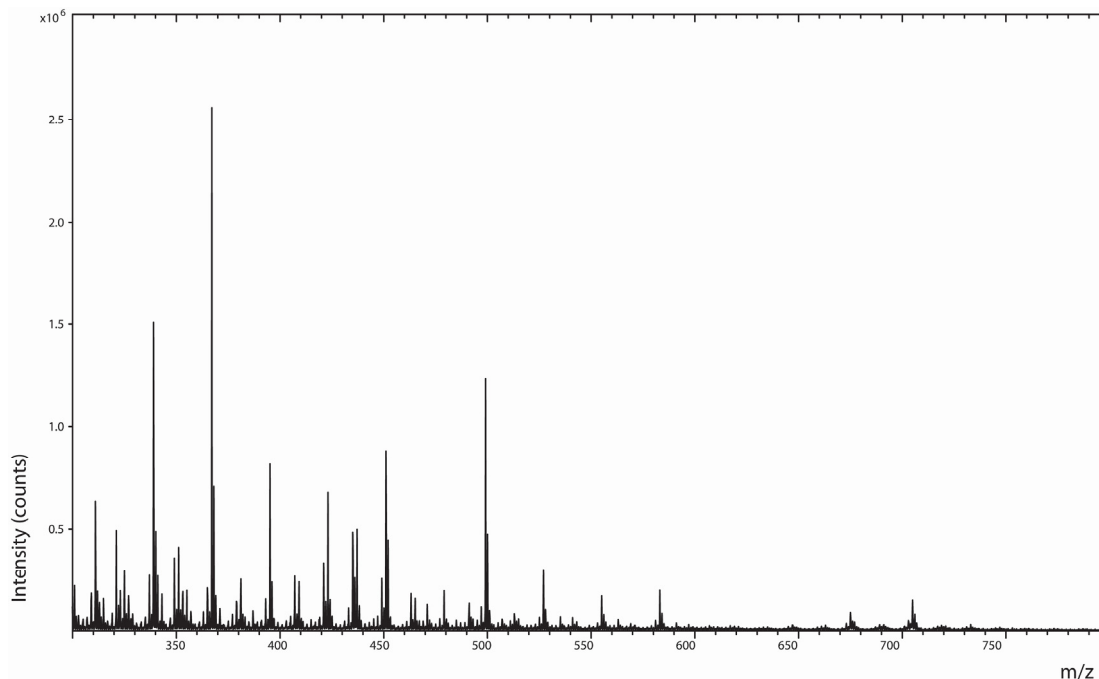


Fig. 29 TOF-SIMS spectrum of EWs isolated from the adaxial side of *P. trichocarpa* leaves using cryo-adhesive isolation method on Si wafer. Negative mode, Bi_3^+ primary ion source.

conventional EI spectra. Ions in the SIMS experiment are more highly vibrationally excited than the ions in a conventional EI mass spectrometer (Thiel and Sjövall, 2011), thus ions may undergo more unusual and rare fragmentations and rearrangements. As a consequence, it is difficult to interpret spectra of complex biological samples, without a priori knowledge about its chemistry (Spool, 2004). In the present study, the assignment of detected compounds in SIMS was facilitated due to the prior characterization of the molecular composition of EWs by GC-MS as well as MALDI-TOF-MS (**Fig. 4, 5**) and literature review (Miller et al., 2005; Siljeström et al., 2009). In order to confirm or at least reinforce mass assignments in SIMS, detected signals were compared with the separately analyzed reference compounds (**Fig. 30**).

The SIMS technique is not equally sensitive to different molecule species; there may be orders-of-magnitude variances in ionization efficiency (Spool, 2004). Therefore, in comparison to the wide range of chemical classes detected by MALDI-TOF-MS and GC-MS, the SIMS spectra provided mainly information about the wax esters (**Table 5**). It is also worth to note, that all those techniques are based on different ionization processes, therefore they cannot be directly compared, but they provide complementary or overlapping information. Both techniques, where samples were prepared in a similar manner (EW

Formula	Assignment	Calculated atomic mass	Detected atomic mass
C ₁₆ H ₃₁ O ₂	[M-H] ⁻ FA – (16:0)	255,23	255,22
C ₁₈ H ₃₅ O ₂	[M-H] ⁻ FA – (18:0)	283,27	283,25
C ₂₀ H ₃₉ O ₂	[M-H] ⁻ FA – (20:0)	311,30	311,28
C ₂₂ H ₄₃ O ₂	[M-H] ⁻ FA – (22:0)	339,33	339,32
C ₂₃ H ₄₃ O ₂	[M-H] ⁻ FA – (23:1)	351,31	351,35
C ₂₃ H ₄₅ O ₂	[M-H] ⁻ FA – (23:0)	353,34	353,34
C ₂₄ H ₄₇ O ₂	[M-H] ⁻ FA – (24:0)	367,36	367,35
C ₂₆ H ₅₁ O ₂	[M-H] ⁻ FA – (26:0)	395,39	395,38
C ₂₇ H ₅₁ O ₂	[M-H] ⁻ FA – (27:1)	407,43	407,39
C ₂₇ H ₅₃ O ₂	[M-H] ⁻ FA – (27:0)	409,41	409,42
C ₂₈ H ₅₃ O ₂	[M-H] ⁻ FA – (28:1)	421,45	421,42
C ₂₈ H ₅₅ O ₂	[M-H] ⁻ FA – (28:0)	423,42	423,41
C ₂₉ H ₅₅ O ₂	[M-H] ⁻ FA – (29:1)	435,47	435,43
C ₂₉ H ₅₇ O ₂	[M-H] ⁻ FA – (29:0)	437,44	437,45
C ₃₀ H ₅₉ O ₂	[M-H] ⁻ FA – (30:0)	451,45	451,44
C ₃₁ H ₆₁ O ₂	[M-H] ⁻ FA – (31:0)	463,50	463,44
C ₃₂ H ₆₃ O ₂	[M-H] ⁻ FA – (32:0)	479,48	479,46
C ₄₄ H ₈₈ O ₂	[M-H] ⁻ WE – (44:0)	647,67	647,65
C ₄₆ H ₉₂ O ₂	[M-H] ⁻ WE – (46:0)	675,70	675,68
C ₄₇ H ₉₄ O ₂	[M-H] ⁻ WE – (47:0)	689,72	689,70
C ₄₈ H ₉₆ O ₂	[M-H] ⁻ WE – (48:0)	703,73	703,71

Table 5 Comparison of detected by TOF-SIMS (negative mode) *m/z* values with the theoretical masses of assigned compounds.

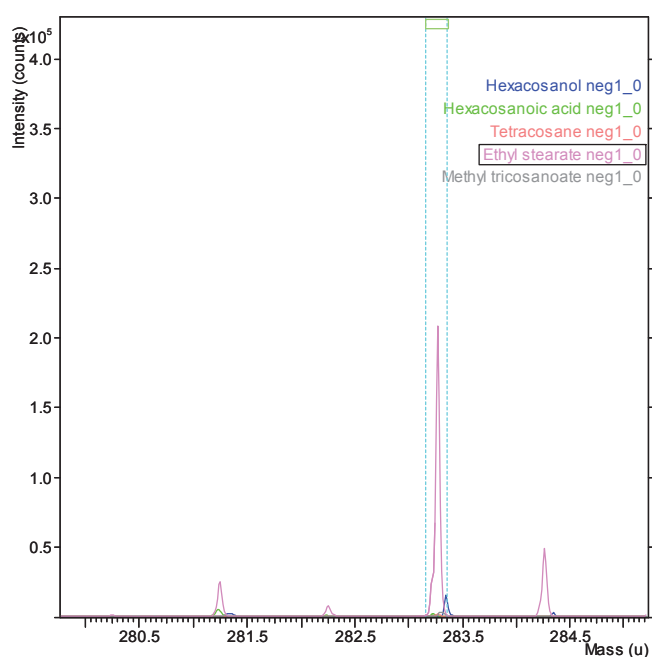
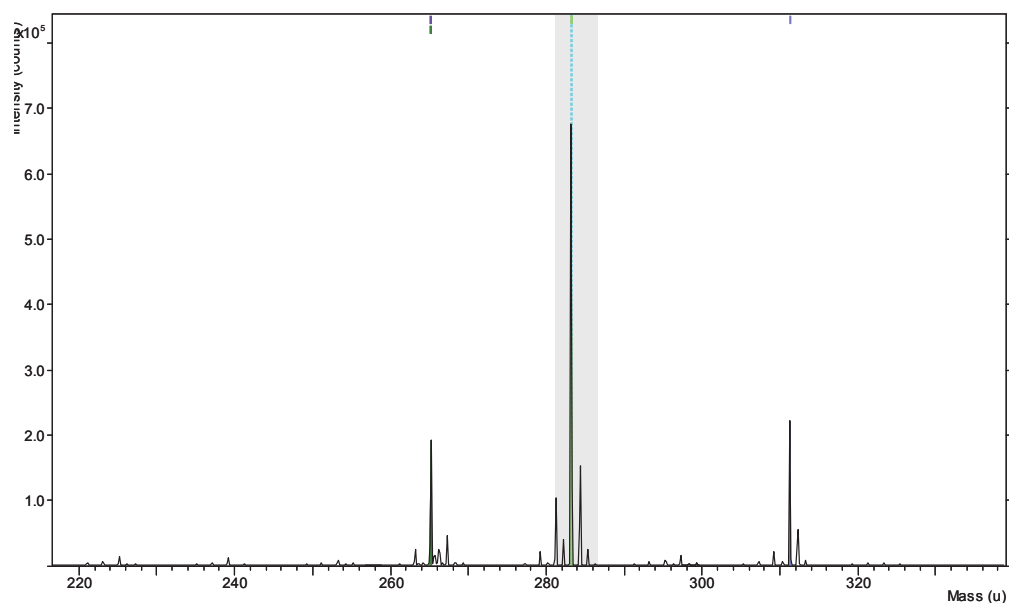


Fig. 30 TOF – SIMS spectrum of ethyl stearate, negative polarity. Strongest peak is observable for ion fragment: $C_{18}H_{35}O_2^-$ corresponding to stearic acid $[M-H]^-$, which indicates that esters undergo decomposition under SIMS conditions.

imprints using the cryo-adhesive method), allowed to detect similar wax esters; $C_{44} - C_{48}$. Those esters are most abundantly present in EWs of *P.trichocarpa* as can be seen in **Fig. 4**. The MALDI-TOF-MS spectrum was acquired for highly concentrated samples of EWs

(obtained by pulling EW imprints with organic solvent and final solvent evaporation). As a result, detection of less abundant wax constituents was also possible, resulting in the whole series of wax ester homologues from C₄₀ – C₅₄ to be found. It is also worth to note, that ionization yield for both techniques (MALDI and SIMS) is usually lower than 0.01%, which results in loss of major ions that remain undetected (Benabdellah et al., 2010).

In addition to intact esters, a series of peaks with masses that can correspond to the molecular formula CH₃(CH₂)_xCOO⁻ (x = 14 – 30) were found in the negative secondary ion mass spectra. They were assigned to species originating from wax ester decomposition. This interpretation was supported by (1) GC-MS analysis, where free fatty acids were detected only in the range of C₁₆ – C₁₈ (with the traces of C₁₃ – C₁₅), (2) the fact that esters belong to wax constituents that are most amenable for ionization, (3) previous report on lipids investigated by SIMS demonstrated a wide range of fatty acids detected in cuticular waxes (Thiel and Sjövall, 2011), and finally (4) measurements of authentic standards that showed that esters undergo decomposition to fatty acid ions (**Fig. 30**).

Although during ionization some esters remained intact (WE C₄₄ – C₄₈), it appears that most of them were partly decomposed. Under SIMS conditions they lost alkyl group and only carboxylate ion (FA C₂₀ – C₃₂) could be detected (**Table 5**). All those ions with defined *m/z* value were selected to display the wax constituent images. Only the high quality mass spectral peaks were chosen for image construction whereas weak peaks were omitted from the analysis. **Fig. 32** represents the whole set of images acquired for one sample whereas **Fig. 31** and **34** show only representative images for selected *m/z* values. In order to achieve better view on the characteristic features for *m/z* = 423, it is recommended to refer to the electronic version of the figures. Due to the fact that SIMS imaging was performed with the high spatial resolution (100 pixels/mm), heterogenous distribution of EW constituents could be here confirmed and investigated in more details.

The false color intensity maps visualize that fragment ion peaks at *m/z* 311, 339, 351, 353, 367 (FA C₂₀ – C₂₄) exhibit the same distribution pattern as ion peaks at *m/z* 647, 675, 689, 703 corresponding to intact esters (**Fig. 32**). Co-localization of those ions is clearly visible in the SIMS images in a form of bright spots, which are distinguishable from the relatively homogenous background and are found to be similar for defined *m/z*. The same observations were made for other samples, **Fig. 34** shows representative images for two biological replicates.

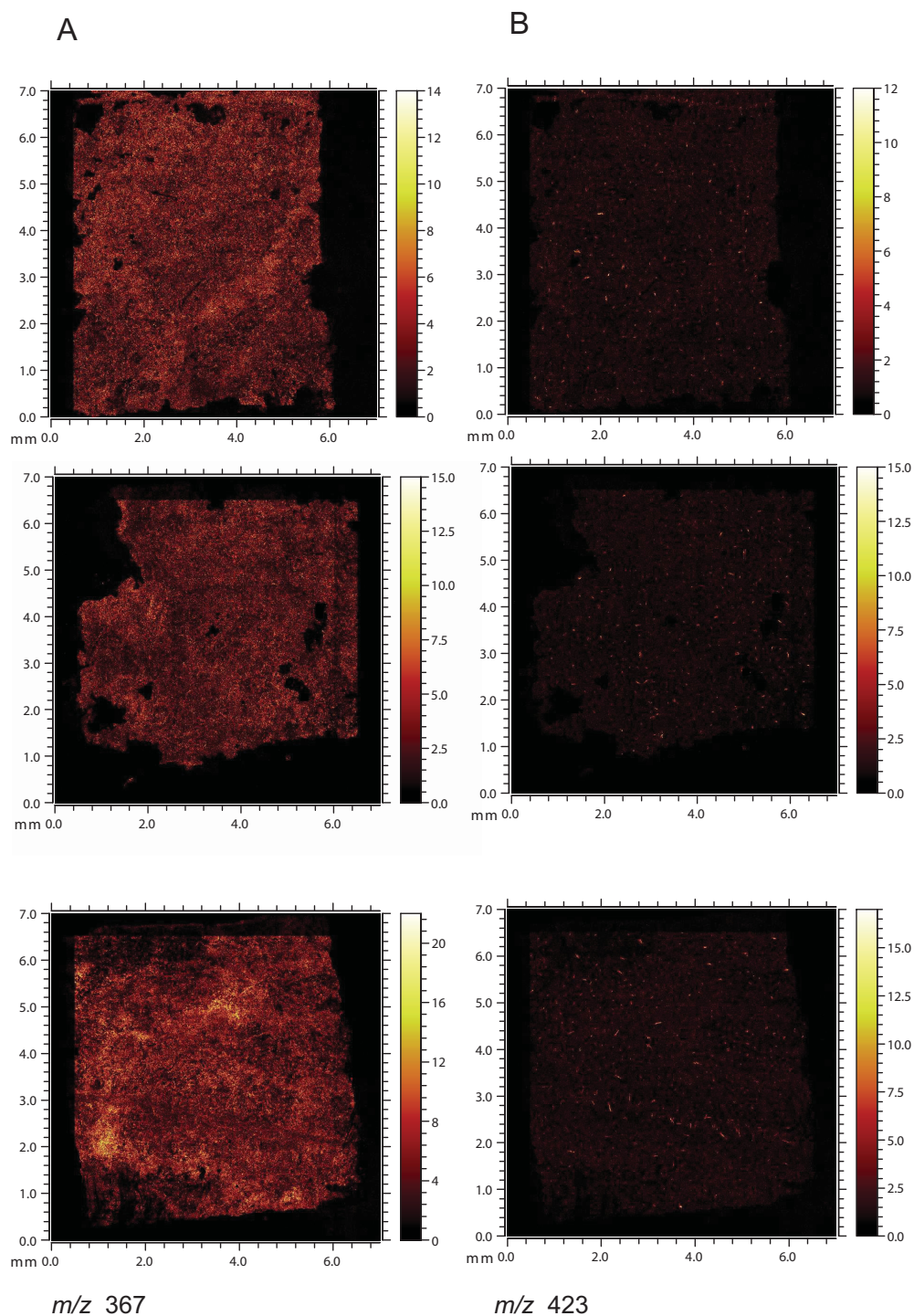
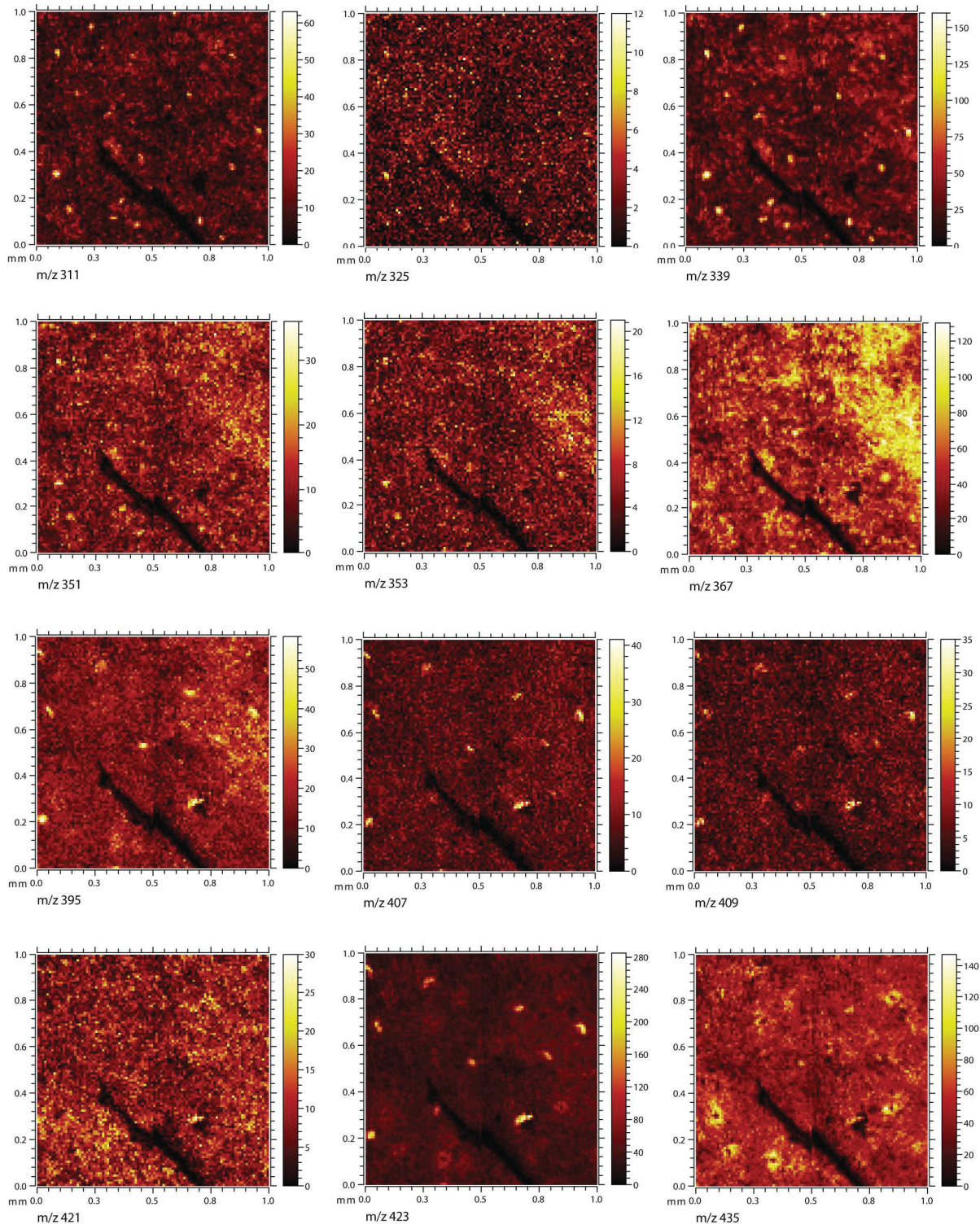


Fig. 31 TOF – SIMS pseudo-color images showing the distribution of m/z 367 (**A**) and m/z 423 (**B**) assigned to $[M-H]^-$ of C24 and C28 fatty acids. Distinctive features in a form of bright spots are present in the images for m/z 423 (better observable in the electronic version). Images are generated using cumulative mass spectra acquired for three different samples. Scanned area: 700 x 700 μm , lateral resolution - 100 pixels/mm.



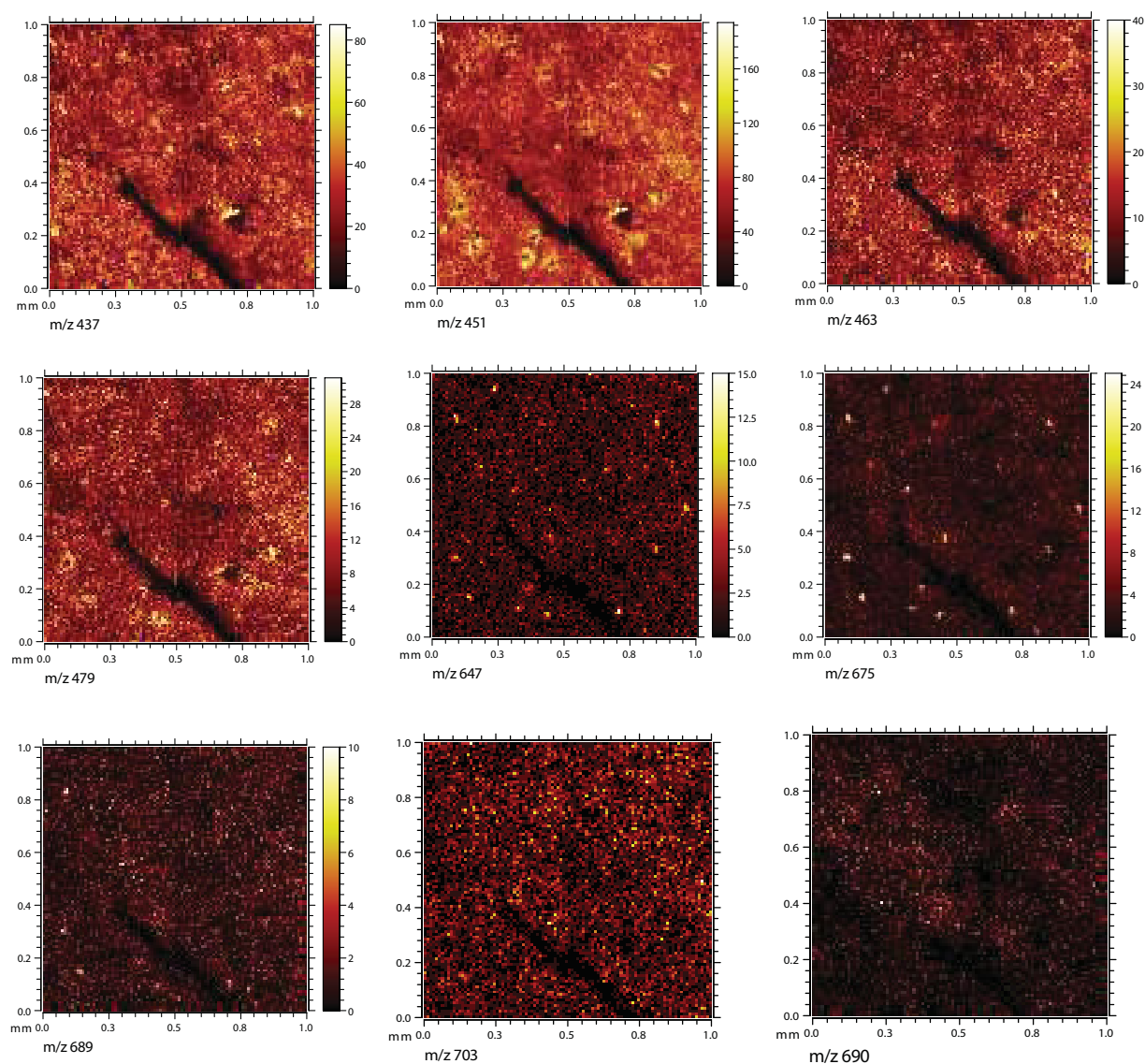


Fig. 32 TOF – SIMS pseudo-color images showing the distribution of defined m/z values (from m/z 311 – 703 assigned to $[M-H]^-$ of wax esters and fatty acids). Distinctive features in a form bright spots with dimensions of ca. 40 μm are observable. Scanned area: 100x100 μm , lateral resolution - 100 pixel/mm. Control: m/z 389.

The second distribution pattern is observable for fragment ion peaks at m/z 395, 407, 409, 421, 423, 435, 437, 451, 463, 479 (FA $C_{26} - C_{32}$) (**Fig 32**). All ions in that range co-aggregate. Intensity of those ions in the SIMS spectrum is lower than the intensity of ions exhibiting the first distribution pattern. It is postulated that this group of ions originate from less abundant wax esters, which were not detected by SIMS. It is worth to mention that when using MALDI, a wider range of wax esters was found (WE $C_{40} - C_{54}$) (**Fig. 4, 6**) and that

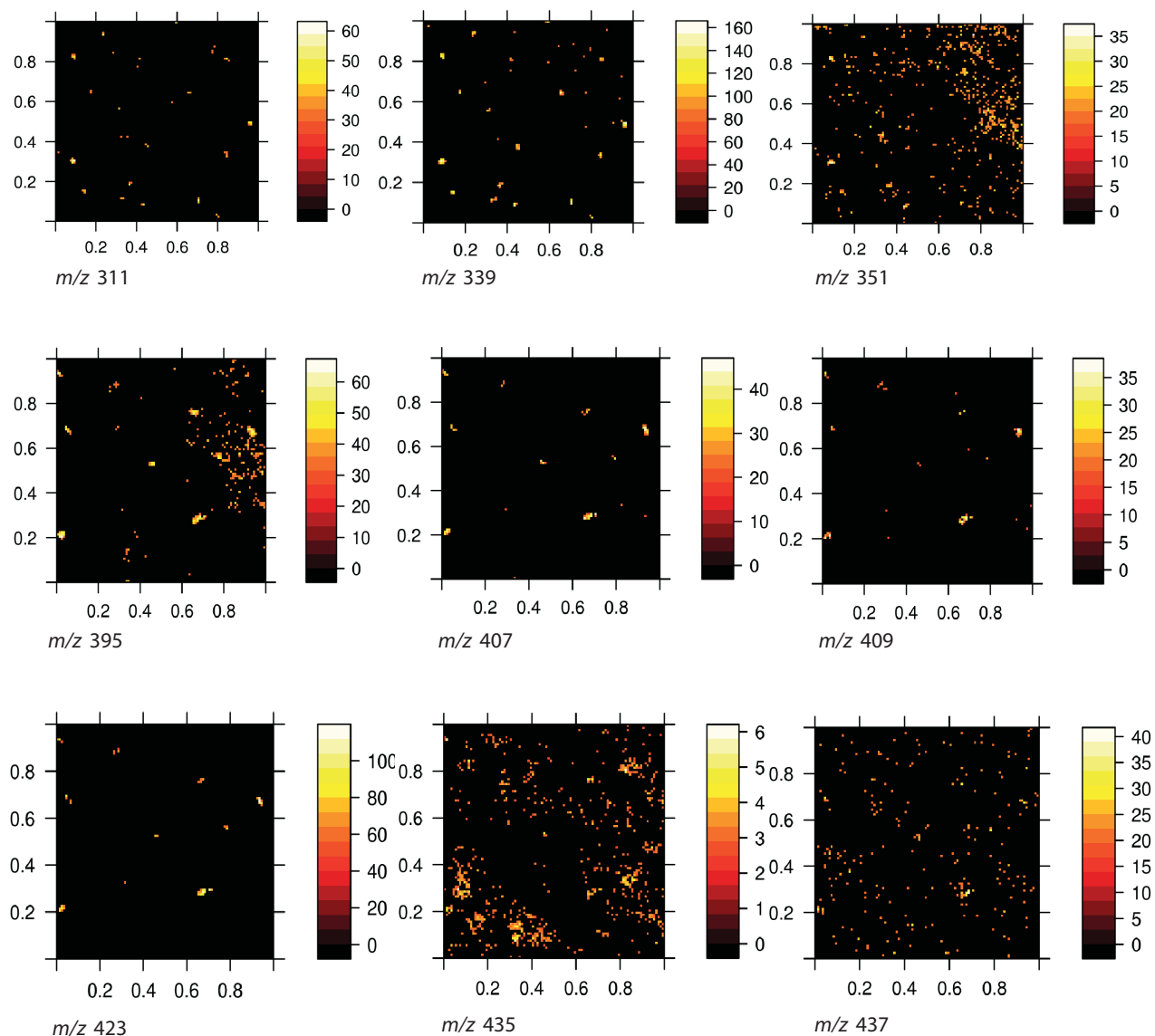
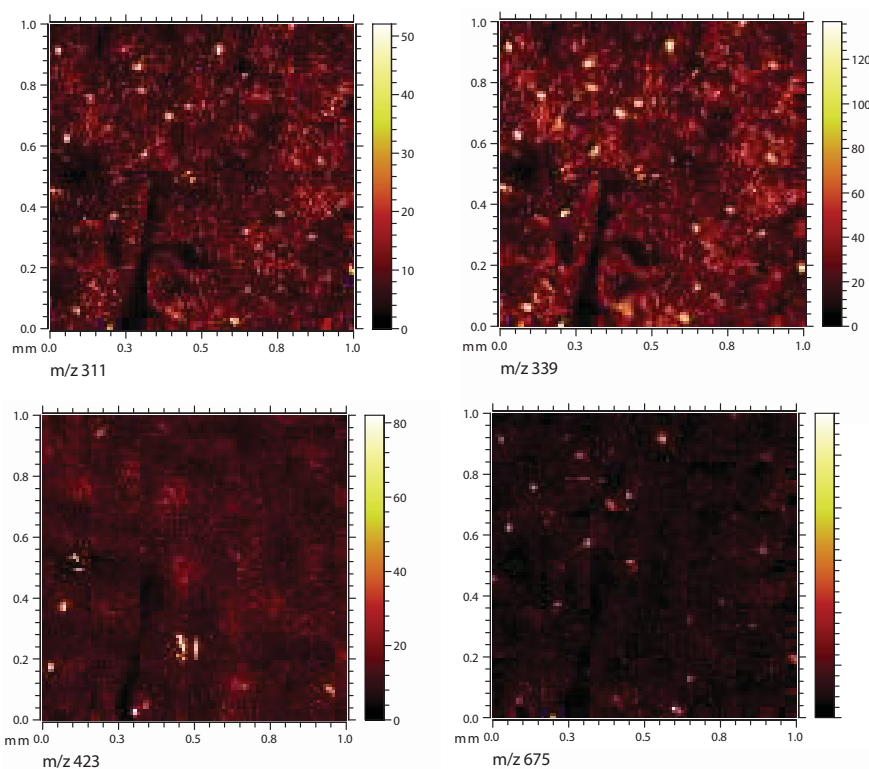


Fig. 33 Representative TOF – SIMS thresholded (pseudo-color) images showing the distribution of defined m/z values. Distinctive features in a form of bright spots with particular spatial arrangement can be observed and classified into two groups; one consists of ions m/z 311 - m/z 367 and m/z 647 - m/z 703, the second group m/z 395 – m/z 479. Scanned area: 100x100 μm , lateral resolution - 100 pixel/mm.

esters detected by SIMS (WE $C_{44} - C_{46}$) belong to the most abundant. It can also be suggested that if wax esters within the range of $C_{47} - C_{54}$ were visible in the SIMS spectra and visual representation of their distribution was possible to acquire, their pattern could be the same as for the series of ions at m/z 395 - 479 (FA $C_{26} - C_{32}$). Thus, SIMS imaging provides at least some evidences for an in situ co-localization of wax compounds, an observation that would not be possible in chemical extracts or MALDI-TOF-MS imaging.

A



B

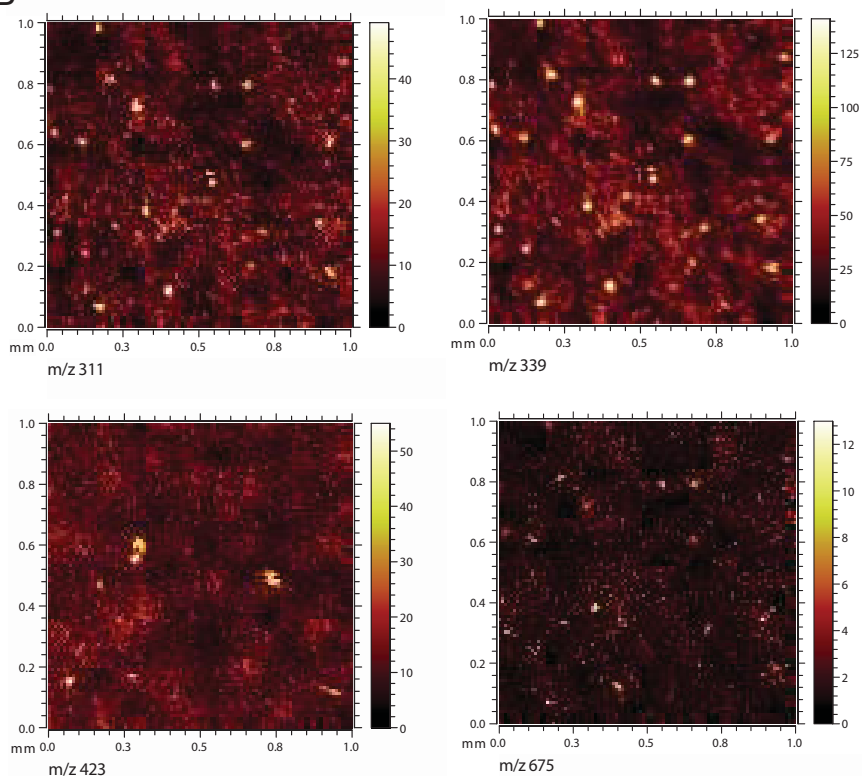


Fig. 34 Representative TOF – SIMS pseudo-color images showing the same spatial distribution of ions with the m/z 311, m/z 339 and m/z 674 and distinctive arrangement of m/z 423. Figures A and B represent different samples. Scanned area: 100x100 μm , lateral resolution - 100 pixel/mm.

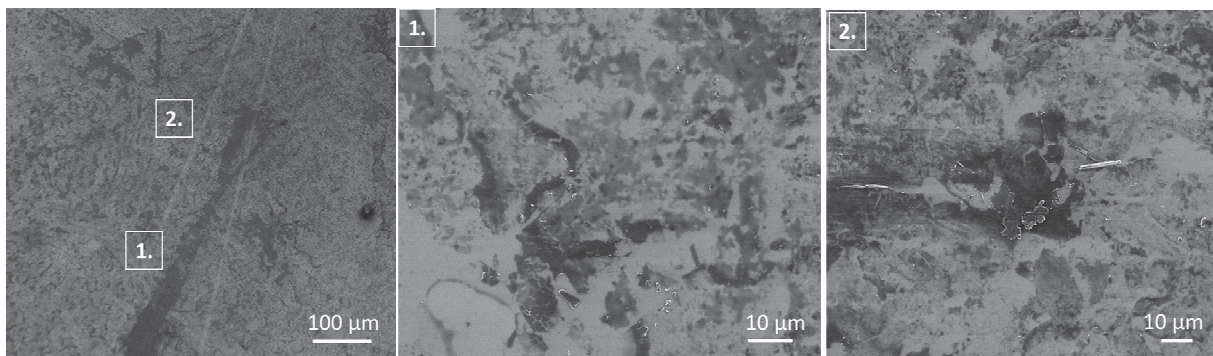


Fig. 35 SEM micrographs of *P. trichocarpa* EW imprint after SIMS experiments confirming absence of morphological structures (including wax crystals) that would correspond to the observed features in the FT-IR images.

Localized features that are observed in the SIMS images allow classification of the detected ions into two groups. To the first group belong ions assigned to fatty acids $C_{20} - C_{24}$ and wax esters $C_{44} - C_{48}$, whereas the second group was assigned to fatty acids $C_{26} - C_{32}$. From these observations we can speculate, that wax esters ranging from C_{44} to C_{48} can be transported to the leaf surface together, whereas the higher homologous, for instance above C_{48} may be transported together. Thus, chain length of wax compounds may determine their joined transport.

The presence of two distinct distribution patterns (specific arrangement of bright spots that emerge from the homogenous background) is better visible in the images generated after employing thresholding (**Fig. 33**).

It is known, that one or more EW constituents may form subtle microscopic structures - wax crystals. For instance, epicuticular crystals in *Eucalyptus*, Poaceae consist of β -diketones and nonacosan-10-ol forms crystals in *Picea pungens* (Jetter and Riederer, 1994). Extensive SEM analysis of *P. trichocarpa* leaf surface showed that EWs create continuous covering without pronounced structures (**Fig. 3**). Thus, association of wax constituents aggregates observed in the SIMS images with the wax crystals is not plausible. Unambiguous evidence is also obtained by the size estimation of observed aggregations. They reach ca. 30-50 μm , whereas typical wax crystals are in the range from hundreds of nanometers to few micrometers (Jetter et al., 2006). Moreover, SEM images acquired after SIMS experiments for the same samples also revealed the absence of any wax crystals (**Fig. 35**).

In order to confirm the molecular heterogeneity present within detected ions, imaging results have been complemented by bioinformatical tools. The data were reduced to the relevant for the analysis mass spectral features. Noise dependent on m/z was calculated, the baseline drift was subtracted from the spectrum, and subsequently interpolation was applied. Due to high quality spectra, the baseline was very low, and the false color images were of high quality even without employment of preprocessing steps. **Fig. 36** represents images before and after preprocessing.

Correlation analyses resulted in the determination of a correlation coefficient (r) that indicates the strength of a relationship between given m/z data. This factor was calculated for each of the two ion groups and allowed the validation of visual observations for the localized features in the SIMS images (**Fig. 37, Table 6**). High correlation between the local distribution of ions was found for m/z 339 with m/z 351 ($r = 0.6449$) and m/z 367 ($r = 0.741$) assigned to fatty acids C_{22} , C_{23} and C_{24} respectively. Small to medium correlation index was calculated for $m/z = 675$ with m/z 339 ($r = 0.299$), m/z 351 m/z 367 and m/z 647 assigned to wax ester C_{46} , fatty acids C_{22} , C_{23} , C_{24} and wax ester C_{44} respectively.

High to medium correlation in local distribution was found for all detected ions from m/z 395 to m/z 479 assigned to fatty acids $C_{26} - C_{32}$ (**Table 5,6**). For example the medium correlation of ion at m/z 395 with ions at m/z 407 ($r = 0.464$) and m/z 409 ($r = 0.407$) as well as high correlation with m/z 423 ($r = 0.579$). Furthermore, the high correlation index confirmed the co-localization of ions at m/z 423 with m/z 407 (0.536).

The co-localization of ions confirmed by correlation analysis demonstrates the spatial association between detected ions. SIMS images provide visual representation for the existence of two groups of distribution patterns; one for ions from m/z 311 to m/z 367 assigned to fatty acids $C_{20} - C_{24}$ and from m/z 647 to m/z 689 assigned to wax esters C_{44} to C_{48} . And the second present among ions from m/z 395 to m/z 479 assigned to fatty acids $C_{26} - C_{32}$. Correlation between defined ions of those two groups was reinforced by high to medium positive correlation indexes. Consequently, depending on the chain length of wax constituents their joint transport to the leaf surface might be a plausible scenario not only for the detected ions, but also for the rest of the EW compounds. Thus, it can be concluded, that EW constituents exhibit properties that favor aggregation. It is displayed either by formation of wax crystals observable in some plant species or aggregations that are plane in form and lack 3 dimensional characteristics as in case of *Populus trichocarpa*.

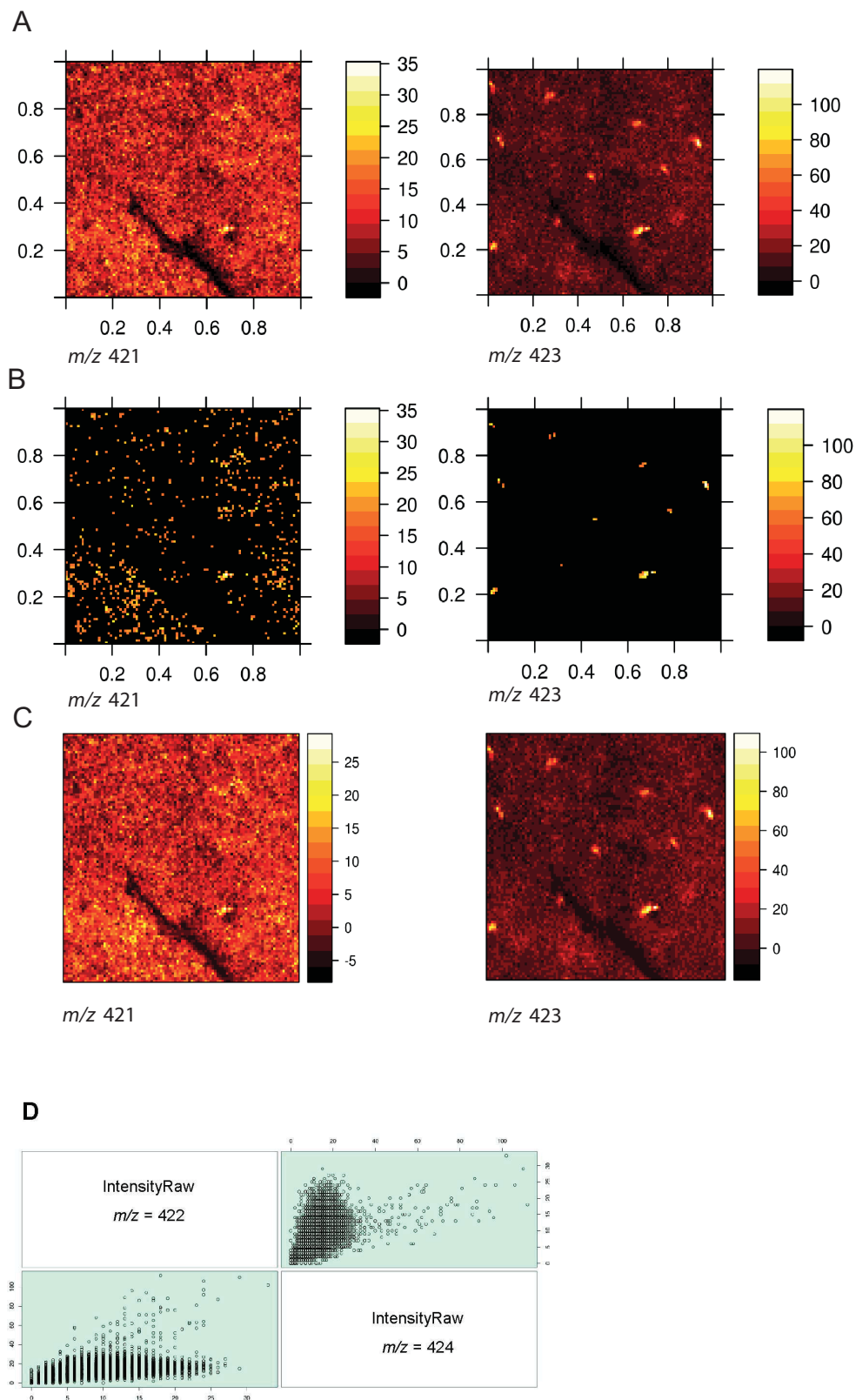


Fig. 36 TOF – SIMS pseudo-color images showing the distribution of m/z 422 and m/z 424 before pre-processing steps (A) thresholded (B) and after pre-processing steps (C). Variables ordered and colored by correlation (D). Images after employing pre-processing deliver similar information as images generated from raw data. Scanned area: 100x100 μm , lateral resolution - 100 pixel/mm.

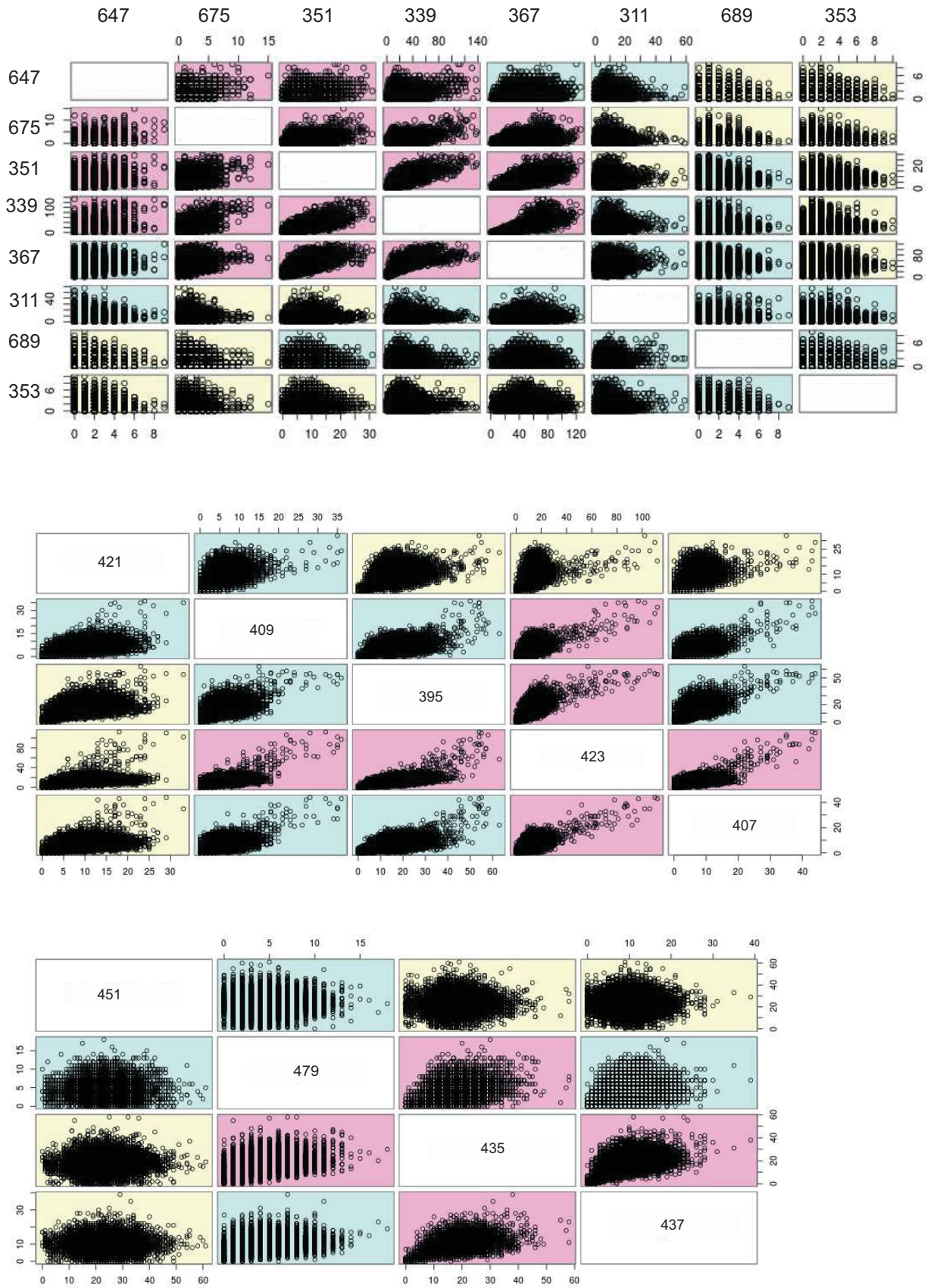


Fig. 37 Graphical representation of correlation analyses. The color scheme used in the scatter plot matrix represents the highest (pink) and the lowest correlation amongst variables (yellow).

<i>m/z</i>	311	339	351	353	367	647	675	689
311	1,00000	0,04668	0,03089	0,06587	0,04975	0,03190	0,01902	0,07774
339	0,04668	1,00000	0,64499	0,010797	0,74156	0,14329	0,29908	0,04648
351	0,03089	0,64499	1,00000	0,01769	0,59459	0,09414	0,20498	0,04454
353	0,06587	0,01079	0,01769	1,00000	0,01729	0,01486	0,00696	0,08222
367	0,04975	0,74156	0,59459	0,01729	1,00000	0,08249	0,20004	0,05546
647	0,03190	0,14329	0,09414	0,01487	0,08249	1,00000	0,11147	0,01566
675	0,01902	0,29908	0,20498	0,00696	0,20004	0,11147	1,00000	0,01566
689	0,07774	0,04648	0,04454	0,08222	0,05546	0,01566	0,01073	1,00000

<i>m/z</i>	395	407	409	421	423
395	1,00000	0,46468	0,40737	0,34327	0,57965
407	0,46468	1,00000	0,39703	0,28979	0,53607
409	0,40737	0,39703	1,00000	0,36562	0,48011
421	0,34327	0,28979	0,36562	1,00000	0,36281
423	0,57965	0,53607	0,48011	0,36281	1,00000

<i>m/z</i>	435	437	451	479
435	1,00000	0,39536	0,02868	0,26123
437	0,39536	1,00000	0,00761	0,2221
451	0,02868	0,00761	1,00000	0,03647
479	0,26123	0,2221	0,03647	1,00000

Table 6. Correlation analyses result in determination of correlation coefficient (r) indicating strength of relationship between given *m/z* data.

3.3 Conclusions

Molecular imaging techniques become more and more widely used methods for the chemical mapping of various biological samples. Due to the constant technological progress in the instrumentation, they offer versatile tools for the detection and localization of wide range of analytes. Those techniques are non-invasive and provide further crucial advantages such as (1) molecular specificity without the usage of exogenous labels, (2) minimum sample preparation, (3) direct and parallel detection of different compound classes, (4) good or very good sensitivity, which for some techniques can be additionally increased by the sample treatments, (5) some techniques, such as SIMS allow depth profiling and 3D imaging (Vickerman, 2011). As a result, molecular imaging techniques have capabilities to provide information that cannot be obtained by other techniques. Their application in the leaf surface studies combined with the selective sampling methods provided spatially resolved chemical information.

The EWs consist of compounds that are IR active, therefore FT-IR spectroscopy imaging appeared to be adequate technique to investigate processes taking place on the leaf surface after insect infestation. In the damaged area, formation of a multilayer of additional wax was detected in 6 h after insect infestation (confirmed also by light microscopy and SEM). Those processes were accompanied by the chemical changes and involved increase of the absorption bands. Detected vibrations could be assigned to different chemical groups present in the EW components (mainly $-CH$, $-OH$, $C-O$). Moreover, injury area exhibited distinguishable IR spectra in comparison to the rest of the sample, which was reinforced by multivariate statistical analysis (HCA).

Acquired results indicate that the EWs play an active role in the wound-healing process. Their deposition on the injury border protects leaf from the destructive consequences of the tissue damage (in particular excessive water loss). Additionally, FT-IR analysis also suggest that the formation of new EW layers involves structural rearrangements where for instance hydrogen bonding or conformational changes could be of particular importance.

In order to investigate the local distribution of individual surface compounds, it was necessary to employ analytical techniques with the potential to achieve better chemical selectivity and high spatial resolution. Mass spectrometry imaging techniques, MALDI-TOF-

MS and particularly TOF-SIMS fulfill those requirements and therefore were employed in the present study. The results show that although EWs of *P. trichocarpa* create a smooth layer (without wax crystals), discrete spatial differentiation exists within EW constituents. SIMS images demonstrated co-localization of ions detected on the leaf surface. They provided visual representation for the existence of two groups of distribution patterns; one occurring for ions assigned to fatty acids C₂₀ – C₂₄ and wax esters C₄₄ - C₄₈. The second is present among ions assigned to fatty acids C₂₆ – C₃₂. Correlation between defined ions of those two groups was reinforced by the high to medium positive correlation indexes. Spatial association between the detected ions assigned to wax esters depends on the chain length of those wax constituents. Thus, it can be postulated that transport of wax esters as well as other wax constituents from the cell to the cuticle surface may also be determined by the chain length. It will be a matter of further investigations with application of all available nowadays instrumentations for the high resolution imaging, to detect a wider range of wax constituents and determine their local distribution. Moreover, also alterations of the EW deposition and local arrangement in the diverse developmental stages and in the response to the environmental changes remain to be determined. Those studies will be very relevant for better understanding of complex processes on the leaf surface, since *P. trichocarpa* is a sequenced plant and therefore investigations on genetic level are available as well.

4. Chapter IV Overall conclusions

All terrestrial plants are covered by cuticle and its most outer layer that creates leaf surface is called epicuticular waxes (EWs). This layer is a first line of interaction between the plant and the environment. Despite its crucial role in plant survival, for decades leaf surface was studied using sampling methods based on solvent extraction. In those methods, spatial discrimination of compounds in various cuticle layers was not preserved; moreover, secondary metabolites from the inner leaf tissue were often co-extracted as well. The main aim of the present study was to apply highly selective sampling methods and a variety of molecular imaging techniques in order to achieve more comprehensive knowledge about the leaf surface. *Populus trichocarpa* (Torr. & Gray) - first long-lived tree that has been sequenced was selected as a model plant.

For the chemical analysis and molecular imaging experiments, epicuticular waxes (EWs) were sampled by cryo-adhesive method, whereas studying the role of leaf surface in plant-insect interaction was performed by a novel *in vivo* method - adhesive tape embedding. The performance of the developed method was carefully investigated and compared with the established in the literature methods for the mechanical EW removal. Adhesive tape embedding appeared to be a promising method for *in vivo* removal of EWs. It offers many advantages such as: (1) surface structures remain mainly intact, (2) simple handling, (3) removed wax layer is visible by naked eye. Consequently, it was applied in the behavioral experiments.

Chemical characterization of EWs was performed by GC-MS as well as MALDI-TOF-MS. The latter technique allowed direct detection of high molecular mass compounds characteristic for plant waxes. The analysis were completed by FT-IR spectroscopy, which confirmed presence of several functional groups such as C=O, C-O and O-H. Those vibrations appeared in the frequency ranges corresponding to alcohols and esters. This complementary approach allowed to conclude, that EWs of *P. trichocarpa* consist of long chain fatty acids (C₁₆, C₁₈), very long chain saturated (C₂₃-C₃₄) and unsaturated alkanes (C₂₅, C₂₇, C₂₉), alcohols (C₂₄-C₃₃) and esters (C₄₀-C₅₄).

An interesting aspect from the ecological point of view was to answer the question if EWs of *P. trichocarpa* provide chemical cues in the host plant recognition process of the specialist

leaf beetles, *Chrysomela populi* (Coleoptera: Chrysomelinae). This model system selected for the experiments represents a naturally occurring interaction between the host plant and the specialist herbivore. EW layer was mechanically and *in vivo* removed from the leaves and response of the beetles to treated and untreated leaves was tested in dual choice experiments. Results demonstrated that EWs do not play a role as decisive chemosensory cues, since leaf beetles were not only able to recognize their host plant after removal of EWs, but even preferred de-waxed leaves over controls. Furthermore, salicin - one of the candidate compounds that may serve as a feeding signal for *C. populi* was not detected among the selectively isolated surface compounds whereas it was present in the whole leaf extract of *P. trichocarpa* leaves.

Complementary chemical characterization analysis of *P. trichocarpa* leaf surface was a first step for investigations aiming determination of the structural arrangement of EW compounds with the employment of molecular imaging techniques. Due to constant technological progress in the instrumentation, molecular imaging techniques offer versatile tools for the detection and localization of wide range of analytes. Those techniques are non-invasive and provide molecular specificity without usage of exogenous labels. They require minimum sample preparation and allow direct and parallel detection of different compound classes.

At present such questions as what is the local distribution of EW compounds and whether they play a role in wound-healing processes were open. By preservation of native, two dimensional arrangement of EWs and employment of molecular imaging techniques it was possible to answer those questions.

Employment of the FT-IR spectroscopy imaging allowed investigation of processes taking place on the leaf surface after insect infestation. In the damaged area, formation of a multilayer of additional EWs was detected in 6 h after insect infestation (confirmed also by light microscopy and SEM). Those processes were accompanied by the chemical changes and involved increase of the absorption bands that are present in the different EW constituents (mainly -CH, -OH, C-O). Moreover, spectra acquired in the injury area exhibited distinguishable profile (e.g. bands shift was detected) comparing to the rest of the sample. This chemical differentiation was confirmed by the multivariate statistical analysis (HCA).

Acquired results indicate that the EWs play an active role in the wound-healing process. Their deposition on the injury border protects leaf from the destructive consequences of the

tissue damage (in particular excessive water loss). Additionally, FT-IR analysis also suggest that the formation of new EW layers involves structural rearrangements where for instance hydrogen bonding or conformational changes could be of special importance.

In order to investigate the local distribution of individual surface compounds, it was necessary to employ analytical techniques with the potential to achieve better chemical selectivity and high spatial resolution. Mass spectrometry imaging techniques, MALDI-TOF-IMS and particularly TOF-SIMS fulfill those requirements and therefore were employed in the present study as well.

Although MALDI-TOF-MS provided chemical specificity and information about the distribution of detected ions could be acquired, this technique does not offer sufficient spatial resolution. The EWs are a mixture of compounds with very similar chemical characteristics (very long chain aliphatic compounds). In case of *P. trichocarpa* they create a thin film that lacks distinguishable structures. Due to those chemical and morphological properties, a distinction of areas that could be differentiated in images by morphological features or varying chemical compositions is rather impossible. Consequently, it is of special importance to employ techniques with the potential to achieve high spatial resolution. Employing TOF-SIMS offered this possibility.

High resolution mass spectrometry imaging provided evidences, that although EWs of *P. trichocarpa* create a smooth layer (without wax crystals), discrete spatial differentiation exists within EW constituents. TOF-SIMS images demonstrated co-localization of ions detected on the leaf surface. They provided visual representation for the existence of two groups of distribution patterns; one occurring for ions assigned to fatty acids $C_{20} - C_{24}$ and wax esters $C_{44} - C_{48}$. The second is present among ions assigned to fatty acids $C_{26} - C_{32}$. Correlation between defined ions of those two groups was reinforced by the statistical analysis. Spatial association between the detected ions assigned to wax esters depends on the chain length of those wax constituents. Thus, it can be postulated that transport of wax esters as well as other wax constituents from the cell to the cuticle surface may also be determined by the chain length.

Understanding the molecular mechanism of wound-induced deposition of EWs or co-aggregation of wax constituents on the leaf surface requires primary understanding the mechanism of wax transportation, which despite the efforts over decades has remained

largely unknown. Next to the understanding the complex network of enzymes and transporters involved in the wax production and export, there are many unresolved questions such as: (1) if the same traffic mechanism serves all lipophilic wax constituents, (2) what is the spatial and temporal aspect of their deposition to the leaf surface, (3) whether chemical structure i.e. chain length or chemical class determines the spatial arrangement on the leaf surface, and (4) how environmental factors (abiotic and biotic) influence the local distribution of EW compounds.

Present study on the *Populus trichocarpa* provides new insight into the processes taking place on the leaf surface that allows to answer some of those questions. Additionally, since molecular imaging techniques were successfully applied to answer biologically relevant questions, present study shows promising directions for future studies in the plant surface research. Further investigations are required in order to detect a wider range of wax constituents and determine their local distribution. Moreover, also alteration of EW deposition and local arrangement of surface compounds in the diverse developmental stages and in the response to the environmental changes is also an interesting direction of the future studies.

Finally, it is worth to underline that *Populus trichocarpa* in opposite to the most common model plant - *Arabidopsis thaliana*, is an economically and ecologically important plant. Thus, research on that plant species delivers considerable benefits, particularly that studies based on chemical analysis can be complemented with the molecular genetic analysis.

5. Materials and Methods

5.1 Plant material

Populus trichocarpa Torr. & Gray (clone 600-25) was cultivated in a growth chamber at 23°C day and 18°C night with 50% relative humidity, light intensity of 30% (Natura deLuxe 36W, Osram) and a diurnal cycle of 12 h light and 12 h dark. Cuttings were kept at 12°C and after 8 weeks when they reached 15-20 cm in length, plants were transferred to 2 L pots. Standard substrate (Klasmann-Deilmann, GmbH, Geeste, Germany) was used as soil and 4 weeks after transfer, plants were fertilized with 1% of 10:15:10 N:P:K supplement (Ferty 3, Planta Düngemittel GmbH, Regenstauf, Germany) every second week. Plants were grown under controlled condition throughout the cultivation and not treated with any pesticides to prevent chemical modification on the leaf surface. Plants used for all experiments were 4-5 months old, for bioassays 4-5 weeks and 7-8 weeks old leaves were used. Other plants used in the study: *Prunus laurocerasus* L., *Armoracia rusticana* G. Gaertn., B. Mey. & Scherb., *Phaseolus lunatus* L. were grown in the similar conditions.

5.2 Isolation of EWs for chemical analysis

EWs were isolated using cryo-adhesive method (Jetter et al., 2000) with water as a transfer medium. *P. trichocarpa* leaves were shortly rinsed with distilled water to remove any contaminating particles. Standard microscopic glass slides (76 x 26 mm, Menzel-Gläser, Thermo Scientific) were chosen as a sample target, they enabled isolation of EWs from a large leaf area. Leaf tissues were cut into rectangle shape pieces with dimensions slightly larger than the glass slides (to avoid contamination from the inner plant tissue). Each leaf cutting was placed on the clean glass slide with evenly distributed 4-5 double distilled water droplets (3 µl each), afterwards a second glass slide was placed on top of it and gently pressed creating a sandwich. The leaf was homogeneously moistened with very thin water film. With the help of tweezers, the whole sandwich was dipped in liquid nitrogen for 30 s. Water droplets served as a medium, which transferred the wax layer from the leaf to the glass slide and the second glass slide enabled putting slight force on the tissue without direct contacting and damaging it. It allowed isolating exclusively EWs with no disturbance to the other cuticle layers. Glass slides were detached from the plant tissue and the same procedure was repeated 10-15 times, until enough wax material was collected for chemical analysis. Subsequent washing of the collected imprints from the targets was done using mixture of solvents, CH₂Cl₂-hexane-MeOH (7:2:1). Washing was repeated three times, the last one was

done with the help of an ultrasonic bath (Bandelin Sonorex) at room temperature for 15 min. In the next step, the solvent was removed under reduced pressure (Büchi Rotavapor R-200) and the dry mass was determined. Samples were ultimately dissolved in CH_2Cl_2 to the required concentration ($0.1\text{-}1\text{ mg mL}^{-1}$) and kept at -20°C . The leaf area was calculated according to the dimensions of the glass slides used for isolation and their number. The same procedure was applied for all replicates. As standards served long chain alkanes, alcohols (eg. cetyl alcohol (C_{16}), heptadecanol (C_{17}), octadecanol (C_{18}), eicosanol (C_{20}), docosanol (C_{22})), acids (eg. heptadecanoic acid (C_{17}), stearic acid (C_{18}), nonadecanoic acid (C_{19}), arachidic acid (C_{20})), esters (eg. ethyl stearate (C_{20}), methyl bohenate (C_{23}), methyl tricosanoate (C_{24}), methyl octacosanoate (C_{29})).

5.3 Isolation of EWs for imaging

The cryo-adhesive method was selected as a sampling method for all imaging analysis according to the procedure presented in the section 5.2. With the modification considering the volume of water used as a transfer medium, that was adequate to the leaf area dimensions. As a sample target were used (1) developed in the lab ZnS plates (FT-IR and Raman/CARS), (2) commercially available MALDI plate for imaging experiments (Waters; Micromass, Manchester, UK) and (3) Si wafers (SIMS). The leaf area used for imaging experiments depended on the target dimensions and for most experiments was as following (1) 10mm x 10 mm for FT-IR and Raman/CARS, (2) 20mm x 20 mm for MALDI-MS and (3) 5mm x 5 mm for SIMS imaging. For the FT-IR, Raman and SIMS imaging, the EW samples were directly used for the analysis, without any treatments.

5.4 Isolation of EWs *in vivo*

EWs were isolated *in vivo* using a new method, which employs commercially available transparent adhesive tape (PVC foil with an adhesive material, adhesive power: 2.2 N cm^{-1} , 50 mm breadth, Lux GmbH&Co.KG). Adhesive tape was 5 cm breadth and was cut with scissors into ca. 10-13 cm pieces (1/4 larger than the leaf size), which were subsequently placed on the adaxial or abaxial leaf side. The tape was gently pressed on the leaf with the special care to bring into close contact both surfaces – the adhesive tape and the leaf along the whole leaf area. Afterwards, the tape with adhered EWs was removed and the procedure was repeated with the fresh tape. The tape transparency allowed to instantly view the EW imprint (**Fig. 9**), which in turn allowed to evaluate the EW removal efficiency and optimize the number of treatments (usually 5-7 times). During the optimization procedure, de-waxed

leaves were examined under light microscope (Stemi SV 11 with Axio Cam HRc camera, Carl Zeiss, Germany) and high resolution SEM to examine potential mechanical damages including removal of trichomes during the applied procedure. EWs were also isolated *in vivo* using gum arabic treatment according to (Buschhaus et al., 2007; Jetter and Schäffer, 2001). An aqueous suspension (1 g mL^{-1}) of gum arabic powder (Acros Organics) was applied on the entire leaf surface with the help of small paintbrush. After 1-1.5 h the polymer dried and could be removed from the leaves, special care was taken not to damage the leaves after applying subsequent treatment. Both *in vivo* isolation procedures were performed in the growth chamber.

For comparison of new sampling method with the established one, intracuticular waxes were extracted twice for 2 minutes with the organic solvent (CH_2Cl_2) after mechanical removal of EW layer. Three methods were employed (1) adhesive tape embedding (2) cryo-adhesive and (3) gum arabic method.

5.5 Insect rearing

Chrysomela populi leaf beetles were collected from the local forests around Jena and afterwards cultivated in ventilated, transparent boxes (20 x 20 cm) lined with moist tissue paper. Boxes were kept at 20°C, 43% air humidity at 14 h light and 10 h dark photoperiod. During autumn and winter season insects were not active and were kept at lower temperature (12°C). Beetles were constantly supplied with fresh *P. trichocarpa* foliage; no starving period was used, also before behavioural experiments.

5.6 Insect behavioral bioassay

Adults of *Chrysomela populi*, representing a specialist herbivore on Poplar plants, were used for dual choice bioassays. EWs were removed *in vivo* using adhesive tape, as well as gum arabic method. Each experimental pair consisting of one intact leaf and one de-waxed leaf was chosen from the opposite sides of the same stem in order to ensure their similar developmental stage. Leaves were harvested, inserted into a signed 2 mL Eppendorf tube filled with water and placed in ventilated, transparent boxes (20 x 20 cm). The bottom of the boxes was covered with the moist tissue paper, which additionally provided relatively high humidity. In each box, leaf pairs and eight insects were placed. Boxes were kept in the darkness, keeping other conditions the same as during insect rearing. For *in vivo* bioassay, leaves were not detached from the plants and insects were trapped through the whole

experiment (**Fig. 15**). Although traps were covering the leaves, they gave insects the opportunity of movement and choice between untreated and treated half of the leaf. After the bioassay, leaves were scanned and consumed leaf area was calculated using Adobe Photoshop software (version 12.0, Adobe Systems, Inc.) or alternatively leaves before and after the bioassay were weighted (XS 205 DualRange, Mettler Toledo). All weight measurements were done on balance with accuracy of 10 µg. The significance of differences in consumed leaf area between intact and de-waxed leaves in all experiments was determined by paired *t*-test (R software, version 2.12.2).

5.7 Insect feeding bioassay for FT-IR imaging experiments

Specialist herbivore on Poplar plants - *Chrysomela populi* adults were used for feeding experiments. Plants were 4-5 months old and kept during bioassay in the same conditions as their cultivation, however in the separate chamber. Insects were trapped in a single leaf (not detached from the plant) using envelope shaped traps made from the commercially available nets for insects (Fliegengitter, Tesa). Light access was thus not disturbed as well as the additional mechanical stress on the plant was excluded, since single trap weighted around 6 g and was externally supported by the ropes. Starting point for the time dependent experiments was defined as a moment when insects were removed from the leaves. The experiments were controlled in that manner, that damage done by insects' feeding did not exceed 25-35% of total leaf area. The mechanical damage was performed by the mechanical caterpillar – MecWorm (Mithöfer et al., 2005) and the damage area was comparable with that done by the insects' feeding. Each plant was used for experiments only once; after collecting leaves from the plant for defined time period, plant was not used further. For each defined time point (**1h, 6h, 24h, 72h**), EWs were isolated from 4-5 damaged leaves and repeated for at least 5 plants, except of 72h and 15 days, which was repeated for 3 plants.

5.8 GC – MS / Electron ionization

GC-MS analyses were performed on a gas-chromatograph coupled to mass spectrometer equipped with EI and quadruple analyser (Thermo Quest Finnigan TraceMS). Three types of column were used: DB-1ms (100% Dimethylpolysiloxan, 30 m x 0.25 mm, film thickness 0.25 µm, Alltech), relatively more polar DB-5ms (5% Phenyl, 95% Dimethylpolysiloxan, 15 m + 10 m precolumn x 0.25 mm, film thickness 0.25 µm, Phenomenex) and midpolar fused silica capillary column Rtx-200MS (Crossbond trifluoropropylmethyl polysiloxane, 30 m x 0.25 mm, film thickness 0.25 µm, Restek). Through usage of columns that differ in polarity,

better chromatographic resolution of compounds present in the complex mixture was achieved. Mass spectra were acquired from 60 to 600 m/z 1 μl of sample was injected in a split (1/10) mode. The injector temperature was 260°C and helium as a carrier gas at a constant flow rate of 1.5 mL min^{-1} was used, detector voltage was 350 V. The temperature program was as follow: 65°C (1 min), then 30°C min^{-1} to 150°C, 8°C min^{-1} to 220°C (hold time 1 min), 5°C min^{-1} to 300°C (hold time 2 min), 10°C min^{-1} to 320°C (3 min). Wax compounds containing hydroxyl group were transferred to the corresponding trimethylsilyl derivatives. Samples were incubated in 10 μl MSTFA and 5 μl pyridine for 30 min in 70°C with constant shaking. In parallel, the same procedure was performed for a blank sample (only MSTFA and pyridine). Pure CH_2Cl_2 served as a blank sample. Identification of wax compounds was based on their mass spectra, fragmentation pattern, literature data and co-injected standards. Relative quantification was done using external standards: eicosane and 1-hexadecanol in an end concentration of 1 $\mu\text{g mL}^{-1}$ each. Both were added to the samples just after the isolation procedure. All standards were purchased from Sigma Aldrich and organic solvents from Carl Roth GmbH (99.9%, HPLC grade).

5.9 GC – MS / Positive chemical ionization

Soft ionization was performed using positive chemical ionization (PCI) with either methane or isobutene as a reagent gas. For those measurements, a mass spectrometer equipped with ion trap analyser (Thermo Scientific, Trace GC Ultra ITQ 900) was used. Flow rate of reagent gas and ion source temperature were optimized and reached value of 0.8 mL min^{-1} and 200°C, respectively. Spectra were acquired in a positive mode in the mass range from 50 to 650 m/z . Temperature program and other settings were according to the description for EI ionisation.

5.10 LC-MS

Sample preparation was performed according to the same protocol as for GC-MS and MALDI-TOF-MS, with the modification that EW imprints were washed from the glass slides in MeOH. Solvent was evaporated, dry mass calculated and samples were dissolved in MeOH- H_2O (8:2) to required concentration (0.1 – 10 mg mL^{-1}). For the whole leaf extraction, leaves freshly harvested from the plant were weighted and crushed in mortar in MeOH- H_2O (8:2). The supernatant was collected to Eppendorf tubes, and centrifuged twice for 10 min (8 000 rpm) and eventually transferred to HPLC vials. Metabolites were separated

by LCMS (LCQ, Finnigan, Thermo Scientific), on a Grom-Sil ODS-3 column (125x2x3 μm , Alltech Grom) with solvents (A) H_2O -THF- FA (97.7:1.8:0.5) and (B) ACN, eluted with gradient program of 10 % B 10 min; 0% B after 11 min. with the flow rate of 0.3 mL min^{-1} . An injection volume of $10 \mu\text{l}$ was used. The eluent was monitored with a DAD detector at 268 nm. The retention time and mass spectrum was compared with standard: D (-)-salicin ($20 \mu\text{g mL}^{-1}$) (Sigma Aldrich).

5.11 MALDI-TOF-MS

The spectra were acquired using a MALDI micro MX mass spectrometer (Waters; Micromass, Manchester, UK) operating in a reflectron mode and positive polarity. EW compounds were ionized and desorbed with a nitrogen UV laser (337 nm, 4 ns laser pulse, firing rate 10 Hz, max 280 μJ per laser pulse, 10 shots per spectrum). Ions were recorded from 200 to 1500 m/z , matrix ions (below 200 m/z) were suppressed, and 70 scans were co-added. Data acquisition and data processing were done with a help of software package Mass Lynx V4.0, (Waters; Micromass, Manchester, UK). Stainless steel MALDI plate (Waters; Micromass, Manchester, UK) served as a target and was cleaned by sonication in MeOH and subsequently in Me_2CO , hexane and CH_2Cl_2 before each usage. For external calibration of mass spectrometer mixture of PEG 600 and PEG 1000 ($1 \mu\text{g mL}^{-1}$ in Me_2CO , Sigma Aldrich) was used. $^7\text{LiDHB}$ prepared from DHB (Sigma Aldrich) and Lithium ^7Li hydroxide (Sigma Aldrich) according to the protocol (Cvačka et al., 2006) was applied as a matrix (10 mg mL^{-1}) in Me_2CO for calibration and in CH_2Cl_2 : Me_2CO (1:1) for sample analysis. All compounds were detected as lithiated (^7Li) adducts. Samples in CH_2Cl_2 were spotted on a target using different sampling techniques (mix technique, Sa/Ma, Ma/Sa, Ma/Sa/Ma), the best results gave “sandwich” technique: matrix, sample, matrix ($0.8 \mu\text{l}$ of 10 mg mL^{-1} each). Six parallel spots were made for each sample and subsequently measured.

5.12 MALDI – TOF – MS imaging

MALDI-TOF-MS imaging requires application of matrix, therefore EW imprint on the MALDI plate was covered homogeneously by the $^7\text{LiDHB}$ matrix solution prepared in Me_2CO : CH_2Cl_2 (9:1, vol/vol) at a concentration of 20 mg/mL . The samples were sprayed from a distance of around 150 mm using a commercial airbrush. Since the matrix was dissolved in a mixture of organic solvents that may dissolve EWs as well, care was taken to keep the appropriate distance and not cause dislocation of analytes by matrix application.

The number of laser shots per pixel for samples coated with DHB was 150 (130 J/shot). The samples were imaged using 200 μ m resolution. The range of the measured masses was set from 250 to 1000 Da. Data were collected with MassLynx 4.0 with a custom-made software MALDI Image Converter (Waters, UK) to obtain spatially differentiated data. Biomap software (Novartis, Switzerland) was employed to generate ion intensity maps. The experiments were performed with 5 replicates.

5.13 Scanning Electron Microscopy (SEM)

EW imprints were prepared on the following sample targets: (1) stainless steel discs (diameter 2 cm), (2) ZnS sample target (FT-IR analysis), (3) standard microscopic glass slides (EW thickness measurements), (4) adhesive tape, (5) gum arabic polymer, (6) Si wafers (SIMS analysis) Imprints were done using three methods, (1) cryo-adhesive with water as a transfer medium, (2) new method – adhesive tape embedding (3) gum arabic method. For trichomes assessment, leaves after the isolation procedures were examined. Samples after SIMS analysis were prepared on Si wafers. All sample targets with EW imprints as well as de-waxed leaves were mounted on the aluminum holders, sputter coated with ca. 10 nm of gold (Bal-Tec SCD005 sputter coater; 60 mA, 10s) and examined by SEM (LEO Gemini 1530) at 1.5 kV. For the evaluation of the new isolation method, particularly considering trichome density, more than 60 micrographs were acquired.

5.14 FT-IR spectroscopy

IR spectra in a transmission mode were recorded on a Bruker FT-IR microspectrometer coupled to a liquid nitrogen cooled the mercury/cadmium telluride detector and linked to a Equinox spectrometer (Bruker Optics, Ettlingen, Germany). ZnS windows, which are infrared-transparent polished crystals, were used for all FT-IR measurements (Crystal, Berlin, Germany). ZnS windows with a diameter of 20mm, thickness of 1mm were fixed in the aluminium plates with the dimension 45x50 mm. Samples were measured in a 700-4000 cm^{-1} range with a spectral resolution of 2 cm^{-1} and 150 scans for a background and 150 scans for samples were co-added. The background spectrum was measured at a position outside the sample. Spectra were recorded using 80x80 μm square aperture size. The interferograms were converted to frequency by standard Fourier transform processing. All spectra were converted from transmittance to absorbance spectra. Software package OPUS 6.5 supplied by Bruker, was used for data acquisition and data processing.

Due to thin EW layer and therefore relatively weak absorbance signals in the IR spectrum, the initial experiment aimed to obtain highly concentrated sample, therefore EW imprints obtained in the cryo-adhesive method were washed with organic solvent, concentrated by removing solvent and spotted on ZnS substrate. In the second experiment, wax imprints from the leaves damaged by insects were isolated on the ZnS substrate, subsequently point measurements were done within one sample on varying distances from the injury boarder, so the spectra could be directly compared. In the third approach, a defined area was scanned for the chemical mapping.

5.15 FT-IR spectroscopy imaging

Images of wax imprints were recorded in a transmission mode with 80 μm step size in x and y direction using controlled by the software motorized stage. For majority of measurements an area of ca. 1500x1500 μm was scanned creating a 20x20 pixel map. Hyperspectral data were collected using FT-IR microspectrometer at 80 μm lateral resolution and spectral resolution of 4cm^{-1} and 50 scans for a background and 50 scans for samples were co-added. In order to minimize contribution of signals from atmospheric constituents (water vapour, CO_2) during long term mapping, background was repeatedly recorded after each 8 measurement point. Raw spectra were transformed to series of pseudo-color chemical maps collected at particular wavelengths or as spectra acquired for individual pixels. All spectra converted from transmittance to absorbance passed tests for the spectral quality; therefore death pixels are not observable in the chemical maps. Software package OPUS 6.5 supplied by Bruker for data acquisition and signal intensity color maps were generated using OPUS 6.5 or CytoSpec 2.00.01.

5.16 Hierarchical Cluster Analysis (HCA)

Before HCA analysis, raw spectroscopic data sets were de-noised by Savitzky-Golay algorithm (13 smoothing points) and baseline corrected. Spectra were subsequently transformed to second derivatives, which help to eliminate anomalous spectral readings due to instrumental variations as well as to extract subtle variations in spectral features among spectra. Subsequent normalization process allowed stressing the differences not in the intensities but in the shapes of the spectra. This in turn allowed to cluster pixels in terms of qualitative classification and not quantitative. Hierarchical cluster analysis of hyperspectral data are displayed as HCA images. Clusters are colour encoded; the coordinates from which a spectrum was collected is indicated in the given color. Mean cluster spectra were calculated

by averaging original (not second derivatives) spectra within single cluster and they represent the chemical composition of all spectra in a cluster. Distance matrix was computed using D-Values method and Ward's algorithm was chosen as a clustering method. Chemical mapping and HCA were performed using IR spectral imaging software (CytoSpec, version 2.00.01).

5.17 Raman and CARS (coherent anti-Stokes Raman scattering) microscopy imaging

Raman spectra were acquired with a Raman microspectrometer (Horiba-Jobin-Yvon, model LabRam). For excitation, the 532 nm, 633 nm HeNe laser (4mW-10 mW at the sample) and 1064 nm was used. The parameters were as follow: slit - 100 μm , exposure time - 10 seconds, 10x – 100x objectives.

The CARS signal was collected in forward (F-CARS) and in epi direction. Images at the different wavelengths around the calculated Raman resonance were recorded, for image generation each pixel was averaged eight times. Both the pump and the Stokes beam were spatially and temporally overlapped and subsequently coupled into a laser scanning microscope (Carl Zeiss, Germany). Short pulse laser source consists of a Ti:sapphire laser (Mira HP Coherent, USA) pumped by a Nd:vanadate laser (Verdi-V 18 Coherent, USA) at 532 nm. The OPO (optical parametric oscillator) generated laser wavelengths around 670 nm with an output power of 48mW - 173 mW. Filters: 2x600, 1x610, 1x630 were used in order to eliminate all higher than required wavelengths. The laser radiation was focused onto the object plane by a 50x objective.

5.18 TOF – SIMS imaging

TOF-SIMS was performed on a TOF.SIMS5 instrument (ION-TOF GmbH, Münster, Germany) The spectrometer is equipped with Bi cluster primary ion source and a reflectron type time-of-flight analyzer. UHV base pressure was $< 5 \times 10^{-9}$ mbar. For high mass resolution the Bi source was operated in the 'high current bunched' mode providing short Bi^+ or Bi_3^+ primary ion pulses at 25 keV energy and a lateral resolution of approx. 4 μm . The pulse length of 1.1 to 1.3 ns allowed high mass resolution. The primary ion beam was raster across 700x700 μm , 500x500 μm and 100x100 μm sample area, and 700x700, 128x128 and 100x100 data points were recorded. Images larger than the maximum deflection range of the primary ion gun were obtained using the manipulator stage scan mode with a lateral resolution of 100 pixel/mm. Primary ion doses were kept below 10^{11} ions/cm² (static SIMS limit). Spectra were calibrated on the C^- , C_2^- , C_3^- , or on the C^+ , CH^+ , CH_2^+ , and CH_3^+ peaks.

Based on these datasets the chemical assignments for characteristic fragments were determined. The experiments were performed with 5 biological and 2 technical replicates for 700x700 μm area, 1 biological replicate for 500x500 μm area and 3 biological replicates for 100x100 μm area. Following standards were implemented: hexacosanoic acid, ethyl stearate, methyl tricosanoate, 1-hexacosanol, tetracosane (Sigma Aldrich).

5.19 TOF - SIMS data analysis

The first set of signal intensity color maps were generated using SurfaceLab 6.3 (ION-TOF GmbH, Münster, Germany). The signal intensity color maps for each m/z value were further reconstructed using the HOT (black-to-yellow) color scheme available in the R `dcmriS4` package (version 0.20.1).

The preprocessing and statistical analysis of all the datasets were performed using R (version 3.0.2). Each dataset comprised of detected m/z values. A single mass file comprised of meta data containing the image dimensions as well as the co-ordinate information and intensity values arranged column wise.

Intensity thresholding was performed in order to segment foreground and background and achieve better visualization of the compound aggregation and their spatial distribution for given m/z values. For the thresholding 0.5 units of the most intense signal was selected, all the signals below this threshold were considered as a background.

In order to validate association within EW compounds, correlation analysis were performed for detected ions. Within each group, the correlation coefficient (r) was calculated to give an indication of the strength of the relationship between m/z values. Positive correlation coefficient corresponds to positive correlation $r = 0.1 - 0.3$ corresponds to small, $r = 0.3 - 0.5$ corresponds to medium, $r = 0.5 - 1.0$ corresponds to strong correlation between two analyzed ions. Negative values would indicate negative correlation.

The scatter plot matrix representing the correlation analysis was generated using the `cpairs()` function in the R `gclus` package (version 1.3.1). The color scheme used in the scatter plot matrix represents the highest and the lowest correlation amongst variables. The highest correlations are between variables that are closest to the principal diagonal and are represented in pink. The variables having lowest correlation are far from the principal diagonal and are represented in yellow.

6. Supplementary materials

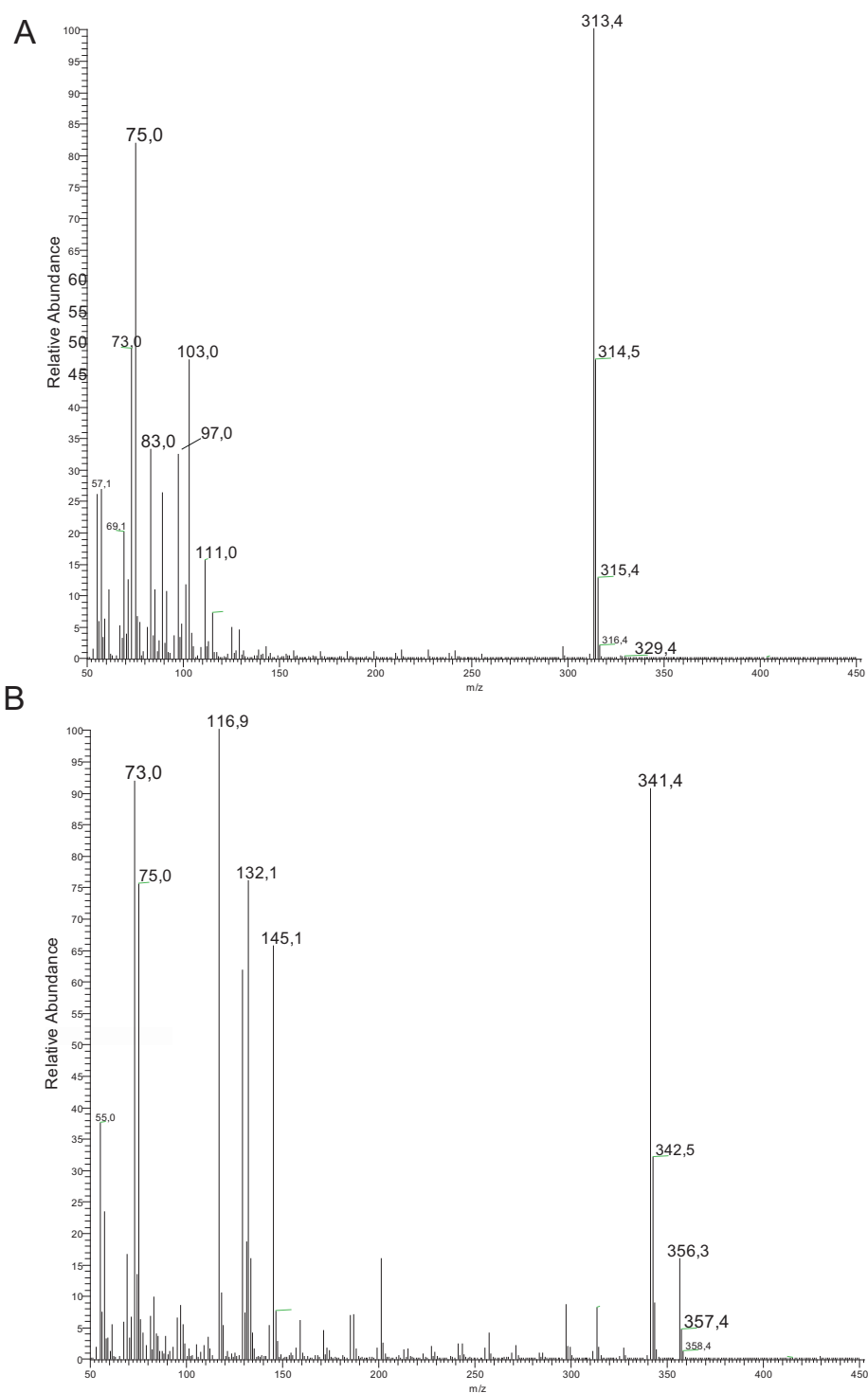


Fig. S1 GC-MS spectra of representative standards (A) heptadecanol (B) stearic acid. Characteristic fragmentation pattern (m/z values as well as signal intensities) of alcohols and fatty acids allowed differentiating those groups of compounds.

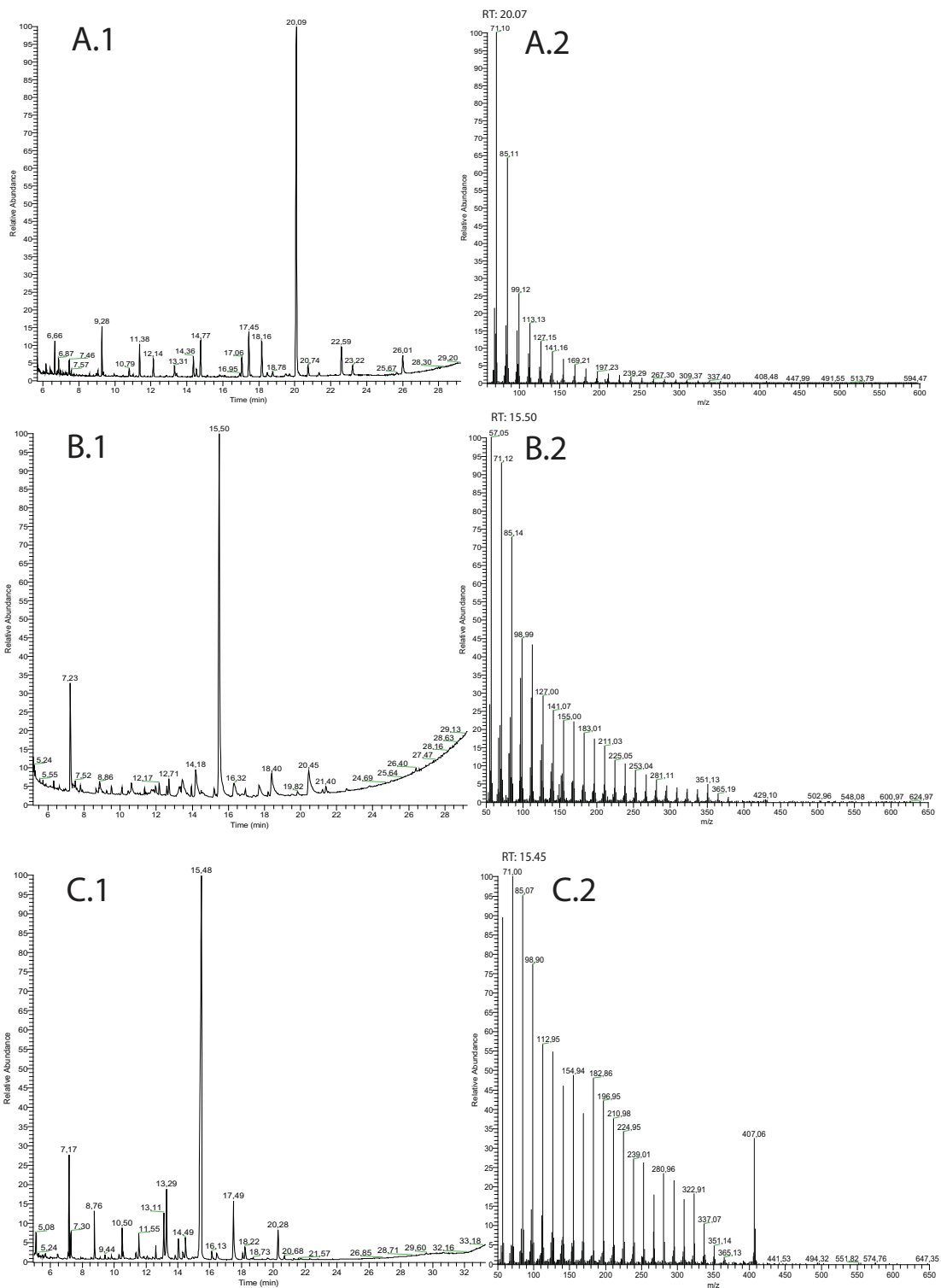


Fig. S2 GC chromatograms and MS spectra of *P. trichocarpa* EWs (adaxial side). EI Quadrupole detector. DB-5 ms column (A.1), fragmentation pattern for nonacosane C₂₉ (A.2). EI Ion Trap detector. Rtx-200MS column (B.1), fragmentation pattern for nonacosane C₂₉ (B.2). PCI Ion Trap detector. Rtx-200MS column (C.1), fragmentation pattern for nonacosane C₂₉ (C.2).

GC-MS					MALDI-TOF-MS			
Chain length	Fatty acids	Alkanes	Alkenes	Alcohols	Alkanes	Alcohols	Chain length	Esters
13	tr	-	-	-	-	-	40	7,87±0,29
14	tr	-	-	-	-	-	41	0,39±0,11
15	tr	-	-	-	-	-	42	2,85±0,30
16	3,44±1,05	-	-	tr	-	-	43	0,52±0,06
18	3,90±1,53	-	-	-	-	-	44	6,62±1,52
23		2,74±1,34	-	-	tr	-	45	1,26±0,14
24			-	6,14±1,77	tr	1,34±0,04	46	16,10±0,73
25	-	9,32±3,67	2,80±0,78		tr	0,73±0,22	47	1,82±0,25
26	-		-	2,0±0,49	tr	2,58±0,36	48	10,58±0,38
27	-	6,77±2,20	3,75±0,92		tr	0,58±0,12	49	1,51±0,24
28	-	-	-	1,74±0,47	-	6,95±0,52	50	2,21±0,07
29	-	42,65±6,66	0,90±0,32		6,26±1,18	1,46±0,18	51	0,29±0,11
30	-		-	2,42±0,65	2,80±0,43	12,19±1,19	52	1,00±0,07
31	-	2,22±1,23	-		3,69±0,35	1,28±0,15	53	0,17±0,01
32	-		-		1,24±0,07	1,26±0,06	54	0,51±0,04
33	-		-		0,39±0,05	0,71±0,16	56	tr
34	-		-		0,30±0,06	tr		

Table S1 Relative abundance of individual homologues [%] detected by GC-MS and MALDI-TOF-MS in EWs isolated from the adaxial side of *P. trichocarpa* leaves using cryo-adhesive method, (tr – traces). Mean value ± S.D., n=6.

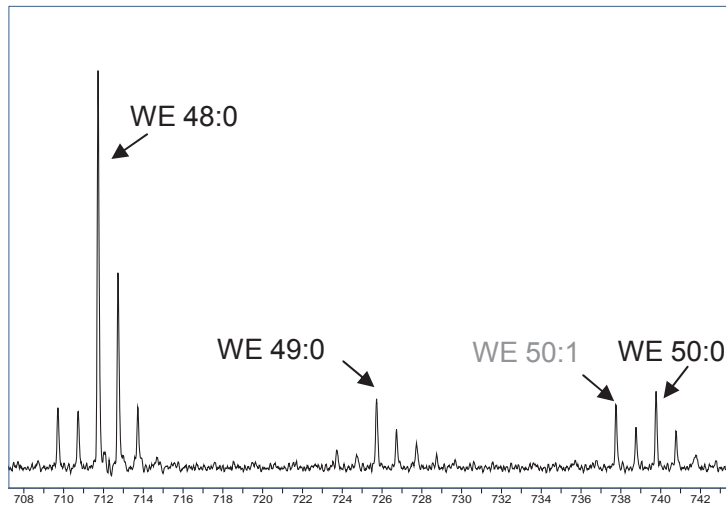


Fig. S3 Isotopic pattern of wax esters detected by MALDI-TOF-MS. An arrow indicate presence of signals that may correspond to unsaturated wax esters. Their signal intensity is comparable with the signal intensity of signals assigned to saturated wax ester and m/z difference corresponds to absence of 2 hydrogen atoms.

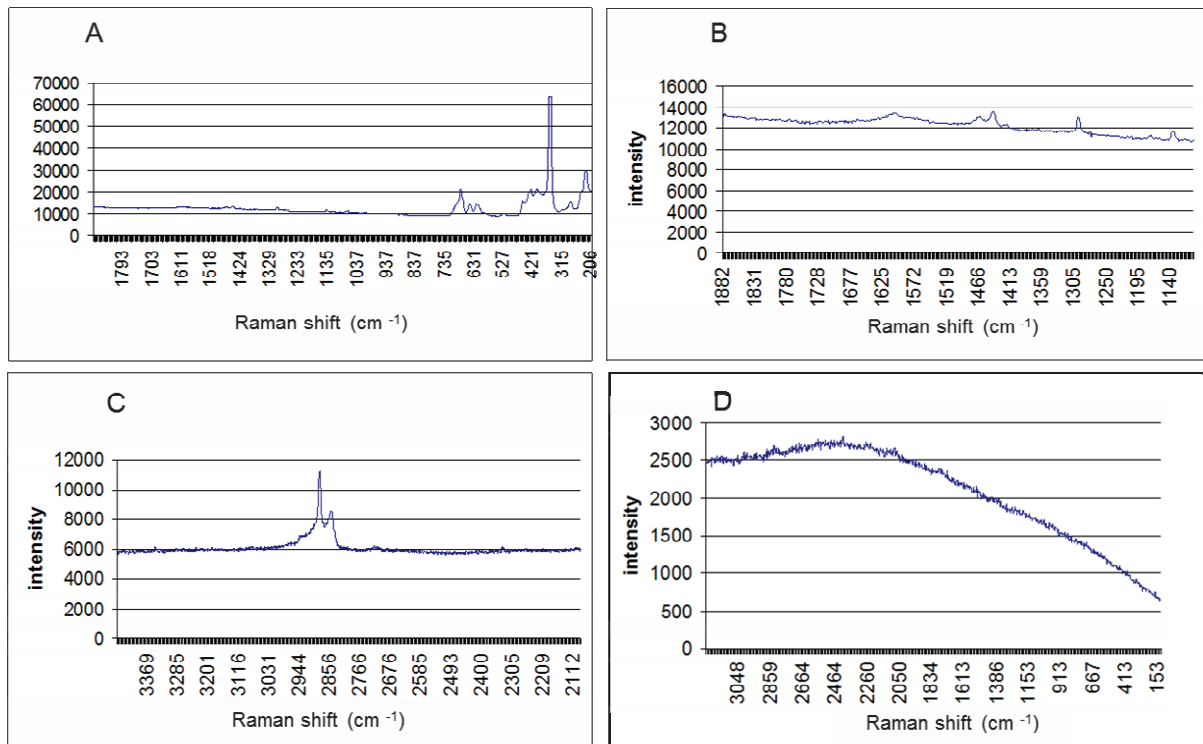


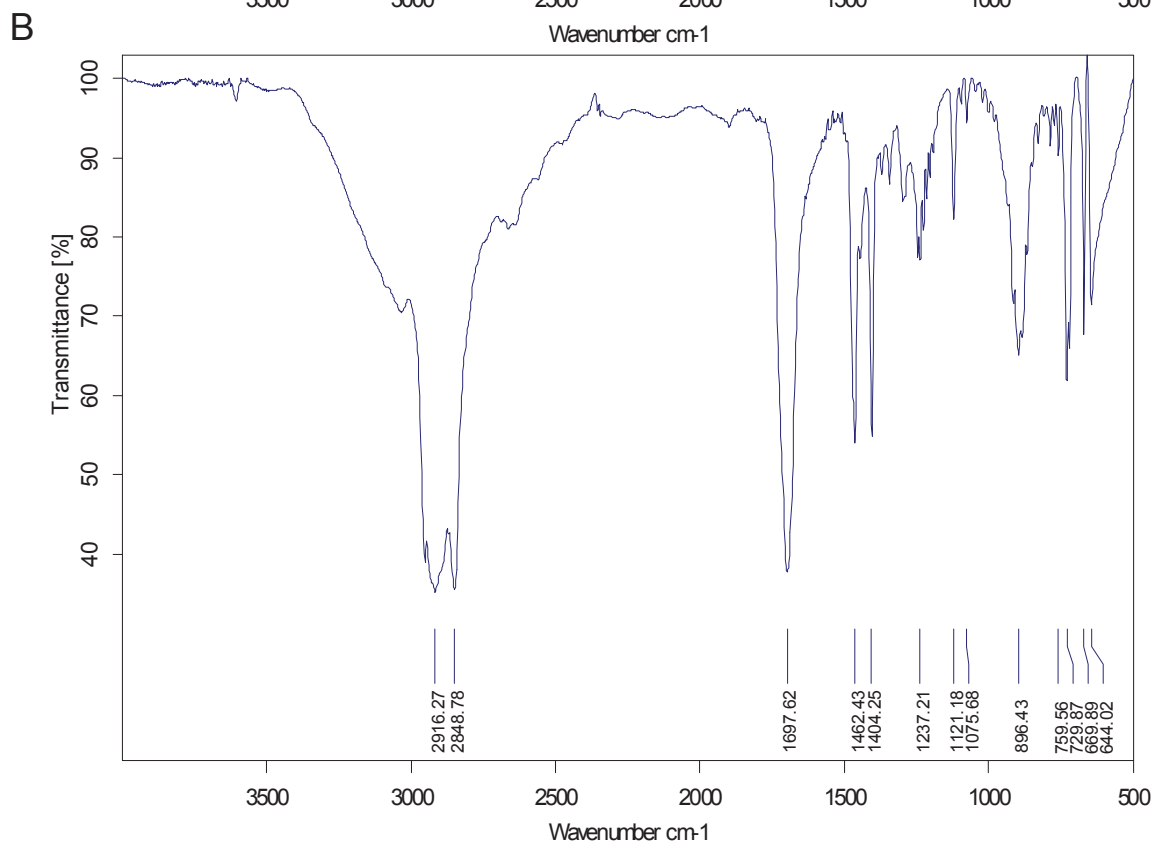
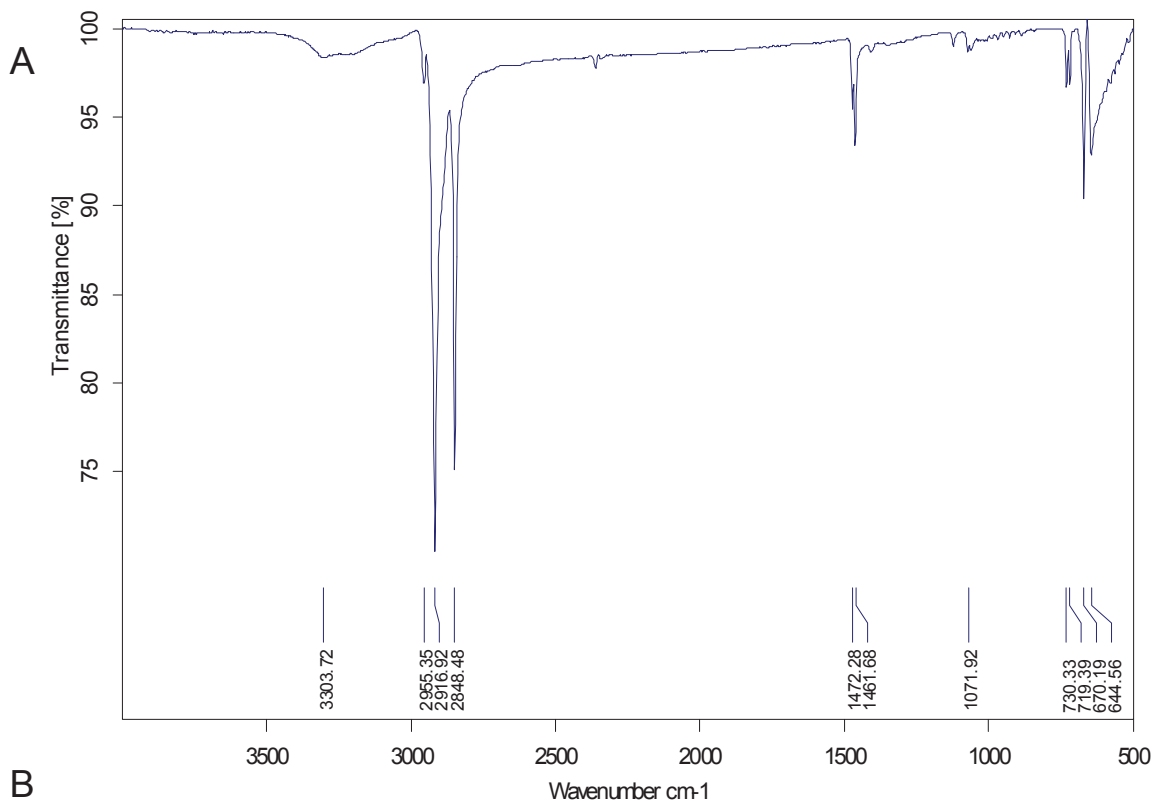
Fig. S4 FT-Raman spectrum of *P. trichocarpa* EW imprint, adaxial side (A – C) and abaxial side (D), laser wavelength - 532 nm.

Vibration/Assignment	Raman shift / wavenumber (cm ⁻¹)	Intensity
= C-H	3008	Not present
ν asym C-H lipids	2881 2848	Strong Strong
ν C = O	1750	Not present
ν C = C cis lipids	1659	Not present
ν C = C	1504	Not present
δ (CH ₃)	1461	Weak
δ (CH ₂) deformation	1443	Weak
t(CH ₂) twisting	1296 1171	Weak Weak
ν C-C	1089	Weak

Table S2. Vibrations detected by Raman microspectroscopic analysis of EWs from *P. trichocarpa*. Excitation with the laser wavelength - 532 nm.

Vibration/Assignment	Raman shift /wavenumber (cm ⁻¹)	Intensity
ν asym C-H lipids (fatty acids)	2881 2848 2840	Strong Strong Medium
ν C-C	2721	Weak
ν C=C cis lipids	1659	Weak
ν C=C	1504	Weak
δ (CH ₃)	1461	Weak
δ (CH ₂) deformation	1440 1416	Weak Weak
t(CH ₂) twisting	1296 1171	Weak Weak
ν C-C	1132 1062 1032	Weak Weak Weak

Table S3. Vibrations detected by Raman microspectroscopic analysis of EWs from *P. trichocarpa* (adaxial side). Excitation with the laser wavelength - 1064 nm and 633 nm.



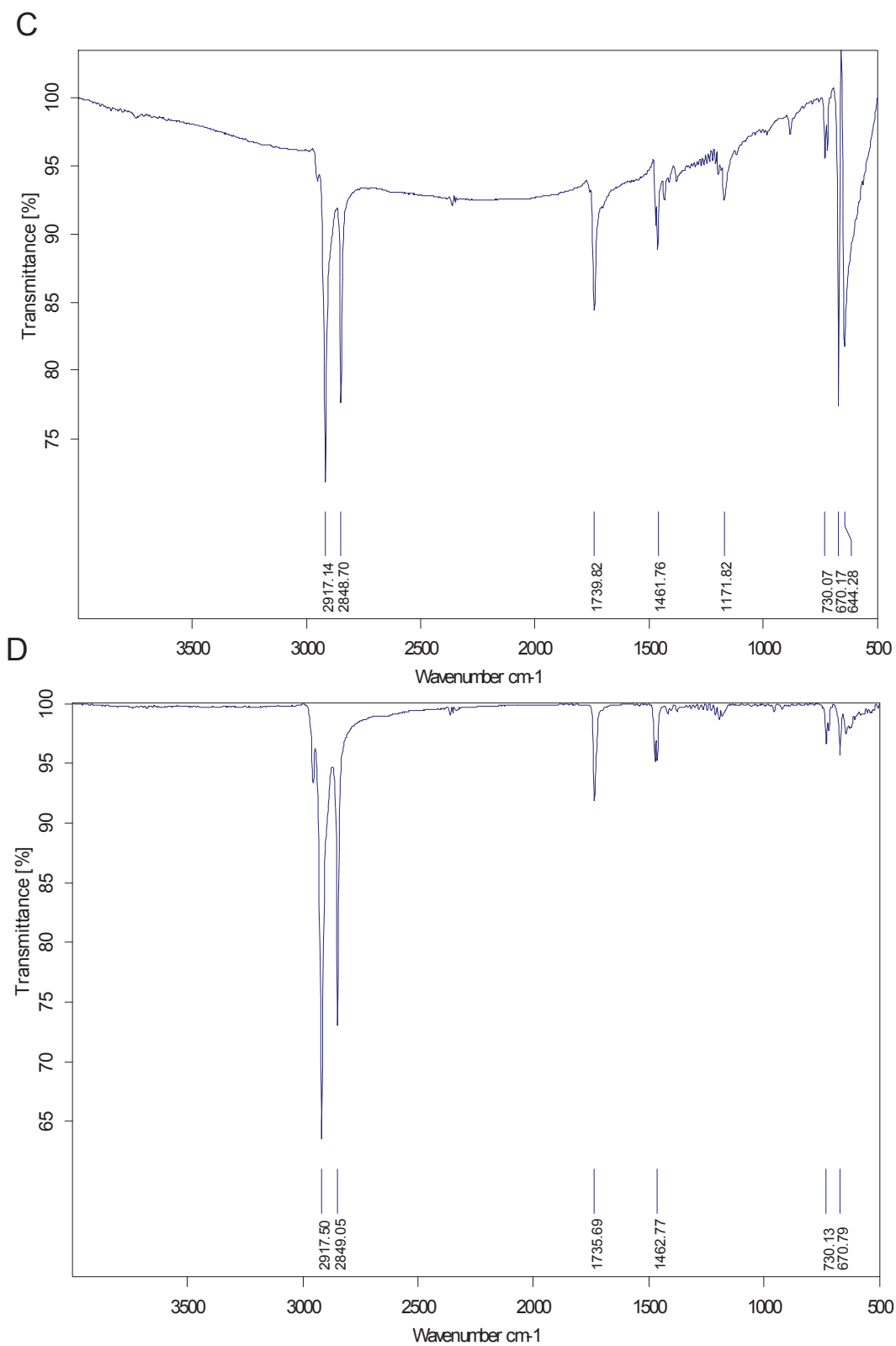


Fig. S5 FT-IR spectra of representative standards (A) octacosanol (B) octacosanoic acid (C) methyl octacosanoate (D) stearyl arachidate.

7. References

- Adati, T., Matsuda, K., 1993. Feeding Stimulants for Various Leaf Beetles (Coleoptera:Chrysomelidae) in the Leaf Surface Wax of Their Host Plants. *Applied Entomology and Zoology* 28, 319-324.
- Alfaro-Tapia, A., Verdugo, J. A., Astudillo, L. A., Ramírez, C. C., 2007. Effect of epicuticular waxes of poplar hybrids on the aphid *Chaitophorus leucomelas* (Hemiptera: Aphididae). *Journal of Applied Entomology* 131, 486-492.
- Amstalden van Hove, E. R., Smith, D. F., Heeren, R. M., 2010. A concise review of mass spectrometry imaging. *Journal of Chromatography A* 1217, 3946-3954.
- Anton, L. H., Ewers, F. W., Hammerschmidt, R., Klomparens, K. L., 1994. Mechanisms of Deposition of Epicuticular Wax in Leaves of Broccoli, *Brassica oleracea* L. var. *capitata* L. *New Phytologist* 126, 505-510.
- Arrondo, J. L. R., Goñi, F. M., 1999. Structure and dynamics of membrane proteins as studied by infrared spectroscopy. *Progress in Biophysics and Molecular Biology* 72, 367-405.
- Baker, E. A., Holloway, P. J., 1970. Scanning electron microscopy of waxes on plant surfaces. *Micron* (1969) 2, 364-380.
- Barron, C., Parker, M. L., Mills, E. N. C., Rouau, X., Wilson, R. H., 2005. FTIR imaging of wheat endosperm cell walls in situ reveals compositional and architectural heterogeneity related to grain hardness. *Planta* 220, 667-677.
- Barthlott, W., 1998. Classification and terminology of plant epicuticular waxes. *Botanical Journal of the Linnean Society*.
- Barthlott, W., Neinhuis, C., 1997. Purity of the sacred lotus, or escape from contamination in biological surfaces. *Planta* 202, 1-8.
- Benabdellah, F., Seyer, A., Quinton, L., Touboul, D., Brunelle, A., Laprèvote, O., 2010. Mass spectrometry imaging of rat brain sections: nanomolar sensitivity with MALDI versus nanometer resolution by TOF-SIMS. *Analytical and Bioanalytical Chemistry* 396, 151-162.
- Bergner, G., Chatzipapadopoulos, S., Akimov, D., Dietzek, B., Malsch, D., Henkel, T., Schlücker, S., Popp, J., 2009. Quantitative CARS Microscopic Detection of Analytes and Their Isotopomers in a Two-Channel Microfluidic Chip. *Small* 5, 2816-2818.
- Bernard, A., Joubes, J., 2013. Arabidopsis cuticular waxes: advances in synthesis, export and regulation. *Progress in Lipid Research* 52, 110-129.
- Bernays, E. A., Blaney, W. M., Chapman, R. F., Cook, A. G., 1976. The Ability of *Locusta migratoria* L. to Perceive Plant Surface Waxes. In: Jermy, T. (Ed.), *The Host-Plant in Relation to Insect Behaviour and Reproduction*. Springer US, pp. 35-40.
- Bhushan, B., Jung, Y. C., Koch, K., 2009. Self-Cleaning Efficiency of Artificial Superhydrophobic Surfaces. *Langmuir* 25, 3240-3248.
- Bianchi, G., Avato, P., Scarpa, O., Murelli, C., Audisio, G., Rossini, A., 1989. Composition and structure of maize epicuticular wax esters. *Phytochemistry* 28, 165-171.
- Blenn, B., Bandoly, M., Küffner, A., Otte, T., Geiselhardt, S., Fatouros, N., Hilker, M., 2012. Insect Egg Deposition Induces Indirect Defense and Epicuticular Wax Changes in *Arabidopsis thaliana*. *Journal of Chemical Ecology* 38, 882-892.
- Bodnaryk, R. P., 1992. Leaf epicuticular wax, an antixenotic factor in Brassicaceae that affects the rate and pattern of feeding of flea beetles, *Phyllotreta cruciferae* (Goeze). *Canadian Journal of Plant Science. Revue Canadienne de Phytotechnie* 72, 1295-1303.

- Bradshaw, H. D., Ceulemans, R., Davis, J., Stettler, R., 2000. Emerging Model Systems in Plant Biology: Poplar (*Populus*) as A Model Forest Tree. *Journal of Plant Growth Regulation* 19, 306-313.
- Brunner, A. M., Busov, V. B., Strauss, S. H., 2004. Poplar genome sequence: functional genomics in an ecologically dominant plant species. *Trends in Plant Science* 9, 49-56.
- Buda, G. J., Barnes, W. J., Fich, E. A., Park, S., Yeats, T. H., Zhao, L., Domozych, D. S., Rose, J. K. C., 2013. An ATP Binding Cassette Transporter Is Required for Cuticular Wax Deposition and Desiccation Tolerance in the Moss *Physcomitrella patens*. *The Plant Cell*.
- Buschhaus, C., Herz, H., Jetter, R., 2007. Chemical composition of the epicuticular and intracuticular wax layers on the adaxial side of *Ligustrum vulgare* leaves. *New Phytologist* 176, 311-316.
- Buschhaus, C., Jetter, R., 2011. Composition differences between epicuticular and intracuticular wax substructures: How do plants seal their epidermal surfaces? *Journal of Experimental Botany* 62, 841-853.
- Cameron, K. D., Teece, M. A., Bevilacqua, E., Smart, L. B., 2002. Diversity of cuticular wax among *Salix* species and *Populus* species hybrids. *Phytochemistry* 60, 715-725.
- Carado, A., Passarelli, M. K., Kozole, J., Wingate, J. E., Winograd, N., Loboda, A. V., 2008. C60 secondary ion mass spectrometry with a hybrid-quadrupole orthogonal time-of-flight mass spectrometer. *Analytical Chemistry* 80, 7921-7929.
- Cervantes, D., Eigenbrode, S., Ding, H. J., Bosque-Pérez, N., 2002. Oviposition Responses by Hessian Fly, *Mayetiola destructor*, to Wheats Varying in Surfaces Waxes. *Journal of Chemical Ecology* 28, 193-210.
- Chapman, R. F., Bernays, E. A., 1989. Insect behavior at the leaf surface and learning as aspects of host plant selection. *Experientia* 45, 215-222.
- Chen, L., Carpita, N. C., Reiter, W.-D., Wilson, R. H., Jeffries, C., McCann, M. C., 1998. A rapid method to screen for cell-wall mutants using discriminant analysis of Fourier transform infrared spectra. *The Plant Journal* 16, 385-392.
- Cheng, J.-X., Volkmer, A., Xie, X. S., 2002. Theoretical and experimental characterization of coherent anti-Stokes Raman scattering microscopy. *J. Opt. Soc. Am. B* 19, 1363-1375.
- Coimbra, M. A., Barros, A., Rutledge, D. N., Delgadillo, I., 1999. FTIR spectroscopy as a tool for the analysis of olive pulp cell-wall polysaccharide extracts. *Carbohydrate Research* 317, 145-154.
- Cottle W., Kolattukudy P.E. 1982. Biosynthesis, Deposition, and Partial Characterization of Potato Suberin Phenolics. *Plant Physiology* 69, 393-399.
- Cvačka, J., Jiros, P., Sobotnik, J., Hanus, R., Svatoš, A., 2006. Analysis of insect cuticular hydrocarbons using matrix-assisted laser desorption/ionization mass spectrometry. *Journal of Chemical Ecology* 32, 409-434.
- Cvačka, J., Svatoš, A., 2003. Matrix-assisted laser desorption/ionization analysis of lipids and high molecular weight hydrocarbons with lithium 2,5-dihydroxybenzoate matrix. *Rapid Communication in Mass Spectrometry* 17, 2203-2207.
- de Boer, G., Hanson, F. E., 1988. The role of leaf lipids in food selection by larvae of the tobacco hornworm, *Manduca sexta*. *Journal of Chemical Ecology* 14, 669-682.
- DeBono, A., Yeats, T. H., Rose, J. K. C., Bird, D., Jetter, R., Kunst, L., Samuels, L., 2009. Arabidopsis LTPG Is a Glycosylphosphatidylinositol-Anchored Lipid Transfer Protein Required for Export of Lipids to the Plant Surface. *The Plant Cell Online* 21, 1230-1238.
- Dragota, S., Riederer, M., 2007. Epicuticular Wax Crystals of *Wollemia nobilis*: Morphology and Chemical Composition. *Annals of Botany* 100, 225-231.
- Dubis, E. N., Dubis, A. T., Morzycki, J. W., 1999. Comparative analysis of plant cuticular waxes using HATR FT-IR reflection technique. *Journal of Molecular Structure* 511-512, 173-179.

- Eigenbrode, S. D., Espelie, K. E., 1995. Effects of Plant Epicuticular Lipids on Insect Herbivores. *Annual Review of Entomology* 40, 171-194.
- Eigenbrode, S. D., Jetter, R., 2002. Attachment to Plant Surface Waxes by an Insect Predator. *Integrative and Comparative Biology* 42, 1091-1099.
- Eigenbrode, S. D., Kabalo, N. N., Rutledge, C. E., 2000. Potential of reduced-waxbloom oilseed Brassica for insect pest resistance. *Journal of Agricultural and Urban Entomology*. 17, 53-63.
- Ensikat, H. J., Neinhuis, C., Barthlott, W., 2000. Direct access to plant epicuticular wax crystals by a new mechanical isolation method. *International Journal of Plant Sciences* 161, 143-148.
- Evans, C. L., Xie, X. S., 2008. Coherent Anti-Stokes Raman Scattering Microscopy: Chemical Imaging for Biology and Medicine. *Annual Review of Analytical Chemistry* 1, 883-909.
- Farmer, E. E., 2001. Surface-to-air signals. *Nature* 411, 854-856.
- Felton, G. W., Tumlinson, J. H., 2008. Plant-insect dialogs: complex interactions at the plant-insect interface. *Current Opinion in Plant Biology* 11, 457-463.
- Fernandez, P., Hilker, M., 2007. Host plant location by Chrysomelidae. *Basic and Applied Ecology* 8, 97-116.
- Filik, J., Frogley, M. D., Pijanka, J. K., Wehbe, K., Cinque, G., 2012. Electric field standing wave artefacts in FTIR micro-spectroscopy of biological materials. *Analyst* 137, 853-861.
- Fletcher, J. S., Lockyer, N. P., Vaidyanathan, S., Vickerman, J. C., 2007. TOF-SIMS 3D Biomolecular Imaging of *Xenopus laevis* Oocytes Using Buckminsterfullerene (C60) Primary Ions. *Analytical Chemistry* 79, 2199-2206.
- Gatehouse, A., 2002. Plant resistance towards insect herbivores: a dynamic interaction. *New Phytologist* 156, 145-169.
- Gaume, L., Gorb, S., Rowe, N., 2002. Function of epidermal surfaces in the trapping efficiency of *Nepenthes alata* pitchers. *New Phytologist* 156, 479-489.
- Gniwotta, F., Vogg, G., Gartmann, V., Carver, T. L. W., Riederer, M., Jetter, R., 2005a. What do microbes encounter at the plant surface ? Chemical composition of pea leaf cuticular waxes. *Plant Physiology* 139, 519-530.
- Gniwotta, F., Vogg, G., Gartmann, V., Carver, T. L. W., Riederer, M., Jetter, R., 2005b. What Do Microbes Encounter at the Plant Surface? Chemical Composition of Pea Leaf Cuticular Waxes. *Plant Physiology* 139, 519-530.
- Goodwin, R. J. A., 2012. Sample preparation for mass spectrometry imaging: Small mistakes can lead to big consequences. *Journal of Proteomics* 75, 4893-4911.
- Gorb, E., Haas, K., Henrich, A., Enders, S., Barbakadze, N., Gorb, S., 2005. Composite structure of the crystalline epicuticular wax layer of the slippery zone in the pitchers of the carnivorous plant *Nepenthes alata* and its effect on insect attachment. *Journal of Experimental Biology* 208, 4651-4662.
- Griffiths, D. W., Deighton, N., Birch, A. N. E., Patrian, B., Baur, R., Städler, E., 2001. Identification of glucosinolates on the leaf surface of plants from the Cruciferae and other closely related species. *Phytochemistry* 57, 693-700.
- Griffiths, J., 2008. Secondary Ion Mass Spectrometry. *Analytical Chemistry* 80, 7194-7197.
- Guhling, O., Hobl, B., Yeats, T., Jetter, R., 2006. Cloning and characterization of a lupeol synthase involved in the synthesis of epicuticular wax crystals on stem and hypocotyl surfaces of *Ricinus communis*. *Archives of Biochemistry and Biophysics* 448, 60-72.
- Haas, K., Rentschler, I., 1984. Discrimination between epicuticular and intracuticular wax in blackberry leaves: ultrastructural and chemical evidence. *Plant Science Letters* 36, 143-147.
- Hauke, V., Schreiber, L., 1998. Ontogenetic and seasonal development of wax composition and cuticular transpiration of ivy (*Hedera helix* L.) sun and shade leaves. *Planta* 207, 67-75.

- Hill, R., Blenkinsopp, P., Thompson, S., Vickerman, J., Fletcher, J. S., 2011. A new time-of-flight SIMS instrument for 3D imaging and analysis. *Surface and Interface Analysis* 43, 506-509.
- Hopkins, R. J., Birch, A. N. E., Griffiths, D. W., Baur, R., Städler, E., McKinlay, R. G., 1997. Leaf Surface Compounds and Oviposition Preference of Turnip Root Fly *Delia floralis*: The Role of Glucosinolate and Nonglucosinolate Compounds. *Journal of Chemical Ecology* 23, 629-643.
- Höfer R. R., Briesen I., Beck M., Pinot F., Schreiber L., Franke R., 2008. The Arabidopsis cytochrome P450 CYP86A1 encodes a fatty acid α -hydroxylase involved in suberin monomer biosynthesis. *Journal of Experimental Botany* 59, 2347–2360,
- Inyang, E. N., Butt, T. M., Beckett, A., Archer, S., 1999. The effect of crucifer epicuticular waxes and leaf extracts on the germination and virulence of *Metarhizium anisopliae* conidia. *Mycological Research* 103, 419-426.
- Jeffree, C. E., 1996. Structure and ontogeny of plant cuticles. In: Kerstiens, G. (Ed.), *Plant Cuticles: an integrated functional approach* BIOS scientific publishers, Oxford, pp. 33 - 82.
- Jetter, R., Riederer, M., 1994. Epicuticular crystals of nonacosan-10-ol: In-vitro reconstitution and factors influencing crystal habits. *Planta* 195, 257-270.
- Jetter, R., Schäffer, S., 2001. Chemical composition of the *Prunus laurocerasus* leaf surface. Dynamic changes of the epicuticular wax film during leaf development. *Plant Physiology* 126, 1725-1737.
- Jetter, R., Schaffer, S., Riederer, M., 2000. Leaf cuticular waxes are arranged in chemically and mechanically distinct layers: evidence from *Prunus laurocerasus* L. *Plant Cell and Environment* 23, 619-628.
- Ji, X., Jetter, R., 2008. Very long chain alkylresorcinols accumulate in the intracuticular wax of rye (*Secale cereale* L.) leaves near the tissue surface. *Phytochemistry* 69, 1197-1207.
- Kacuráková, M., Capek, P., Sasinková, V., Wellner, N., Ebringerová, A., 2000. FT-IR study of plant cell wall model compounds: pectic polysaccharides and hemicelluloses. *Carbohydrate Polymers* 43, 195-203.
- Kappers, I. F., Aharoni, A., van Herpen, T. W., Luckerhoff, L. L., Dicke, M., Bouwmeester, H. J., 2005. Genetic engineering of terpenoid metabolism attracts bodyguards to Arabidopsis. *Science* 309, 2070-2072.
- Kaspar, S., Peukert, M., Svatos, A., Matros, A., Mock, H.-P., 2011. MALDI-imaging mass spectrometry – An emerging technique in plant biology. *PROTEOMICS* 11, 1840-1850.
- Kendrick, A., Raffa, K., 2006. Sources of Insect and Plant Volatiles Attractive to Cottonwood Leaf Beetles Feeding on Hybrid Poplar. *Journal of Chemical Ecology* 32, 2585-2594.
- Kerstiens, G., 1996. Signalling across the divide: a wider perspective of cuticular structure—function relationships. *Trends in Plant Science* 1, 125-129.
- Kessler, A., Baldwin, I. T., 2001. Defensive Function of Herbivore-Induced Plant Volatile Emissions in Nature. *Science* 291, 2141-2144.
- Koch, K., Bhushan, B., Barthlott, W., 2010. Multifunctional Plant Surfaces and Smart Materials. In: Bhushan, B. (Ed.), *Springer Handbook of Nanotechnology*. Springer Berlin Heidelberg, pp. 1399-1436.
- Koch, K., Bhushan, B., Ensikat, H.-J., Barthlott, W., 2009a. Self-healing of voids in the wax coating on plant surfaces. *Philosophical Transactions of the Royal Society A: Mathematical, Physical and Engineering Sciences* 367, 1673-1688.
- Koch, K., Bhushan, B., Ensikat, H. J., Barthlott, W., 2009b. Self-healing of voids in the wax coating on plant surfaces. *Philosophical Transactions of the Royal Society* 367, 1673-1688.
- Koch, K., Dommissé, A., Niemietz, A., Barthlott, W., Wandelt, K., 2009c. Nanostructure of epicuticular plant waxes: Self-assembly of wax tubules. *Surface Science* 603, 1961-1968.

- Koch, K., Neinhuis, C., Ensikat, H. J., Barthlott, W., 2004. Self assembly of epicuticular waxes on living plant surfaces imaged by atomic force microscopy (AFM). *Journal of Experimental Botany* 55, 711-718.
- Kolattukudy, P. E., 1996. Biosynthetic pathways of cutin and waxes, and their sensitivity to environmental stresses. In: Kerstiens, G. (Ed.), *Plant Cuticles: an integrated functional approach* BIOS Scientific Publishers, Oxford, pp. 83 - 108.
- Kolattukudy, P. E., Rogers, L. M., Li, D., Hwang, C. S., Flaishman, M. A., 1995. Surface signaling in pathogenesis. *Proceedings of the National Academy of Sciences* 92, 4080-4087.
- Kondo, T., Sawatari, C., 1996. A Fourier transform infra-red spectroscopic analysis of the character of hydrogen bonds in amorphous cellulose. *Polymer* 37, 393-399.
- Kosma, D. K., Bourdenx, B., Bernard, A., Parsons, E. P., Lu, S., Joubes, J., Jenks, M. A., 2009. The impact of water deficiency on leaf cuticle lipids of *Arabidopsis*. *Plant Physiology* 151, 1918-1929.
- Krafft, C., Ramoji, A. A., Bielecki, C., Vogler, N., Meyer, T., Akimov, D., Rösch, P., Schmitt, M., Dietzek, B., Petersen, I., Stallmach, A., Popp, J., 2009. A comparative Raman and CARS imaging study of colon tissue. *Journal of Biophotonics* 2, 303-312.
- Krauss, P., Markstadter C., Riederer M., 1997. Attenuation of UV radiation by plant cuticles from woody species. *Plant, Cell and Environment* 20, 1079-1085.
- Kühn, G., Weidner, S., Just, U., Hohner, G., 1996. Characterization of technical waxes comparison of chromatographic techniques and matrix-assisted laser-desorption/ionization mass spectrometry. *Journal of Chromatography A* 732, 111-117.
- Kühnle, A., Müller, C., 2011. Relevance of visual and olfactory cues for host location in the mustard leaf beetle *Phaedon cochleariae*. *Physiological Entomology* 36, 68-76.
- Kunst, L., Samuels, A. L., 2003. Biosynthesis and secretion of plant cuticular wax. *Progress in Lipid Research* 42, 51-80.
- Kunst, L., Samuels, L., 2009. Plant cuticles shine: advances in wax biosynthesis and export. *Current Opinion in Plant Biology* 12, 721-727.
- Lammers, K., Arbuckle-Keil, G., Dighton, J., 2009. FT-IR study of the changes in carbohydrate chemistry of three New Jersey pine barrens leaf litters during simulated control burning. *Soil Biology and Biochemistry* 41, 340-347.
- Lasch, P., Waesche, W., McCarthy, W. J., Mueller, G. J., Naumann, D., 1998. Imaging of human colon carcinoma thin sections by FT-IR microspectrometry. *SPIE* 3257, 187-198.
- Lee, S. B., Suh, M. C., 2012. Recent Advances in Cuticular Wax Biosynthesis and Its Regulation in *Arabidopsis*. *Molecular Plant* 6, 246-249
- León, J., Rojo, E., Sánchez-Serrano, J. J., 2001. Wound signalling in plants. *Journal of Experimental Botany* 52, 1-9.
- Lin, S., Binder, B. F., Hart, E. R., 1998. Insect Feeding Stimulants from the Leaf Surface of *Populus*. *Journal of Chemical Ecology* 24, 1781-1790.
- Loon, J. A., Blaakmeer, A., Griepink, F., Beek, T., Schoonhoven, L., Groot, A., 1992. Leaf surface compound from *Brassica oleracea* (Cruciferae) induces oviposition by *Pieris brassicae* (Lepidoptera: Pieridae). *Chemoecology* 3, 39-44.
- Maffei, M. E., Mithofer, A., Boland, W., 2007. Before gene expression: early events in plant-insect interaction. *Trends in Plant Science* 12, 310-316.
- Maloney, P. J., Albert, P. J., Tulloch, A. P., 1988. Influence of epicuticular waxes from white spruce and balsam fir on feeding behavior of the eastern spruce budworm. *Journal of Insect Behavior* 1, 197-208.

- Mankovska, B., Percy, K. E., Karnosky, D. F., 2005. Impacts of greenhouse gases on epicuticular waxes of *Populus tremuloides* Michx.: results from an open-air exposure and a natural O₃ gradient. *Environmental Pollution* 137, 580-586.
- Maréchal, Y., Chanzy, H., 2000. The hydrogen bond network in Iβ cellulose as observed by infrared spectrometry. *Journal of Molecular Structure* 523, 183-196.
- Markstadter, C., Federle, W., Jetter, R., Riederer, M., Holldobler, B., 2000. Chemical composition of the slippery epicuticular wax blooms on *Macaranga* (Euphorbiaceae) ant-plants. *Chemoecology* 10, 33-40.
- Martin, P., 1997. Wound Healing--Aiming for Perfect Skin Regeneration. *Science* 276, 75-81.
- McCann, M. C., Chen, L., Roberts, K., Kemsley, E. K., Sene, C., Carpita, N. C., Stacey, N. J., Wilson, R. H., 1997. Infrared microspectroscopy: Sampling heterogeneity in plant cell wall composition and architecture. *Physiologia Plantarum* 100, 729-738.
- McCann, M. C., Hammouri, M., Wilson, R., Belton, P., Roberts, K., 1992. Fourier Transform Infrared Microspectroscopy Is a New Way to Look at Plant Cell Walls. *Plant Physiology* 100, 1940-1947.
- McFarlane, H. E., Shin, J. J., Bird, D. A., Samuels, A. L., 2010. Arabidopsis ABCG transporters, which are required for export of diverse cuticular lipids, dimerize in different combinations. *The Plant Cell* 22, 3066-3075.
- Merk, S., Blume, A., Riederer, M., 1997. Phase behaviour and crystallinity of plant cuticular waxes studied by Fourier transform infrared spectroscopy. *Planta* 204, 44-53.
- Meusel, I., Leistner, E., Barthlott, W., 1994. Chemistry and micromorphology of compound epicuticular wax crystalloids (*Strelitzia* type). *Plant Systematics and Evolution* 193, 115-123.
- Miller, D. J., Sun, L., Walzak, M. J., McIntyre, N. S., Chvedov, D., Rosenfeld, A., 2005. Static SIMS studies of fatty alcohols, amines and esters on gold and aluminium–magnesium alloy surfaces. *Surface and Interface Analysis* 37, 499-508.
- Miller, R. H., 1982. Apple Fruit Cuticles and the Occurrence of Pores and Transcuticular Canals. *Annals of Botany* 50, 355-371.
- Mithöfer, A., Wanner, G., Boland, W., 2005. Effects of Feeding *Spodoptera littoralis* on Lima Bean Leaves. II. Continuous Mechanical Wounding Resembling Insect Feeding Is Sufficient to Elicit Herbivory-Related Volatile Emission. *Plant Physiology* 137, 1160-1168.
- Mithöfer, A., Boland, W., 2012. Plant Defense Against Herbivores: Chemical Aspects. *Annual Reviews of Plant Biology*. 63, 431-50.
- Mohlenhoff, B., Romeo, M., Diem, M., Wood, B. R., 2005. Mie-Type Scattering and Non-B Beer-Lambert Absorption Behavior of Human Cells in Infrared Microspectroscopy. *Biophysical Journal* 88, 3635-3640.
- Molina I., Li-Beisson Y., Beisson F., Ohlrogge J.B., Pollard M., 2009. Identification of an Arabidopsis Feruloyl-Coenzyme A Transferase Required for Suberin Synthesis. *Plant Physiology*, 151, 1317–1328.
- Müller, C., Riederer, M., 2005. Plant Surface Properties in Chemical Ecology. *Journal of Chemical Ecology* 31, 2621-2651.
- Murayama, C., Kimura, Y., Setou, M., 2009. Imaging mass spectrometry: principle and application. *Biophysical Reviews* 1, 131-139.
- Nallala, J., Gobinet, C., Diebold, M.-D., Untereiner, V., Bouché, O., Manfait, M., Sockalingum, G. D., Piot, O., 2012. Infrared spectral imaging as a novel approach for histopathological recognition in colon cancer diagnosis. *Journal of Biomedical Optics* 17, 116013-116013.
- Nan, X., Potma, E. O., Xie, X. S., 2006. Nonperturbative chemical imaging of organelle transport in living cells with coherent anti-stokes Raman scattering microscopy. *Biophysical Journal* 91, 728-735.

- Neinhuis, C., Koch, K., Barthlott, W., 2001. Movement and regeneration of epicuticular waxes through plant cuticles. *Planta* 213, 427-434.
- Palaniswamy, P., Lamb, R. J., 1993. Wound-induced antixenotic resistance to flea beetles, *Phyllotreta cruciferae* (Goeze) (Coleoptera: Chrysomelidae), in crucifers. *The Canadian Entomologist* 125, 903-912.
- Palo, R. T., 1984. Distribution of birch (*Betula* SPP.), willow (*Salix* SPP.), and poplar (*Populus* SPP.) secondary metabolites and their potential role as chemical defense against herbivores. *Journal of Chemical Ecology* 10, 499-520.
- Panikashvili, D., Aharoni, A., 2008. ABC-type transporters and cuticle assembly: Linking function to polarity in epidermis cells. *Plant Signaling and Behavior* 3, 806-809.
- Park, I.-K., Lee, S.-G., Shin, S.-C., Kim, C.-S., Ahn, Y.-J., 2004. Feeding and Attraction of *Agelastica coerulea* (Coleoptera: Chrysomelidae) to Betulaceae Plants. *Journal of Economic Entomology* 97, 1978-1982.
- Passarelli, M. K., Winograd, N., 2011a. Lipid imaging with time-of-flight secondary ion mass spectrometry (ToF-SIMS). *Biochimica and Biophysica Acta* 1811, 976-990.
- Passarelli, M. K., Winograd, N., 2011b. Lipid imaging with time-of-flight secondary ion mass spectrometry (ToF-SIMS). *Biochimica et Biophysica Acta (BBA) - Molecular and Cell Biology of Lipids* 1811, 976-990.
- Pearl, I. A., Darling, S. F., 1971. Phenolic extractives of the leaves of *Populus balsamifera* and of *P. trichocarpa*. *Phytochemistry* 10, 2844-2847.
- Perkins, M., Roberts, C., Briggs, D., Davies, M., Friedmann, A., Hart, C., Bell, G., 2005. Surface morphology and chemistry of *Prunus laurocerasus* L. leaves: a study using X-ray photoelectron spectroscopy, time-of-flight secondary-ion mass spectrometry, atomic-force microscopy and scanning-electron microscopy. *Planta* 221, 123-134.
- Philippe, R. N., Bohlmann, J., 2007. Poplar defense against insect herbivores. *Canadian Journal of Botany* 85, 1111-1126.
- Podila, G. K., Rogers, L. M., Kolattukudy, P. E., 1993. Chemical Signals from Avocado Surface Wax Trigger Germination and Appressorium Formation in *Colletotrichum gloeosporioides*. *Plant Physiology* 103, 267-272.
- Post-Beittenmiller, D., 1996. Biochemistry and molecular biology of wax production in plants. *Annual Review of Plant Physiology and Plant Molecular Biology* 47, 405-430.
- Potma, E. O., Xie, X. S., 2003. Detection of single lipid bilayers with coherent anti-Stokes Raman scattering (CARS) microscopy. *Journal of Raman Spectroscopy* 34, 642-650.
- Pyee, J., Yu, H. S., Kolattukudy, P. E., 1994. Identification of a lipid transfer protein as the major protein in the surface wax of broccoli (*Brassica-oleracea*) leaves. *Archives of Biochemistry and Biophysics* 311, 460-468.
- Rank, N. E., 1994. Host-plant effects on larval survival of a salicin-using leaf beetle *Chrysomela aeneicollis* Schaeffer (Coleoptera: Chrysomelidae). *Oecologia* 97, 342-353.
- Reifenrath, K., Riederer, M., Müller, C., 2005. Leaf surface wax layers of Brassicaceae lack feeding stimulants for *Phaedon cochleariae*. *Entomologia Experimentalis et Applicata* 115, 41-50.
- Renwick, J. A. A., Radke, C. D., Sachdev-Gupta, K., Städler, E., 1992. Leaf surface chemicals stimulating oviposition *Pieris rapae* (Lepidoptera: Pieridae) on cabbage. *Chemoecology* 3, 33-38.
- Reynhardt, E. C., 1997. The role of hydrogen bonding in the cuticular wax of *Hordeum vulgare* L. *European Biophysics Journal* 26, 195-201.
- Ribeiro da Luz, B., 2006. Attenuated total reflectance spectroscopy of plant leaves: a tool for ecological and botanical studies. *New Phytologist* 172, 305-318.

- Riedel, M., Eichner, A., Jetter, R., 2003. Slippery surfaces of carnivorous plants: composition of epicuticular wax crystals in *Nepenthes alata* Blanco pitchers. *Planta* 218, 87-97.
- Riedel, M., Eichner, A., Meimberg, H., Jetter, R., 2007. Chemical composition of epicuticular wax crystals on the slippery zone in pitchers of five *Nepenthes* species and hybrids. *Planta* 225, 1517-1534.
- Riederer, M., Schneider, G., 1989. Comparative study of the composition of waxes extracted from isolated leaf cuticles and from whole leaves of *Citrus*: Evidence for selective extraction. *Physiologia Plantarum* 77, 373-384.
- Rinia, H. A., Bonn, M., Müller, M., Vartiainen, E. M., 2007. Quantitative CARS spectroscopy using the maximum entropy method: the main lipid phase transition. *Chemphyschem: a European Journal of Chemical Physics and Physical Chemistry* 8, 279-287.
- Rinia, H. A., Burger, K. N., Bonn, M., Müller, M., 2008. Quantitative label-free imaging of lipid composition and packing of individual cellular lipid droplets using multiplex CARS microscopy. *Journal of Biophysics* 95, 4908-4914.
- Rowell-Rahier, M., Pasteels, J. M., 1989. Phenolglucosides and Interaction at Three Tropic Levels: Salicaceae - Herbivores - Predators. In: Bernays, E. A. (Ed.), *Insect-Plant Interactions*, vol. II. CSR Press, pp. 75-94.
- Salzer, R., Siesler, H. (Eds.), 2009. *Infrared and Raman Spectroscopic Imaging*. WILEY-VCH.
- Schaller A. (Ed.), 2008. *Induced Plant Resistance to Herbivory*. Springer Netherlands.
- Schnitzler, J. P., Louis, S., Behnke, K., Loivamaki, M., 2010. Poplar volatiles - biosynthesis, regulation and (eco)physiology of isoprene and stress-induced isoprenoids. *Plant Biology* 12, 302-316.
- Schone, C., Hofler, H., Walch, A., 2013. MALDI imaging mass spectrometry in cancer research: combining proteomic profiling and histological evaluation. *Clinical Biochemistry* 46, 539-545.
- Schönherr, J., 1976. Water permeability of isolated cuticular membranes: The effect of cuticular waxes on diffusion of water. *Planta* 131, 159-164.
- Schönherr, J., 2006. Characterization of aqueous pores in plant cuticles and permeation of ionic solutes. *Journal of Experimental Botany* 57, 2471-2491.
- Schreiber, L., 2001. Effect of temperature on cuticular transpiration of isolated cuticular membranes and leaf discs. *Journal of Experimental Botany* 52, 1893-1900.
- Schreiber, L., 2005. Polar Paths of Diffusion across Plant Cuticles: New Evidence for an Old Hypothesis. *Annals of Botany* 95, 1069-1073.
- Schreiber, L., 2006. Review of sorption and diffusion of lipophilic molecules in cuticular waxes and the effects of accelerators on solute mobilities. *Journal of Experimental Botany* 57, 2515-2523.
- Schulz, H., Baranska, M., 2007. Identification and quantification of valuable plant substances by IR and Raman spectroscopy. *Vibrational Spectroscopy* 43, 13-25.
- Schwanninger, N. G. a. M., 2007. The potential of Raman microscopy and Raman imaging in plant research. *Spectroscopy: An International Journal* 21 69-89.
- Sene, C., McCann, M. C., Wilson, R. H., Grinter, R., 1994. Fourier-Transform Raman and Fourier-Transform Infrared Spectroscopy (An Investigation of Five Higher Plant Cell Walls and Their Components). *Plant Physiology* 106, 1623-1631.
- Shepherd, T., Robertson, G. W., Griffiths, D. W., Birch, A. N. E., Duncan, G., 1995. Effects of environment on the composition of epicuticular wax from kale and swede. *Phytochemistry* 40, 407-417.
- Siljeström, S., Hode, T., Lausmaa, J., Sjövall, P., Toporski, J., Thiel, V., 2009. Detection of organic biomarkers in crude oils using ToF-SIMS. *Organic Geochemistry* 40, 135-143.
- Simmons, A. T., Gurr, G. M., 2005. Trichomes of *Lycopersicon* species and their hybrids: effects on pests and natural enemies. *Agricultural and Forest Entomology* 7, 265-276.

- Smith, W. K., McClean, T. M., 1989. Adaptive Relationship Between Leaf Water Repellency, Stomatal Distribution, and Gas Exchange. *American Journal of Botany* 76, 465-469.
- Socrates, G., 1994. Infrared Characteristic Group Frequencies. John Wiley&Sons, West Sussex, UK.
- Soler M., Serra O., Molinas M., Huguet G., Fluch S., Figueras M., 2007. A Genomic Approach to Suberin Biosynthesis and Cork Differentiation. *Plant Physiology* 144, 419-431
- Spencer, J. L., 1996. Waxes enhance *Plutella xylostella* oviposition in response to sinigrin and cabbage homogenates. *Entomologia Experimentalis et Applicata* 81, 165-173.
- Spool, A. M., 2004. Interpretation of static secondary ion spectra. *Surface and Interface Analysis* 36, 264-274.
- Städler, E., Reifenrath, K., 2009. Glucosinolates on the leaf surface perceived by insect herbivores: review of ambiguous results and new investigations. *Phytochemistry Reviews* 8, 207-225.
- Steinbauer, M., Schiestl, F., Davies, N., 2004. Monoterpenes and Epicuticular Waxes Help Female Autumn Gum Moth Differentiate Between Waxy and Glossy Eucalyptus and Leaves of Different Ages. *Journal of Chemical Ecology* 30, 1117-1142.
- Steiner, G., Koch, E., 2009. Trends in Fourier transform infrared spectroscopic imaging. *Analytical and Bioanalytical Chemistry* 394, 671-678.
- Stewart, D., 1996. Furier Transform Infrared Microspectroscopy of Plant Tissues. *Applied Spectroscopy* 50, 357-365.
- Stoner, K. A., 1990. Glossy leaf wax and plant resistance to insects in *Brassica oleracea* under natural infestation. *Environmental Entomology* 19, 730-739.
- Stork, N. E., 1980. Role of wax blooms in preventing attachment to Brassicas by the mustard beetle, *Phaedon cochlearie* *Entomologia Experimentalis et Applicata* 28, 100-107.
- Strehle, K. R., Rösch, P., Berg, D., Schulz, H., Popp, J., 2006. Quality Control of Commercially Available Essential Oils by Means of Raman Spectroscopy. *Journal of Agricultural and Food Chemistry* 54, 7020-7026.
- Svatoš, A., 2010. Mass spectrometric imaging of small molecules. *Trends in Biotechnology* 28, 425-434.
- Tahallah, N., Brunelle, A., De La Porte, S., Laprévotte, O., 2008. Lipid mapping in human dystrophic muscle by cluster-time-of-flight secondary ion mass spectrometry imaging. *Journal of Lipid Research* 49, 438-454.
- Taylor, G., 2002. *Populus: Arabidopsis for Forestry*. Do We Need a Model Tree? *Annals of Botany* 90, 681-689.
- Termonia, A., Hsiao, T. H., Pasteels, J. M., Milinkovitch, M. C., 2001. Feeding specialization and host-derived chemical defense in Chrysomeline leaf beetles did not lead to an evolutionary dead end. *Proceedings of the National Academy of Sciences* 98, 3909-3914.
- Thiel, V., Sjövall, P., 2011. Using Time-of-Flight Secondary Ion Mass Spectrometry to Study Biomarkers. *Annual Review of Earth and Planetary Sciences* 39, 125-156.
- Toole, G. A., Kačuráková, M., Smith, A. C., Waldron, K. W., Wilson, R. H., 2004. FT-IR study of the *Chara corallina* cell wall under deformation. *Carbohydrate Research* 339, 629-635.
- Touboul, D., Kollmer, F., Niehuis, E., Brunelle, A., Laprévotte, O., 2005. Improvement of biological time-of-flight-secondary ion mass spectrometry imaging with a bismuth cluster ion source. *Journal of the American Society for Mass Spectrometry* 16, 1608-1618.
- Tsumuki, H., Kanehisa, K., Kawada, K., 1989. Leaf Surface Wax as a Possible Resistance Factor of Barley to Cereal Aphids. *Applied Entomology and Zoology* 24, 295-301.
- Tulloch, A. P., 1973. Composition of leaf surface waxes of *Triticum* species: Variation with age and tissue. *Phytochemistry* 12, 2225-2232.
- Tuskan, G. A., DiFazio, S., Jansson, S., Bohlmann, J., Grigoriev, I., Hellsten, U., Putnam, N., Ralph, S., Rombauts, S., Salamov, A., Schein, J., Sterck, L., Aerts, A., Bhalerao, R. R., Bhalerao, R.

- P., Blaudez, D., Boerjan, W., Brun, A., Brunner, A., Busov, V., Campbell, M., Carlson, J., Chalot, M., Chapman, J., Chen, G.-L., Cooper, D., Coutinho, P. M., Couturier, J., Covert, S., Cronk, Q., Cunningham, R., Davis, J., Degroeve, S., Déjardin, A., dePamphilis, C., Detter, J., Dirks, B., Dubchak, I., Duplessis, S., Ehrling, J., Ellis, B., Gendler, K., Goodstein, D., Gribskov, M., Grimwood, J., Groover, A., Gunter, L., Hamberger, B., Heinze, B., Helariutta, Y., Henrissat, B., Holligan, D., Holt, R., Huang, W., Islam-Faridi, N., Jones, S., Jones-Rhoades, M., Jorgensen, R., Joshi, C., Kangasjärvi, J., Karlsson, J., Kelleher, C., Kirkpatrick, R., Kirst, M., Kohler, A., Kalluri, U., Larimer, F., Leebens-Mack, J., Leplé, J.-C., Locascio, P., Lou, Y., Lucas, S., Martin, F., Montanini, B., Napoli, C., Nelson, D. R., Nelson, C., Nieminen, K., Nilsson, O., Pereda, V., Peter, G., Philippe, R., Pilate, G., Poliakov, A., Razumovskaya, J., Richardson, P., Rinaldi, C., Ritland, K., Rouzé, P., Ryaboy, D., Schmutz, J., Schrader, J., Segerman, B., Shin, H., Siddiqui, A., Sterky, F., Terry, A., Tsai, C.-J., Uberbacher, E., Unneberg, P., Vahala, J., Wall, K., Wessler, S., Yang, G., Yin, T., Douglas, C., Marra, M., Sandberg, G., Van de Peer, Y., Rokhsar, D., 2006. The Genome of Black Cottonwood, *Populus trichocarpa* (Torr. & Gray). *Science* 313, 1596-1604.
- Uppalapati, S. R., Ishiga, Y., Doraiswamy, V., Bedair, M., Mittal, S., Chen, J., Nakashima, J., Tang, Y., Tadege, M., Ratet, P., Chen, R., Schultheiss, H., Mysore, K. S., 2012. Loss of Abaxial Leaf Epicuticular Wax in *Medicago truncatula* *irg1/palm1* Mutants Results in Reduced Spore Differentiation of Anthracnose and Nonhost Rust Pathogens. *The Plant Cell Online* 24, 353-370.
- Urban, J., 2006. Occurrence, bionomics and harmfulness of *Chrysomela populi* L. (Coleoptera, Chrysomelidae). *Journal of Forest Science* 52, 255-284.
- van de Voort, F. R., Sedman, J., Russin, T., 2001. Lipid analysis by vibrational spectroscopy. *European Journal of Lipid Science and Technology* 103, 815-826.
- Vickerman, J. C., 2011. Molecular imaging and depth profiling by mass spectrometry-SIMS, MALDI or DESI? *Analyst* 136, 2199-2217.
- Villena, J. F., Domínguez, E., Heredia, A., 2000. Monitoring Biopolymers Present in Plant Cuticles by FT-IR Spectroscopy. *Journal of Plant Physiology* 156, 419-422.
- Vrkoslav, V., Muck, A., Cvačka, J., Svatoš, A., 2010. MALDI imaging of neutral cuticular lipids in insects and plants. *J. American Society of Mass Spectrometry* 21, 220-231.
- Walsh, M. J., German, M. J., Singh, M., Pollock, H. M., Hammiche, A., Kyrgiou, M., Stringfellow, H. F., Paraskevaidis, E., Martin-Hirsch, P. L., Martin, F. L., 2007. IR microspectroscopy: potential applications in cervical cancer screening. *Cancer Letters* 246, 1-11.
- Warren, J. M., Bassman, J. H., Fellman, J. K., Mattinson, D. S., Eigenbrode, S., 2003. Ultraviolet-B radiation alters phenolic salicylate and flavonoid composition of *Populus trichocarpa* leaves. *Tree Physiology* 23, 527-535.
- Wen, M., Buschhaus, C., Jetter, R., 2006. Nanotubules on plant surfaces: Chemical composition of epicuticular wax crystals on needles of *Taxus baccata* L. *Phytochemistry* 67, 1808-1817.
- Winograd, N., 2005. The Magic of Cluster SIMS. *Analytical Chemistry* 77, 142 A-149 A.
- Wong, P. T. T., Capes, S. E., Mantsch, H. H., 1989. Hydrogen bonding between anhydrous cholesterol and phosphatidylcholines: an infrared spectroscopic study. *Biochimica et Biophysica Acta (BBA) - Biomembranes* 980, 37-41.
- Woodhead, S., 1983. Surface chemistry of *Sorghum bicolor* and its importance in feeding by *Locusta migratoria*. *Physiological Entomology* 8, 345-352.
- Wu, J. H., 1973. Wound-healing as a factor in limiting the size of lesions in *Nicotiana glutinosa* leaves infected by the very mild strain of tobacco mosaic virus (TMV-VM). *Virology* 51, 474-484.

- Yang, G., Espelie, K. E., Wiseman, B. R., Isenhour, D. J., 1993. Effect of Corn Foliar Cuticular Lipids on the Movement of Fall Armyworm (Lepidoptera: Noctuidae) Neonate Larvae. *The Florida Entomologist* 76, 302-316.
- Yang, J., Yen, H. E., 2002. Early Salt Stress Effects on the Changes in Chemical Composition in Leaves of Ice Plant and Arabidopsis. A Fourier Transform Infrared Spectroscopy Study. *Plant Physiology* 130, 1032-1042.
- Yeats, T. H., Rose, J. K. C., 2013. The Formation and Function of Plant Cuticles. *Plant Physiology* 163, 5-20.

Summary

The most common approach to localize biomolecules in plant is to use labels or staining. However tagging with the external marker may change the structure and activity of studied biomolecules. Similarly, extraction of interesting plant structures (e.g. cell walls) prior analysis leads to distortion of chemical and structural information. And in studies on whole intact leaf, special attention needs to be devoted to the vertical discrimination in order to ensure the surface origin of the acquired data. In the present research, the leaf surface was investigated using selective sampling methods (cryo-adhesive, gum arabic, adhesive tape embedding) and molecular imaging tools: (1) MALDI-TOF-IMS (matrix assisted laser/desorption ionization time-of-flight imaging mass spectrometry), (2) TOF-SIMS (time-of flight secondary ion mass spectrometry) imaging, (3) FT-IR (Fourier transform infrared) as well as (4) Raman spectroscopy imaging. These tools provide molecular specificity and spatially resolved information. The results were complemented with SEM (scanning electron microscopy) and statistical analysis.

The first sequenced tree, *Populus trichocarpa*, along with the leaf beetle *Chrysomela populi* were chosen as a model system. This system represents a naturally occurring interaction between a specialist herbivore and its host plant.

The chemical characterization of the leaf surface represented by epicuticular waxes (EWs) was performed by mass spectrometry (GC-MS and MALDI-TOF-MS) and vibrational spectroscopy (FT-IR and Raman). EWs are complex mixture of very long chain saturated (C₂₃-C₃₄) and unsaturated alkanes (C₂₅, C₂₇, C₂₉), fatty acids (C₁₆, C₁₈), alcohols (C₂₄-C₃₃) and wax esters (C₄₀-C₅₄). All these highly lipophilic wax constituents determine the primary role of the EW layer, namely its barrier function on the plant-environment interface.

By preserving the two dimensional arrangement of the EWs, it was possible to determine local distribution of the leaf surface compounds and monitor processes occurring after insect. FT-IR imaging appeared to be an adequate technique to detect changes on the leaf surface after insect feeding. The alterations were observed in 6 h after insect infestation and were localized in the damaged area. They involve an increase of the absorption bands that are present in the different EW constituents (mainly -CH, -OH, C-O). Moreover, spectra acquired in the injury area exhibited distinguishable profile (e.g. bands shift was detected)

comparing to the rest of the sample. This chemical differentiation was confirmed by the multivariate statistical analysis (HCA). Formation of a multilayer of an additional wax on the injury border (confirmed by SEM) indicate that EWs play an active role in the wound-healing processes. This process aims to protect the leaf from the destructive consequences of tissue damage (in particular excessive water loss).

Reported in the literature role of EWs in the host plant recognition would potentially mean that deposition of additional waxes in the injury area would potentially increase attractiveness of damaged leaves. In order to study that aspect, behavioral bioassays and selective sampling methods were employed including novel, *in vivo* method for selective EW removal – adhesive tape embedding. Results demonstrated that leaf beetles were not only able to recognize their host plant after removal of EW layer, but even preferred de-waxed leaves over controls. Further, salicine – compound reported to influence food selection in leaf beetles, was not detected among surface compounds. Outcome of those studies leads to the conclusion that compounds on the EW layer (leaf surface) of *P. trichocarpa* do not provide chemosensory cues necessary in the host recognition process of specialist leaf beetles, *C. populi*.

In order to achieve better chemical selectivity and spatial resolution, next to FT-IR imaging, mass spectrometry imaging techniques were employed as well. MALDI-TOF-MS and particularly TOF-SIMS imaging allowed investigating the local distribution of individual surface compounds. SIMS images demonstrated the co-localization of ions detected on the leaf surface. They provided a visual representation for the existence of two groups of distribution patterns; one occurring for ions assigned to fatty acids C₂₀ – C₂₄ and wax esters C₄₄ to C₄₈. And the second present among ions assigned to fatty acids C₂₆ – C₃₂. Correlation between defined ions of those two groups was confirmed by the statistical analysis. Spatial association between the detected ions assigned to wax esters depends on the chain length of those wax constituents.

Although many studies over the past decade increased our understanding of processes involved in the wax production and its export from the plant cell to the cuticle, major questions still remain to be resolved. In order to answer those questions comprehensively, a multidisciplinary approach is required. In the present study, the application of selective sampling methods combined with the many advantages of the molecular imaging techniques provided new insights into the processes occurring on the leaf surface of *P. trichocarpa*. The

employed approaches delivered information not obtainable by most of the traditional techniques and therefore have the potential to contribute to the present knowledge in the plant surface research.

8. Zusammenfassung

Das häufigste Verfahren ein Biomolekül in Pflanzen- oder Tiergewebe zu lokalisieren, ist dessen Markierung mit Hilfe von Farbstoffen. Diese Strategie hat jedoch mehrere Nachteile. Zum Beispiel kann die Verknüpfung mit einem externen Marker (z.B. GFP-ähnliche Proteine) die Struktur sowie die Funktion von dem untersuchten Makromolekül ändern. Darüber hinaus gibt es zwei Hauptstrategien bei der Analyse von Pflanzengeweben. Die Erste basiert auf der Extraktion von interessanten Pflanzenstrukturen, wie z. B. Zellwänden. Nach Anwendung dieser Strategie sind jedoch chemische und strukturelle Informationen gestört, oder die Mehrheit der Strukturinformationen verloren gegangen. Eine andere Strategie basiert auf der Analyse des gesamten Pflanzengewebes, wie z.B. vollständig intakte Blätter. Für die Untersuchung biologischer Oberflächen ist es jedoch von großer Bedeutung woher die erhaltenen Informationen stammen. In der vorliegenden Doktorarbeit wurde die Blattoberfläche mit Hilfe eines selektiven Probenahme Verfahrens gesammelt und mittels molekularer bildgebender Verfahren wie der (1) MALDI-TOF-IMS (Matrix assistierter Laser - Desorption und Ionisation mit bildgebender Flugzeit Massenspektrometrie), (2) TOF-SIMS (Flugzeitsekundärionen-Massenspektrometrie)-Bildgebung, (3) FT-IR (Fourier-Transformierter-Infrarot) sowie (4) Raman Spektroskopie untersucht. Diese Methoden ermöglichen die Untersuchung molekularer Spezifitäten ohne die Verwendung von externen Markern und liefern räumlich aufgelöste Informationen. Die Ergebnisse wurden darüber hinaus mittels REM (Rasterelektronenmikroskopie) und statistischer Analysen ergänzt.

Als Modellsystem wurde der erste sequenzierte Baum, *Populus trichocarpa* und der Blattkäfer *Chrysomela populi* gewählt. Dieses Modellsystem repräsentiert eine natürlich auftretende Interaktion zwischen einem spezialisiertem Pflanzenfresser und seiner Futterpflanze.

Die chemische Charakterisierung der epikutikulären Wachse (EWs) auf der Blattoberfläche wurde mittels Massenspektrometrie (GC-MS und MALDI-MS) und Schwingungsspektroskopie (FT-IR- und Raman) durchgeführt. Die EWs stellen eine komplexe Mischung aus sehr langkettigen gesättigten (C₂₃-C₃₄) und ungesättigten Alkanen (C₂₅, C₂₇, C₂₉), Fettsäuren (C₁₆, C₁₈), Alkoholen (C₂₄-C₃₃) und Wachsestern (C₄₀-C₅₄) dar.

Gemeinsam bestimmen diese sehr lipophilen Wachsbestandteile die primäre Funktion der EW Schicht als Barriere zwischen Pflanze und Umwelt.

Ein interessanter Aspekt aus ökologischer Sicht war die Frage, ob die EWs von *P. trichocarpa* ein chemisches Signal für die Erkennung durch spezialisiert Blattkäfer darstellen. Dieser Aspekt wurde mit Verhaltenstests und neuen, *in-vivo* Methoden zur selektiven Entfernung der EWs untersucht. Die Ergebnisse zeigten, dass EWs keine entscheidende Rolle als chemosensorische Signale spielen. Die Blattkäfer waren nicht nur in der Lage, ihre Futterpflanze auch nach der Entfernung des EWs zu erkennen, sondern bevorzugten sogar die entwachsten Blätter gegenüber der Kontrolle.

Die Erhaltung der zweidimensionalen Anordnung der EWs ermöglichte es darüberhinaus die Verteilung der Verbindungen auf der Blattoberfläche und ihre Veränderungen im Verlauf von Fraßschädigung zu untersuchen

Die Anwesenheit von IR-aktiven Verbindungen auf der Blattoberfläche, erlaubte die Anwendung von bildgebender FT-IR Spektroskopie, um Änderungen auf der Blattoberfläche nach Insektenfraß zu erkennen. Diese Änderungen der Oberflächenchemie wurden 6 Stunden nach dem Frasschaden in den beschädigten Regionen lokalisiert. Sie beinhalten eine Erhöhung der Absorptionsbanden für unterschiedlichen EW-Komponenten (insbesondere CH, -OH, C-O) entsprechen und eine Verschiebung der Absorptionsfrequenzen. Die Bildung einer mehrschichtigen zusätzlichen EW Schicht an der Grenze zum Frasschaden wurde darüberhinaus mittels REM bestätigt und dessen chemische Abgrenzung mittels multivariater statistischer Analyse bestätigt.

Um eine bessere chemische Selektivität und räumliche Auflösung zu erreichen, wurden massenspektrometrische bildgebende Verfahren eingesetzt. Die MALDI-TOF-IMS und besonders die TOF-SIMS ermöglichten die lokale Verteilung der einzelnen Oberflächenverbindungen zu charakterisieren. SIMS-Bilder zeigen eine gemeinsame Lokalisierung detektierter Ionen aus der Blattoberfläche. Sie liefern eine visuelle Darstellung für das Vorhandensein von zwei Gruppen von Verteilungsmustern: Eines wurde den Ionen von Fettsäuren C₂₀ - C₂₄ und Wachsester C₄₄ - C₄₈ zugeordnet während das zweite Verteilungsmuster unter Fettsäuren C₂₆ - C₃₂ zu beobachten ist. Die Korrelation zwischen definierten Ionen dieser beiden Gruppen wurde durch die statistische Analyse bestätigt. Obwohl in den letzten zehn Jahren viele Studien zu einem besseren Verständnis der Prozesse bei der Wachsproduktion und dessen Export aus Pflanzenzellen beigetragen haben, bleiben

noch wichtige Fragen offen. Um diese Fragen umfassend zu beantworten, wäre ein multidisziplinärer Ansatz erforderlich. In der vorliegenden Doktorarbeit wurden neue Erkenntnisse zu Prozessen auf der Blattoberfläche von *P. trichocarpa* gewonnen. Die gelieferten Erkenntnisse hätten nicht mit anderen, traditionellen Techniken erreicht werden können und besitzen somit das Potenzial unsere heutigen Kenntnisse in der Erforschung der Pflanzenoberfläche-Forschung zu bereichern.

10. Acknowledgements

I would like to thank Prof. Wilhelm Boland for the opportunity to work on this exciting project and JSMC as well as MPG for the PhD scholarship.

My acknowledgments are addressed to all my advisors for the constructive discussions - Prof. Wilhelm Boland, Prof. Ralf Oelmüller and Prof. Benjamin Dietzek.

I am also grateful to Dr. Axel Mithöfer, Dr. Ales Svatos, Dr. Alexander Welle, Frank Steiniger (Centrum of Electron Microscopy, FSU Jena) for their fruitful discussions. I cordially thank Dr. Stephan von Reuss for his valuable comments and suggestions.

I thank Prof. Benjamin Dietzek for possibility to perform Raman and CARS imaging measurements at the IPHT, Jena and Gero Bergner and Denis Akimov for their technical assistance.

I thank Dr. Alexander Welle and Özgül Demir (Karlsruhe Institute of Technology, Institute for Biological Interfaces) for the TOF- SIMS measurements and successful cooperation. I thank Purva Kulkarni (Department of Bioinformatics, FSU Jena) for bioinformatical analysis of TOF-SIMS data.

My special thanks are addressed to service groups at the Max Planck Institute for Chemical Ecology – HT, IT, and GH. I am particularly grateful to Christian Gast, Daniel Veit and Karsten Wesser for their technical support.

I cordially thank all colleagues in the Department of Biorganic Chemistry, particularly Anja D., Grit, Angelika, Marrita, Andrea, Kerstin for any help I received during my PhD work.

I greatly appreciate all scientific courses organized by the doctoral schools JSMC and IMPRS, which significantly enriched my PhD studies. I am especially grateful to Prof. Małgorzata Barańska and Tomasz Wróbel (Raman Imaging Group, Faculty of Chemistry, Jagiellonian University) for a comprehensive course about the vibrational spectroscopy imaging.

The PhD work would not have been possible without support of my family. I thank them for their love, understanding and patience.

11. Curriculum vitae

February 2010 – April 2015

PhD student – JSMC fellow

Max Planck Institute for Chemical Ecology, Friedrich Schiller University, Jena, Germany

Research project: Discovering the cover. Molecular imaging of *Populus trichocarpa* leaf surface by FT-IR spectroscopy and mass spectrometry techniques.

October 2008 – December 2009

Research fellow of the EU-Marie Curie research and training network: GRASP

Centrum for CO₂ Storage, GFZ German Research Centre for Geosciences, Potsdam, Germany

Research project: Characterization of microbial community in the Altmark natural gas reservoir – potential site for CO₂ storage

January 2007 - June 2008

Institute of Biochemistry and Biophysics, Polish Academy of Science, Warsaw, Poland

Research project: Annexin1 from *Arabidopsis thaliana* – localization and function in the plant cell.

February 2006 – June 2006

Research fellow of the Leonardo da Vinci program

Analytic Jena AG, Jena, Germany

Practical aspects of biotechnology and biomedicine

Education

October 2000 – June 2005

Faculty of Chemistry, Jagiellonian University, Krakow, Poland

Title awarded: M.Sc. in Chemistry (Biological Chemistry Specialization)

August 2004 – April 2005

Neurobiochemistry Department, Faculty of Chemistry, Jagiellonian University, Krakow

Identification and comparison of proteom from astrocytes and neurons (primary cell cultures) in response to specific drugs using MALDI-TOF-MS and LC-MS techniques.

October 2002 – October 2004

The Pedagogical Studium of Jagiellonian University, Krakow

Department of Chemical Education Jagiellonian University, Krakow

Qualification awarded: Teacher of Chemistry in primary and high school

Awards

Student Travel Award, International Society of Chemical Ecology Meeting 2012

Publications

Morozova D., Alawi M., Shaheed M., Krüger M., Kock D., Würdemann H. (2011). The influence of microbial activity on rock fluid interaction: baseline characterization of deep biosphere for Enhanced Gas Recovery in the Altmark natural gas reservoir. *Energy Procedia*, 4, 4633–4640.

Oral Presentations

1. Shaheed M. Local distribution of epicuticular wax compounds on the leaf surface of *Populus trichocarpa*. 28th ISCE Meeting, International Society of Chemical Ecology, Vilnius, Lithuania, July 2012
2. Shaheed M. Discovering the cover. Leaf surface chemistry of *Populus trichocarpa* and its biological role. JSMC Retreat 2012, Bad Sulza, Germany, July 2012

Poster Presentations

1. Dost M. Leaf surface of *Populus trichocarpa* and its role in defense studied by MS and FT-IR microspectroscopy. International Conference on Photochemistry (ICP 2013), Leuven, Belgium, July 2013

2. Dost M. Chemistry and spatial distribution of *Populus trichocarpa* surface compounds and its role in plant defense studied by MS and FT-IR microspectroscopy. 539th WE-Heraeus-Seminar on 'Micro- and Nanostructured Interfaces for Biological and Medical Research', Bad Honnef, Germany, July 2013

3. Shaheed M. Leaf surface of *Populus trichocarpa* and its role in plant defense. MiCom 2011 – 2nd International Student Conference on Microbial Communication, Jena, Germany, September 2011

4. Shaheed M. Localization of elicitors and defensive compounds on plant leaf surface. MiCom 2010 - 1st International Student Conference on Microbial Communication, Jena, Germany, October 2010

Conference Papers

1. Morozova, D.; Shaheed, M.; Vieth, A.; Krüger, M.; Kock, D.; Würdemann, H. Characterization of the deep microbial life in the Altmark natural gas reservoir. GeoDarmstadt 2010 – Geowissenschaften sichern Zukunft, Darmstadt 2010. Schriftenreihe der Deutschen Gesellschaft für Geowissenschaften; 68 10. - 13. Oktober 2010

2. Morozova, D.; Shaheed, M.; Vieth, A.; Krüger, M.; Kock, D.; Würdemann, H. Deep microbial life in the Altmark natural gas reservoir: baseline characterization prior to CO₂ injection. General Assembly European Geosciences Union, Vienna, Austria 2010. Geophysical Research Abstracts; Vol. 12, EGU2010-9431-4

3. Morozova, D.; Shaheed, M.; Vieth, A.; Krüger, M.; Kock, D.; Würdemann, H. The influence of microbial activities on long-term CO₂ storage: baseline characterization of deep microbial life in the Altmark natural gas reservoir 10th International Conference on Greenhouse Gas Control Technologies -GHGT-10, Amsterdam 2010. 19-23 September 2010



12. Independency statement

According to the graduation regulations of the Faculty of Biology and Pharmacy, Friedrich-Schiller-University Jena (No. V, § 8), I declare that the applicable graduation regulations of the Faculty are known by me. I have prepared the present doctoral thesis independently and only using stated auxiliary materials, resources, literature as well as personal contributions. All persons who have supported me in the assessment of materials and assembly of the manuscripts are named in the "Acknowledgments". I have not received the help of a graduation counselor, nor have third parties received direct or indirect monetary benefits for work in connection with the contents of this dissertation. I have not yet submitted this dissertation as an examination paper for a governmental or other scientific examination. Furthermore, I have not submitted this work to another university as a doctoral thesis.

Mina Dost



Selbständigkeitserklärung

Entsprechend der Promotionsordnung der Biologisch-Pharmazeutischen Fakultät der Friedrich-Schiller-Universität Jena (Nr. V, § 8) erkläre ich, dass mir die geltende Promotionsordnung der Fakultät bekannt ist. Die vorliegende Arbeit habe ich selbständig und nur unter Verwendung der angegebenen Hilfsmittel, persönlichen Mitteilungen, Quellen und Literatur angefertigt. Alle Personen, die mir bei der Auswertung des Materials sowie bei der Verfassung der Manuskripte unterstützt haben, sind in der Danksagung genannt. Ich habe weder die Hilfe eines Promotionsberaters in Anspruch genommen, noch haben Dritte unmittelbar oder mittelbar geldwerte Leistungen für Arbeiten erhalten, die in Zusammenhang mit dem Inhalt der vorliegenden Dissertation stehen. Ich habe die Dissertation noch nicht als Prüfungsarbeit für eine staatliche oder andere wissenschaftliche Prüfung eingereicht. Ferner habe ich nicht diese Arbeit bei einer anderen Hochschule als Dissertation eingereicht.

Mina Dost

